Agrociencia

eISSN: 2521-9766

VOLUME 58, NUMBER 7 | OCTOBER 01 - NOVEMBER 15, 2024 | MEXICO

AGRICULTURA

SECRETARÍA DE AGRICULTURA

All correspondence (subscription information, sales, advertising, author contributions, etc.) should be addressed to:

Central Office:

Agrociencia
Guerrero No. 9, Esquina con Avenida Hidalgo,
San Luis Huexotla, Texcoco 56220,
State of Mexico. MEXICO
Tel.: +52-595 92 84427

https://agrociencia-colpos.org/index.php/agrociencia

Cover: Broilers
Photography and credits: Diego Zárate Contreras

AGRICULTURA
SECRETARÍA DE AGRICULTURA Y DESARROLLO RURAL

Contents

Volume 58, Number 7 | October 01 - November 15, 2024

Agricultural Machinery

Animal Science

Agrociencia

INNOVATIVE TECHNOLOGIES IN SPRINKLER IRRIGATION: AN OVERVIEW

Chao **Chen**[1], Zawar **Hussain**[1,2], Junping **Liu**[1]*, Muhammad **Zaman**[3], Muhammad **Akhlaq**[4]

[1]Jiangsu University. Research Centre of Fluid Machinery Engineering and Technology. Zhenjiang, China. 212013.
[1,2] Bahauddin Zakariya University. Department of Agricultural Engineering. Multan, Pakistan. 60800.
[3]University of Agriculture. Department of Irrigation and Drainage. Faisalabad, Pakistan. 30800.
[4]Jiangsu University. School of Agricultural Engineering. Zhenjiang, China. 212013.
* Author for correspondence: liujp@ujs.edu.cn

Citation: Chen C, Hussain Z, Liu J, Zaman M, Akhlaq M. 2024. Innovative technologies in sprinkler irrigation: An overview. **Agrociencia** 58(7): 799-816. https://doi.org/ 10.47163/ agrociencia.v58i7.3191

Editor in Chief:
Dr. Fernando C. Gómez Merino

Received: April 02, 2024.
Approved: September 12, 2024.
Published in Agrociencia: October 14, 2024.

ABSTRACT

The overuse of water in conventional irrigation at the farm level is a global issue that can be addressed by improving irrigation techniques. Sprinkler irrigation can reduce water losses by carefully planning the crop, soil, landscape, and weather conditions, as well as installing the proper sprinkler hardware. The application efficiency of sprinkler systems may be enhanced when these systems are coupled with automation for precise irrigation. Sprinkler irrigation has advanced significantly, but new ideas and current practices are driving further progress. These novel ideas include low-pressure sprinklers, smart controllers, fertigation, water-pesticide integrated sprinkler systems, and variable-rate irrigation. The objective of this work is to highlight the introduction of innovative technologies to optimize sprinkler irrigation systems. Suggestions for the future development of sprinkler irrigation technology are offered to ensure its long-term viability.

Keywords: fertigation, water-pesticide integration, variable rate irrigation, water use efficiency, irrigation efficiency, internet of things (IoT).

INTRODUCTION

Irrigation is the artificial application of water to soil or plants at the appropriate time and quantity, lowering the risk of production loss due to drought by supplying soil moisture to meet crop water requirements. Watering cans, sprinklers, drip irrigation, surface irrigation systems, and other methods can be used to practice irrigation, which is typically done using surface and pressurized systems and is distinguished by how water is transported to the application site (Keller and Bliesner, 1990).

The world's irrigated area accounts for 272 million ha at present, which represents 18 % of the cultivated area. Irrigated agricultural land accounts for approximately 90 % of total crop production (Khan *et al*., 2016). According to world statistics, India has the most irrigated agricultural land (55 ha), followed by China, the USA, Pakistan, Iran, Mexico, Thailand, Indonesia, Russia, and Turkey (Figure 1) (Schultz *et al*., 2005).

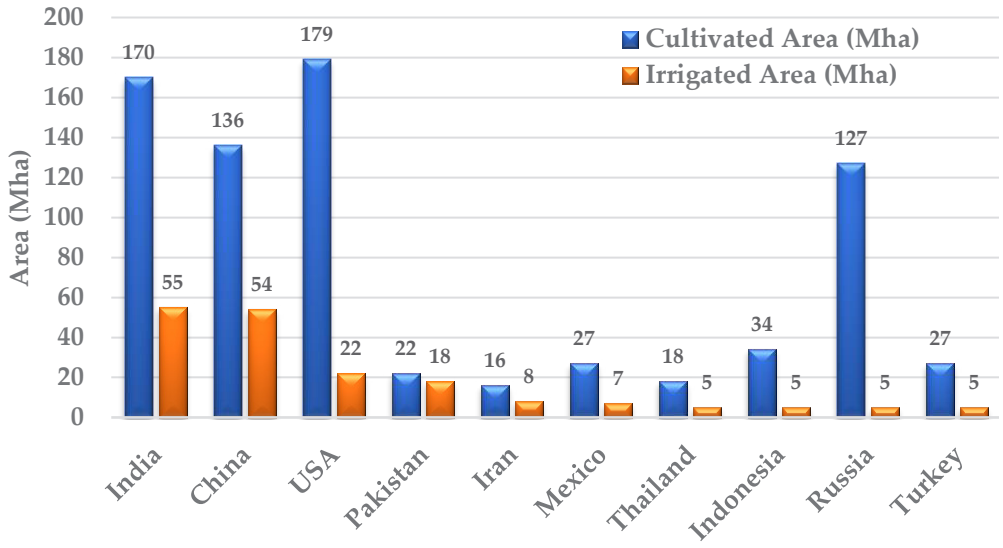

Figure 1. Cultivated and irrigated areas of the top ten countries (Schultz *et al.*, 2005).

Agriculture is the most water-intensive sector, accounting for 70 % of total freshwater withdrawals. However, in some developing countries, this percentage can reach as high as 95 % (FAO, 2015, 2017). The agricultural sector is often criticized for having low efficiency and high-water use. It is highly unlikely that more significant water resources will be made available to agriculture in the future because of the competing water needs of other sectors. Also, because of an increase in population and prosperity, there is an ongoing grow in demand for food, fiber, and housing to satisfy basic needs. Therefore, irrigated agriculture must be more efficient, cost-effective, and flexible. This is possible by updating and modernizing the irrigation systems.

The lack of effective irrigation techniques causes the overuse of water, which lowers crop productivity in most parts of the world. Research shows that most irrigation methods are inefficient because less than half of the water reaches the crop (Li *et al.*, 2019; IFPRI, 2014). Therefore, irrigation system reforms are required to enhance crop yield and satisfy future food needs. Irrigation can boost crop yield per hectare by 2.3 times compared to rainfed areas (Kannan, 1986; Siebert and Doll, 2010).

Sprinkler irrigation systems are becoming increasingly popular, particularly in regions where the terrain is not conducive to traditional irrigation methods. Its adoption in America, Europe, Asia, Africa, and Oceania is 13.3, 10.1, 6.8, 1.9, and 0.9 Mm^2, respectively (Xia *et al.*, 2017). Sprinklers discharge water as tiny droplets when highly pressurized water is forced through them. A sprinkler system is especially suitable for sandy soil, but it is adaptable to almost all soil types. The average application rate of water must be less than the basic infiltration rate of the soil just to prevent water from ponding on the soil surface.

Mechanical and hydraulic devices are used in sprinklers to apply water to the soil surface. With sprinkler irrigation systems, it is possible to apply water, fertilizer, and pesticides efficiently in the right amount at the appropriate times, reducing the occurrence of plant diseases, inhibiting weed growth, and creating favorable conditions for crop growth. This enhances crop productivity and product quality (Kulkarni, 2011). Using sprinkler irrigation, field crop yields may be raised by 10–20 %, while vegetable crop yields could be enhanced by 30 % (Zou *et al.*, 2012). However, sprinkler fertigation keeps crop foliage wet, increasing the risk of pests, diseases, and foliage burn. Additionally, the nutrients may spread to other locations where roots are dormant, reducing the effectiveness of fertilizers.

Sprinkler irrigation with proper design offers higher application efficiency and helps to prevent runoff. It can also help reduce water loss by planning the crops, soil, landscape, and weather conditions when installing the proper sprinkler hardware. Different types of nozzles can be used in pivoting and lateral move sprinkler irrigation systems. The sprinkler head can be altered by nozzles into different devices that utilize 20 % less water (Urrego-Pereira *et al.*, 2013; Wang *et al.*, 2015). Under certain operational conditions, the water is sprayed by these nozzles in multiple streams that combat the winds more effectively and uniformly than conventional sprays (Rahman and Singh, 2014).

Many new technologies have been introduced in sprinkler systems to increase their adaptability and to save water and chemicals like fertilizer and pesticides. This review depicts the induction of innovative technologies and ideas in sprinkler irrigation systems to optimize system productivity.

HISTORY OF DEVELOPMENT IN SPRINKLER IRRIGATION

Sprinkler irrigation technology was introduced almost a century ago, but its application in large areas has only occurred in the past eight decades. As of the end of 1970, more than 3 million hectares of land in the USA and 2.5 million ha in Europe had sprinkler irrigation. In many regions of the world, salinity problems were caused by poorly managed surface irrigation. Fixed sprinkler systems were the first application of sprinkler irrigation. In the 1930s, rotating sprinklers were gradually introduced in the USA, UK, France, Germany, and Italy. After the Second World War, tremendous improvements occurred due to the development of plastics, light aluminum pipes, internal combustion engines, efficient pumps, and electric motors. At that time, towed, center-pivot, mobile, self-propelled, reel traction, and other sprinklers were developed, improving sprinkler irrigation technology worldwide (Shankar *et al.*, 2018).

There are two types of sprinkler irrigation: low-pressure and high-pressure sprinklers (Ella *et al.*, 2008; Li, 2020). Every country develops sprinkler systems and equipment based on prevalent local conditions. In the USA, for instance, self-propelled and center-pivot sprinklers are encouraged. Australia, France, and Germany employ hose reel irrigation systems, whereas Russia uses double cantilever sprinklers. Since the

1950s, China has been at the forefront of development, promoting and implementing sprinkler irrigation as one of the most effective methods for conserving water during irrigation. The first significant change occurred when sprinkler-irrigated acreage increased from 0.03 % in 1974 to 1.42 % in 1985.

The Chinese government adopted water-saving irrigation as a key national policy in the middle of the 1990s because of growing public awareness of worldwide water concerns and the rising need for water resources for economic development. Since then, large amounts of funding have been dedicated to the research and promotion of water-saving irrigation technologies, and sprinkler irrigation development has advanced to a new stage (Yan *et al.*, 2020). In 2008, the Chinese government determined a new strategy for land transfer reforms in rural areas, creating agricultural business units that include family farms, major growers, and agricultural cooperatives. The sprinkler-irrigated area in China reached 4.6 million hectares by the end of 2020 (Figure 2), but this only accounts for 6.3 % of the irrigated area in China (Feng *et al.*, 2023).

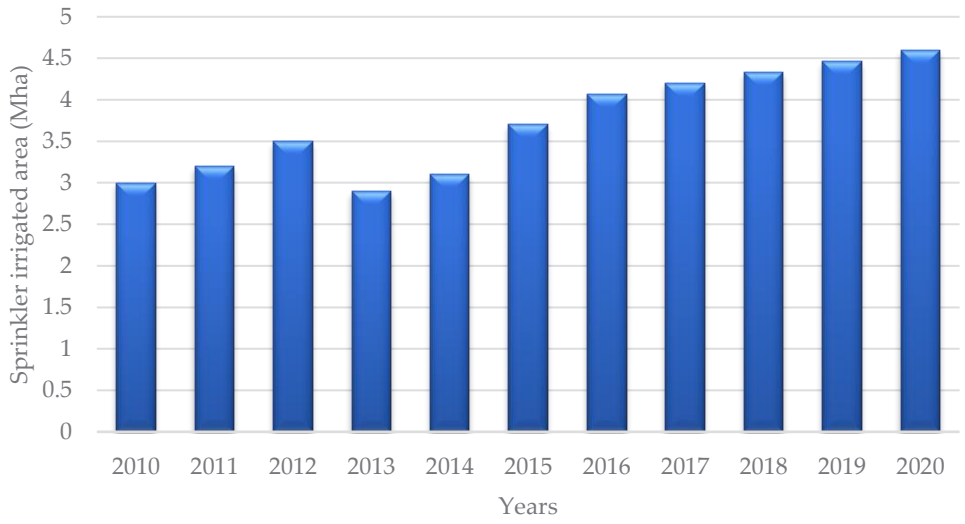

Figure 2. Sprinkler-irrigated area in China (Yan *et al.*, 2020; Feng *et al.*, 2023).

China still has substantial development potential for sprinkler irrigation technologies. To improve efficiency and minimize the management and labor costs of sprinkler irrigation systems, many countries are increasing the area under single-machine control. Worldwide research is also being explored on sprinkler irrigation-based fertigation. Because of rising energy costs worldwide, there has been a paradigm shift away from using high-pressure sprinklers and toward low-pressure sprinklers. As a result, researchers are working to enhance the performance of high-pressure

sprinklers in low-pressure conditions, and irrigators around the world are becoming more interested in the development of water-pesticide-fertilizer integrated sprinkler irrigation and intelligent controllers.

NEW AND ADVANCED TECHNOLOGIES IN SPRINKLER IRRIGATION

Low-pressure sprinklers for the sustainability of farming

New technologies have emerged in sprinkler irrigation to increase system efficiency, water use efficiency, and reduce labor and operating costs. Unpredictable precipitation and rising temperatures already make agriculture challenging. The increasing electricity costs and decreasing the economic feasibility of farming complicate things more. Improving irrigation practices is one of the most straightforward actions to maintain sustainable earnings. Water pumping is often considered the largest energy consumer at the farm level. While farmers cannot simply terminate their field irrigation systems, they may adopt innovative energy-saving technologies.

The first step is to convert high-pressure irrigation to low-pressure, energy-efficient systems. Impact sprinklers release high volumes of water at pressures of 200 to 415 kPa. Most effective systems employ low-pressure sprinkler heads operating at 65 to 175 kPa. These sprinklers lower the need for pumping without considerably lowering the flow, enabling farmers to ensure that their crops have an adequate water supply while reducing the size of their pumps or allowing the modification of their impellers to lower the horsepower requirements (Alvarez, 2015).

By improving irrigation efficiency, low-pressure sprinklers save energy. A concentrated stream of tiny water droplets is released into the atmosphere using high-pressure impact sprinklers. High-pressure sprinklers produce small droplets that are easily dispersed by the wind and rapidly evaporate in dry weather. Meanwhile, low-pressure sprinklers produce larger droplets that are more resistant to high winds and evaporation. Impact sprinklers distribute water in a concentrated stream that severely disturbs the soil, compacting the surface and creating runoff. They generally cover their circle area in 60 to 120 s.

Sprinklers cannot be utilized at lower operating pressures if designed for higher operating pressures. Every type of sprinkler can perform its intended function within a range of flow rates and pressures. This helps them to maintain a proper droplet size and uniform application patterns. Impact sprinkler application patterns are distorted, and their efficiency is reduced when operated at 70 to 100 kPa. Also, they are forced to disperse water in large droplets, which may result in runoff and soil sealing (Li *et al.*, 2019).

When impact sprinklers are operated in low-pressure conditions, water is spread unevenly, leading to water loss. To maximize water distribution under low-pressure conditions, it is necessary to break up the jet mechanically with a fixed water dispersion device. Low-pressure sprinklers can be improved in a number of ways by adding

fluidic devices, orifice nozzles, non-circular nozzles, vanes, and more. In recent years, technological advancements have led to the widespread adoption of rotating spray plate sprinklers (RSPSs), which have a spray plate with grooves that rotate under the force of a water jet (Figure 3). These sprinklers are used in irrigation machinery because their varying plates allow for a variety of droplet sizes and spray patterns (Faci *et al*., 2001; Hanson and Orloff, 1996; Liu *et al*., 2017).

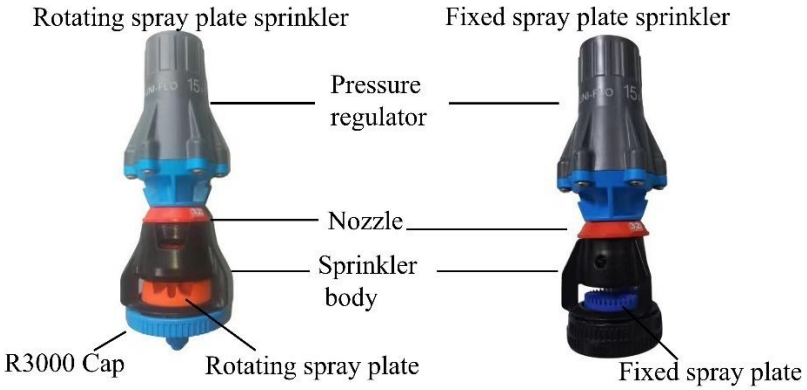

Figure 3. Low-pressure spray plate sprinklers of Nelson Irrigation.

The fluidic sprinkler is an innovative sprinkler head. It operates on the Coanda Effect principle, in which water flows from the nozzle into a tube fitted in the fluidic component to create a low-pressure area with a simple design, low energy loss, and low cost. Numerous studies have been conducted to improve the hydraulic performance, stability, and reliability of fluidic sprinklers in windless conditions (Li *et al.*, 2011; Zhu *et al.*, 2012). There are still issues with the fluidic sprinkler's uniform rotation, even though this application enhanced the water distribution.

Low-cost sprinklers retain the advantages of conventional sprinklers while eliminating the factors that kept small farmers from using them, including the required amount of pressure and expense and the intricacy involved in their use and maintenance. Effective water loss reduction requires careful sprinkler selection in addition to improved crop, soil, and climate management. With the purpose of making the selection of pivoting sprinklers more effective, a runoff-potential index was developed (Hasheminia, 1994; Luz and Heerman, 2005; Rogers *et al*., 2017).

Pivoted sprinklers can improve water distribution by controlling evapotranspiration, which varies according to the crop type, irrigation method, climate, and soil condition. Low-pressure sprinkler systems that apply water within or near the crop canopy may consume less energy and result in less evaporation, but may be less effective due to runoff. To make it easier to select moving spray-plate sprinklers for center-pivot and lateral-move sprinkler irrigation systems, King (2016) developed a quantitative, soil-independent runoff potential indicator. Many commercially available sprinkler

packages were used to evaluate the approach, revealing significant variations that show the runoff potential of several packages might be similar. A runoff index is a valuable tool for comparing different types of sprinklers, indicating which one possesses large droplets and small wetted diameters.

Fertigation in sprinkler irrigation

Chemigation refers to the practice of applying several chemicals to a crop by means of irrigation. When using sprinkler irrigation, fertilizer is dissolved, dispersed, and sprayed into the air by a nozzle with water. Many different types of chemicals, including fertilizers, pesticides, insecticides, fungicides, herbicides, nematicides, and growth regulators may be used (Johnson *et al*., 1986; Threadgill, 1985). On the other hand, the most prevalent type of chemigation involves the injection of water-soluble fertilizers (Bar-Yosef, 1999; Holzapfel *et al*., 2009; Kant and Kafkafi, 2013).

Since the early 1950s, fertilizers have been applied through irrigation in greenhouses in the Netherlands. At the same time, US farmers started small-scale trials incorporating fertilizers like ammonium nitrate and gaseous and liquid ammonia in surface, flood, and furrow irrigation systems. Micro-irrigation was developed and put into practice at the same time that fertigation technology advanced in Israel in the early 1960s. For the precise application of nutrients, electrical pumps and mixing tanks were developed. In the early stages, the distribution of nutrients through fertigation exhibited a certain degree of unevenness, particularly in cases where fertilizer tanks were employed. Subsequently, a greater degree of uniformity in distribution was attained by the utilization of venturi suction pumps and fertilizer injectors.

Micro-irrigation systems and fertigation will continue to become more popular due to their numerous advantages. Fertigation allows the timely application of the appropriate fertilizer dosage, resulting in minimal environmental impact while reducing the amount of the fertilizer by 25–50 %. The precise application of fertilizers directly to the root zone results in efficient fertilizer use and reduced nitrogen leaching below the root zone. Fertigation also saves energy and labor costs associated with fertilizer application (Shukla *et al*., 2018; Ranjan and Sow, 2021). Some good fertilizers commonly used for fertigation are listed below (Table 1).

Table 1. Fertilizers suitable for fertigation.

Nutrient	Fertilizer
Nitrogen (N)	Urea, ammonium sulphate, urea ammonium nitrate (liquid), ammonium nitrate
Nitrogen and phosphorus (N and P)	Mono ammonium phosphate, urea phosphate
Phosphorus (P)	Phosphoric acid
Phosphorus and potassium (P and K)	Mono potassium phosphate
Potassium (K)	Potassium chloride, potassium sulfate, potassium nitrate, potassium thiosulphate
Magnesium and calcium (Mg and Ca)	Magnesium nitrate, calcium nitrate

Fertigation improves crop production management. In 1999 and 2000, a study was conducted in an acid sulfate soil in central Thailand to investigate the impact of various nitrogen (N) fertigation rates on maize yield and nitrate leaching. There were four nitrogen fertigation treatments, i.e., 0, 100, 150, and 200 kg N ha^{-1}, each with three replications set up in a randomized complete block design. The source of nitrogen was urea. The results demonstrated that a fertigation system can be a successful and novel way to deliver water and plant nutrients simultaneously to a crop (Asadi *et al.*, 2002).

China uses more than 60 million Mg of fertilizer annually, one-third of all fertilizers used worldwide. However, the fertilizer use efficiency in China is only 30 % because of excessive application rates and outdated fertilization technologies (Tang *et al.*, 2019), severely hindering the sustainable development of agriculture. Fertigation has gained popularity in China since 2010 due to its numerous benefits. Among the current sprinkler irrigation projects, it is estimated that more than 20 % of sprinkler-irrigated land uses fertigation.

To provide technological support for the widespread adoption of fertigation in center-pivot irrigation systems and to evaluate fertilization uniformity, a fertilizer injection device with a plunger pump was developed. Field experiments were conducted on a system fitted with a fertilizer injection device (Yan *et al.*, 2015). In the meantime, field tests were conducted to find the optimal method for controlling water and nitrogen for wheat, maize, and potato (Cai *et al*., 2018; Li *et al.,* 2018; Zang *et al.*, 2018). Zhang *et al*. (2018) studied water and fertilizer evaporation and drift losses in a center-pivot irrigation system through field experiments. Recently, the Chinese government has been encouraging the development of integrated crop-livestock production systems that use sprinkler irrigation to apply the processed liquid waste of livestock to the field. However, there are still several significant concerns with this technology, like agricultural non-point source contamination, heavy metal residues in crops, and inadequate standards (Dong *et al.*, 2019).

Water-pesticide integration technology

Water and pesticide integration technologies can efficiently solve water and pesticide use in agriculture while also supporting high-yield agricultural farming. Pesticide irrigation has several benefits, including reduced pesticide use, increased crop production and quality, and a better soil environment. Water and pesticide integration is one of the most valuable water-saving irrigation technologies in China due to its high effectiveness and time management (Liu *et al.*, 2016; Prabakaran *et al.*, 2018; Zhu *et al.*, 2016).

Researchers have worked to develop and optimize an integrated sprinkler irrigation system for the application of pesticides. Tsaboula *et al.* (2016) used a particle image velocimeter and variables such as working pressure and nozzle diameter to investigate spraying outflow and discovered changing rules for the outflow field, droplet velocity, and spray angle. Guler *et al.* (2020) evaluated the effects of varying wind speeds on droplet accumulation for five different orifice sizes used in rotary micro sprinkler nozzles in orchard systems. The results showed that the rotational micro sprinkler

nozzles created medium to coarse droplets, which might be employed to reduce spray drift while maintaining pesticide efficiency.

Micro-sprinklers are important components of integrated water and pesticide technology, and their hydraulic performance has a significant impact on the quality of water-pesticide integrated irrigation systems. Wang *et al.* (2022) developed an integrated micro-sprinkler and investigated how the structural parameters affected irrigation and pesticide spraying performance. Using single-factor and three-factor four-level orthogonal tests, the structural optimization of the sprinkler was evaluated. The irrigation flow rate, wetted radius, and uniformity coefficient were used to evaluate the performance of the sprinklers, while the flow rate, spray cone angle, and relative droplet size range were used to assess the performance of the pesticide sprayer. The results of this study offer a theoretical basis for the practical application of sprinklers. Liu *et al.* (2023) designed a water-pesticide integrated micro-sprinkler irrigation system for grape plantings on flat frame installations. Under low pressure, it can irrigate crop roots; under medium pressure, it can apply pesticides to the crop leaves. The flow field of the micro sprinkler was simulated using computational fluid dynamics software to find out the influence and change in main structural parameters. In their study, the structural parameters for the micro sprinklers were optimized. Several operating pressure levels were used to compare the hydraulic performance of the optimized and original sprinklers.

Smart irrigation technologies

Smart irrigation controllers save water by monitoring and analyzing data regarding site conditions such as soil moisture, rain, wind, slope, soil, and type of kind. Based on these parameters, the controllers deliver the right amount of water (Dukes, 2009). Smart sprinkler technologies (Figure 4A) are the latest development in the field of

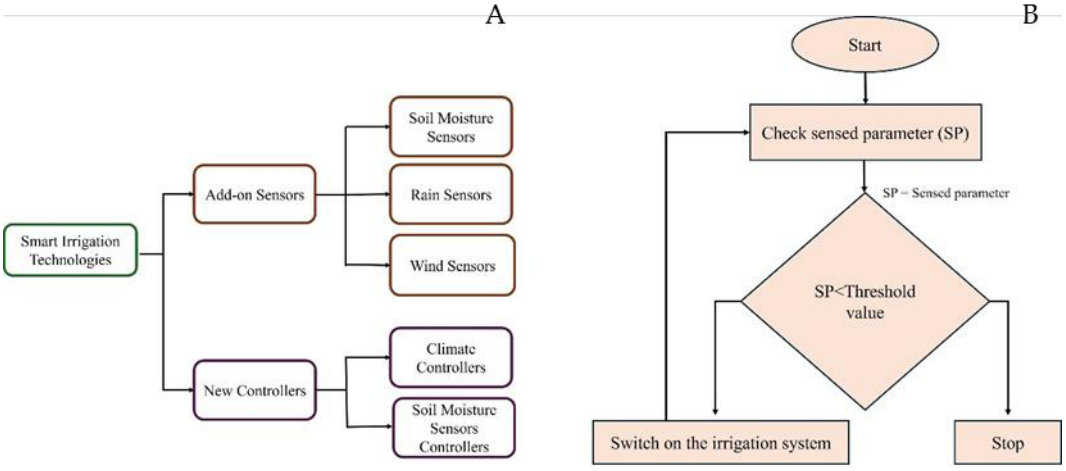

Figure 4. A: Smart irrigation technologies; B: working mechanism of a microcontroller (Difallah *et al.*, 2018).

irrigation. In essence, they collect feedback from the irrigation system and schedule or alter the duration and frequency per that information (Gotcher *et al.*, 2017). Smart controllers plan irrigation based on landscape and weather to avoid overwatering and runoff. The working flowchart of the microcontroller is shown (Figure 4B) (Difallah *et al.*, 2018).

According to the findings of two demonstration studies in California utilizing evapotranspiration (ET) controllers, some irrigation savings are possible, but more extensive comparisons are needed. ET controllers can change irrigation in response to plant needs (Dukes *et al.*, 2009). Similar to ET controllers, soil moisture controllers can decrease irrigation while maintaining turfgrass quality. Soil moisture controllers saved 72 % of irrigation and 34 % of water, compared to homeowner irrigation schedules. A rain sensor stops an automatic sprinkler system from turning on during and after a rainstorm. The rain shut-off gadget stops irrigation when it detects water, and irrigation restarts after the evaporation of rainwater from the sensor. Rain sensors are important devices for preventing wasteful irrigation (Cardenas-Lailhacar *et al.*, 2010).

Kumar *et al.* (2013) investigated a prototype of intelligent irrigation system that uses microcontrollers. It allows irrigation to occur in areas that need watering while avoiding areas where adequate soil moisture is indicated. The pesticide sprinkling system was another highlight of this prototype; it automatically prepares the mixture in the proportions necessary for the plants and minimizes human error. Low-cost sensors and basic circuitry make this tool affordable.

Another project conducted by Ismail *et al*. (2019) focused on the development of a smart irrigation system based on Internet of Things (IoT) technology. The primary objective was to regulate and manage water consumption. This irrigation system was made up of a few sensors, including soil moisture, humidity, and pressure sensors used to monitor soil conditions. To increase sensitivity, these sensors were also connected to the internet via a Wi-Fi module. The users can supervise the irrigation system through the report displayed from the mobile application, which displays sensor readings and controls the water pump in emergencies. The project met its goals for water consumption, minimal project cost, less labor cost, minimum power usage, and reliability.

Islam *et al*. (2020) proposed a model of an IOT-based smart irrigation system in agriculture and used a variety of sensors to monitor the temperature, humidity, pH, and water level in agricultural fields. The data from the sensors was transmitted via wireless transmission to a web server database, and the irrigation system was operated using a smart irrigation mobile application.

Variable rate irrigation technology

Sprinkler irrigation systems can apply water and fertilizers precisely. Manually operated systems require labor for their intended operations. Moreover, it is challenging to irrigate based on real-time crop water requirements (Bitella *et al.*, 2014; Elshaikh *et*

al., 2018; Semananda *et al.*, 2018). The water application rate varies both spatially and temporally based on the actual crop water requirements (Cambra *et al.*, 2018; El-Chami *et al.*, 2019). Hence, to achieve the objectives of precision agriculture, it is important to evaluate the crop water requirements, establish proper irrigation scheduling, and regulate the application process to ensure that only the required amount of water and nutrients are applied.

Precision irrigation should integrate modern techniques and application methods with sophisticated modeling/simulation, sensing, and control technologies to achieve its optimal performance (Baruah *et al.*, 2024; Chauhdary *et al.*, 2023). The physical infrastructure that conveys the water to the crop and the controls that run and manage the system are the two major components of precision irrigation. Data collection is the first step in the management system, and various sensors and instruments are used to obtain precise information about the crop, soil, and weather. The next step is data interpretation, which involves using different modeling and simulation software to predict crop behavior in response to various applications. After this, field irrigation is done based on crop water requirements, and finally, the agronomic, engineering, and economic performance of the system is evaluated (Anjum *et al.*, 2023).

Variable rate irrigation (VRI) is a technique that provides water to the crop precisely at the right time and place to improve water use efficiency and production, save energy, and reduce nutrient leaching (Pan *et al.*, 2013). A very basic form of VRI provides speed control, which adjusts the amount of water applied by changing the lateral's speed as it moves over the field. This strategy can yield the advantages of full VRI in certain cases while being more cost-effective and less difficult (Evans *et al.*, 2012).

Center-pivot and linear-move sprinkler machines are widely used as pressurized irrigation systems worldwide and have a high irrigation efficiency potential (Faci *et al.*, 2001). Farmers use these sprinkler irrigation systems because they cover a large area and have a high level of automation; therefore, they are most suitable for variable application rates (Evans *et al.*, 2012). Hedley and Yule (2009) studied the comparison between VRI and conventional irrigation methods and found that VRI saved 9–19 % more irrigation water. In 2018, a sprinkler prototype with a novel concept of an iris mechanism for variable-rate sprinkler irrigation was developed in Brazil. The suggested approach allows flow rates to be obtained closer to the required values, providing better flexibility and accuracy in applying the target irrigation depth (Sobenko *et al.*, 2018).

VRI systems regulate the center-pivot's travel speed and the duty cycle of solenoid valves placed in front of each sprayer. A control device with a geo-recognizer, like a global positioning system (GPS) unit, is used to locate specific sites and establish unique irrigation zones. The system may apply VRI to center-pivot irrigation systems in both the radial and circumferential directions by altering the pivot rotation speed (Zhang *et al.*, 2018). The uniformity of sprinkler irrigation in each management zone directly impacts crop growth and production. Using a linear-move sprinkler irrigation system with different nozzle diameters, VRI can be readily and economically achieved.

Liu *et al.* (2021) developed a variable rate irrigation uniformity model for linear-move sprinkler irrigation systems. The sprinkler uniformity under various circumstances can be predicted using this model for any linear move irrigation system.

VRI entered commercial production with a sprinkler hardware control system that enhanced control accuracy and reduced expenses. Examples of proper VRI prescriptions that hindered the promotion and deployment of the technology are management zone demarcation, which is mainly determined by soil available water content (AWC) and soil electrical conductivity (EC) (Sui and Yan, 2017; Zhao *et al.*, 2017), and the irrigation decision support system. Direct or indirect attention is paid to the soil in both AWC and EC techniques. However, irrigating the crop rather than the soil is the primary purpose of irrigation.

DISCUSSION

For the precise application of nutrients and water, the present work refers to cutting-edge and innovative sprinkler irrigation technologies. In addition, to save water and energy, sprinkler irrigation equipped with advanced technologies can precisely apply the required amount of water, fertilizers, and other chemicals to the crops. It is possible to reduce energy costs by substituting low-pressure sprinklers with high-pressure sprinklers. As high-pressure impact sprinklers require a minimum operating pressure of approximately 300 kPa, when the operating pressure is increased from 400 to 450 kPa, energy costs increase by up to 18 % (Sheikhesmaeili *et al.*, 2016). Low-pressure sprinklers require 65–175 kPa for effective operation, resulting in lower energy costs without compromising the flow rate.

Fertilizers can be applied effectively through sprinkler irrigation, saving 25–50 %. Similarly, water-pesticide integration technologies in sprinkler irrigation have several benefits, including reduced pesticide use, increased crop production and quality, and a better soil environment. Smart irrigation controllers save water by monitoring and analyzing data regarding site conditions such as soil moisture, rain, wind, slope, soil, plants, and more. Based on these parameters, these controllers deliver the right amount of water at the right time. VRI is a technique of precision agriculture that allows the application of water to crops at a desired location based on actual crop water demand. It is clear that information and results evaluation will enable students and researchers to generate new ideas for future innovations in the field of water-saving irrigation techniques, as well as improvements in the design of existing sprinkler systems.

Sprinkler irrigation is a water-saving technology that promotes green agriculture and improves water productivity. Some factors should be considered for the future promotion of sprinkler irrigation technologies. Although sprinkler irrigation offers excellent uniformity, controllability, and easy operation and maintenance, regional compatibility is a major issue. It is essential to select the appropriate sprinkler system depending on regional conditions. The development of high-uniformity sprinkler fertilizing equipment and control systems is also essential. Multifunctional equipment

that applies water, fertilizer, and pesticide simultaneously is critical to maximizing operational efficiency.

It is recommended to use information technology, such as rainwater irrigation systems and crop water collection equipment with high control precision, intelligence, dependability, ease of use, and wired or wireless sensor network technology. As part of an integrated water, fertilizer, and pesticide irrigation control system, variable irrigation devices, water supply, positioning devices, and control devices should be considered. Developing solar and wind-powered sprinklers should be prioritized for regions with abundant sunshine and plentiful wind energy, respectively.

CONCLUSIONS

This study looked into the major emerging technologies in sprinkler irrigation systems and their significance in conserving water and increasing agricultural yield. To cover investment costs, it is critical to prioritize irrigation engineering and research, incorporating new technologies that build on prior knowledge and aim to maximize crop yield. Although the application technology has been established for many years, one of the outstanding research areas in sprinkler irrigation is the development of an optimal approach for irrigation scheduling.

ACKNOWLEDGMENTS

This work was funded by the National Natural Science Foundation of China (No. 52279036), the Key R&D plan project of Jiangsu Province (No.BE2021341), Project of Faculty of Agricultural Equipment of Jiangsu University (No. NZXB20210101).

REFERENCES

Alvarez N. 2015. Low pressure sprinklers make farming more sustainable: Energy efficiency. SABI Magazine 7 (3).

Anjum MN, Cheema MJM, Hussain F, Wu RS. 2023. Precision irrigation: challenges and opportunities. *In* Precision Agriculture: Evolution, Insights and Emerging Trends. Academic Press: Cambridge, MA, USA, pp: 85–101. https://doi.org/10.1016/B978-0-443-18953-1.00007-6

Asadi ME, Clemente RS, Gupta AD, Loof R, Hansen GK. 2002. Impacts of fertigation via sprinkler irrigation on nitrate leaching and corn yield in an acid-sulphate soil in Thailand. Agricultural Water Management 52 (3): 197–213. https://doi.org/10.1016/s0378-3774(01)00136-6

Baruah VJ, Begum M, Sarmah B, Deka B, Bhagawati R, Paul S, Dutta M. 2024. Precision irrigation management: A step toward sustainable agriculture. *In* Remote Sensing in Precision Agriculture: Transforming Scientific Advancement into Innovation. Academic Press: Cambridge, MA, USA, pp: 189–215. https://doi.org/10.1016/b978-0-323-91068-2.00021-7

Bar-Yosef B. 1999. Advances in fertigation. *In* Advances in Agronomy. Academic Press: Cambridge, MA, USA, pp: 1–77. https://doi.org/10.1016/s0065-2113(08)60910-4

Bitella G, Rossi R, Bochicchio R, Perniola M, Amato M. 2014. A novel low-cost open-hardware platform for monitoring soil water content and multiple soil-air-vegetation parameters. Sensors 14 (10): 19639–19659. https://doi.org/10.3390/s141019639

Cai D, Zhou L, Gu T, Yan H. 2018. Yield and nitrogen utilization of winter wheat under different nitrogen application frequencies with sprinkler irrigation system. Nongye Jixie Xuebao/ Transactions of the Chinese Society for Agricultural Machinery 49 (6): 278–286. https://doi.org/10.6041/j.issn.1000-1298.2018.06.033

Cambra C, Sendra S, Lloret J, Lacuesta, R. 2018. Smart system for bicarbonate control in irrigation for hydroponic precision farming. Sensors 18 (5): 1333. https://doi.org/10.3390/s18051333

Cardenas-Lailhacar B, Dukes MD, Miller GL. 2010. Sensor-based automation of irrigation on bermudagrass during dry weather conditions. Journal of Irrigation and Drainage Engineering 136 (3): 184–193. https://doi.org/10.1061/(asce)ir.1943-4774.0000153

Chauhdary JN, Li H, Jiang Y, Pan X, Hussain Z, Javaid M, Rizwan M. 2023. Advances in sprinkler irrigation: A review in the context of precision irrigation for crop production. Agronomy 14 (1): 47. https://doi.org/10.3390/agronomy14010047

Difallah W, Benahmed K, Bounnama F, Draoui B, Saaidi A. 2018. Intelligent irrigation management system. International Journal of Advanced Computer Science and Applications 9 (9): 429–433. https://doi.org/10.14569/ijacsa.2018.090954

Dong H, Zuo L, Wei S, Zhu Z, Yin F. 2019. Establish manure nutrient management plan to promote green development of integrated crop-livestock production system. Bulletin of Chinese Academy of Sciences 34 (2): 180–189. https://doi.org/10.16418/j.issn.1000-3045.2019.02.007

Dukes MD, Shedd ML, Davis SL. 2009. Smart irrigation controllers: operation of evapotranspiration-based controllers. EDIS (2): AE446. https://doi.org/10.32473/edis-ae446-2009

Dukes MD. 2009. Smart irrigation controllers: What makes an irrigation controller smart? EDIS (2): AE442. https://doi.org/10.32473/edis-ae442-2009

El-Chami D, Knox JW, Daccache A, Weatherhead EK. 2019. Assessing the financial and environmental impacts of precision irrigation in a humid climate. Horticultural Science 46 (1): 43–52. https://doi.org/10.17221/116/2017-hortsciElla VB, Reyes MR, Yoder R. 2008. Effect of hydraulic head and slope on water distribution uniformity of a low-cost drip irrigation system. Applied Engineering in Agriculture 25 (3): 1551–1567. https://doi.org/10.13031/2013.26885

Elshaikh AE, Jiao X, Yang SH. 2018. Performance evaluation of irrigation projects: Theories, methods, and techniques. Agricultural Water Management 203: 87–96. https://doi.org/10.1016/j.agwat.2018.02.034

Evans RG, LaRue J, Stone KC, King BA. 2012. Adoption of site-specific variable rate sprinkler irrigation systems. Irrigation Science 31 (4): 871–887. https://doi.org/10.1007/s00271-012-0365-x

Faci JM, Salvador R, Playán E, Sourell H. 2001. Comparison of fixed and rotating spray plate sprinklers. Journal of Irrigation and Drainage Engineering 127 (4): 224–233. https://doi.org/10.1061/(asce)0733-9437(2001)127:4(224)

FAO (Food and Agriculture Organization). 2015. Towards a water food secure future: Critical perspective for policy makers. Marseille, France. 76 p.

FAO (Food and Agriculture Organization). 2017. Water for sustainable food and agriculture: A report produced for the G20 presidency of Germany. Rome, Italy. 33 p.

Feng X, Liu H, Feng D, Tang X, Li L, Chang J, Tanny J. 2023. Quantifying winter wheat evapotranspiration and crop coefficients under sprinkler irrigation using eddy covariance technology in the North China Plain. Agricultural Water Management 277: 108–131. https://doi.org/10.1016/j.agwat.2022.108131

Gotcher M, Taghuaeian S, Moss QJ. 2017. Smart irrigation technology: Controllers and sensors. Oklahoma State University: Stillwater, OK, USA. 4 p.

Guler H, Zhang Z, Zhu H, Grieshop M, Ledebuhr M. 2020. Spray characteristics of rotary micro sprinkler nozzles used in orchard pesticide delivery. Transactions of the ASABE 63 (6): 1845–1853. https://doi.org/10.13031/trans.13445

Hanson BR, Orloff SB. 1996. Rotator nozzles more uniform than spray nozzles on center-pivot sprinklers. California Agriculture 50 (1): 32–35. https://doi.org/10.3733/ca.v050n01p32

Hasheminia SM. 1994. Controlling runoff under low pressure center pivot irrigation systems. Irrigation and Drainage Systems 8 (1): 25–34. https://doi.org/10.1007/bf00880796

Hedley CB, Yule IJ. 2009. Soil water status mapping and two variable-rate irrigation scenarios. Precision Agriculture 10: 342–355. https://doi.org/10.1007/s11119-009-9119-z

Holzapfel EA, Pannunzio A, Lorite I, de Oliveira AS, Farkas I. 2009. Design and management of irrigation systems. Chilean Journal of Agricultural Research 69 (1): 17–25. https://doi.org/10.4067/s0718-58392009000500003

IFPRI (International Food Policy Research Institute). 2014. Global nutrition report 2014: Actions and accountability to accelerate the world's progress on nutrition. Washington, DC, USA. https://doi.org/10.2499/9780896295643

Islam MdM, Al-Momin Md, Tauhid ABM, Hossain MdK, Sarker S. 2020. IoT based smart irrigation monitoring and controlling system in agriculture. International Journal of Recent Technology and Engineering 8 (6): 2436–2439. https://doi.org/10.35940/ijrte.e6851.038620

Ismail N, Rajendran S, Chee Tak W, Ker Xin T, Shazatushima Shahril Anuar N, Aiman Zakaria F, Mohammed Salleh Al Quhaif Y, Hasan Karakhan HAM, Rahim HA. 2019. Smart irrigation system based on internet of things (IOT). Journal of Physics: Conference Series 1339 (1): 012012. https://doi.org/10.1088/1742-6596/1339/1/012012

Johnson AW, Young JR, Threadgill ED, Dowler CC, Summer DR. 1986. Chemigation for crop production management. Plant Disease 70 (11): 998–1004.

Kannan S. 1986. Physiology of foliar uptake of inorganic nutrients. Proceedings / Indian Academy of Sciences 96 (6): 457–470. https://doi.org/10.1007/bf03053540

Kant S, Kafkafi, U. 2013. Fertigation. *In* Encyclopedia of Soils in the Environment. Elsevier: Amsterdam, Netherlands. https://doi.org/10.1016/b978-0-12-409548-9.05161-7

Keller J, Bliesner RD. 1990. Sprinkle and trickle irrigation. Springer: New York, NY, USA. 584 p. https://doi.org/10.1007/978-1-4757-1425-8

Khan MU, Tayyab M, Majeed M, Shariati MA, Rashidzade S, Mohammadlou A, Plygun S. 2016. Drip irrigation in Pakistan: Status, challenges and future prospects. Russian Journal of Agricultural and Socio-Economic Sciences 56 (8): 114–126. https://doi.org/10.18551/rjoas.2016-08.15

King BA. 2016. Moving spray-plate center-pivot sprinkler rating index for assessing runoff potential. Transactions of the ASABE 59 (1): 225–237. https://doi.org/10.13031/trans.59.11162

Kulkarni S. 2011. Innovative technologies for water saving in irrigated agriculture. International Journal of Water Resources and Arid Environments 1 (3): 226–231.

Kumar ND, Pramod S, Sravani CH. 2013. Intelligent irrigation system. International Journal of Agricultural Science and Research 3 (3): 23–30.

Li H, Issaka Z, Jiang Y, Tang P, Chen C. 2019. Overview of emerging technologies in sprinkler irrigation to optimize crop production. International Journal of Agricultural and Biological Engineering 12 (3): 1–9. https://doi.org/10.25165/j.ijabe.20191203.4310

Li H, Yuan S, Xiang Q, Wang C. 2011. Theoretical and experimental study on water offset flow in fluidic component of fluidic sprinklers. Journal of Irrigation and Drainage Engineering 137 (4): 234–243. https://doi.org/10.1061/(asce)ir.1943-4774.0000288

Li J, Zang W, Li Y, Heeren D, Yan H. 2018. Comparison of nitrogen fertigation management strategies for center-pivot irrigated maize in the sub-humid area of China. *In* ASABE 2018 Annual International Meeting. American Society of Agricultural and Biological Engineers: St. Joseph, MI, USA. https://doi.org/10.13031/aim.201801036

Li J. 2020. Microirrigation in China: History, current situation and future. Irrigation and Drainage 69 (S2): 88–96. https://doi.org/10.1002/ird.2442

Li Y, Zhang Z, Yan H, and Gu T. 2018. Hydraulic performance analysis and optimization for water turbine of JP75 hose reel irrigation machine. Nongye Jixie Xuebao/Transactions of the Chinese Society for Agricultural Machinery 49 (1): 100–107. https://doi.org/10.6041/j.issn.1000-1298.2018.01.012

Liu J, Gull U, Putnam DH, Kisekka I. 2021. Variable-rate irrigation uniformity model for linear-move sprinkler systems. Transactions of the ASABE 66 (4): 1295–1302. https://doi.org/10.13031/trans.14313

Liu J, Hussain Z, Wang X, Li Y. 2023. Optimization and numerical simulation of the internal flow field of water–pesticide integrated microsprinklers. Irrigation and Drainage 72 (2): 328–342. https://doi.org/10.1002/ird.2789

Liu J, Liu W, Bao Y, Zhang Q, Liu X. 2017. Drop size distribution experiments of gas-liquid two phases fluidic sprinkler. Paiguan Jixie Gongcheng Xuebao/Journal of Drainage and Irrigation Machinery Engineering 35 (8): 731.

Liu J, Yuan S, Darko RO. 2016. Characteristics of water and droplet size distribution from fluidic sprinklers. Irrigation and Drainage 65 (4): 522–529. https://doi.org/10.1002/ird.2061

Luz PB, Heerman, D. 2005. A statistical approach to estimating runoff in center pivot irrigation with crust conditions. Agricultural Water Management 72 (1): 33–46. https://doi.org/10.1016/j.agwat.2004.09.013

Pan L, Adamchuk VI, Martin DL, Schroeder MA, Ferguson RB. 2013. Analysis of soil water availability by integrating spatial and temporal sensor-based data. Precision Agriculture 14 (4): 414–433. https://doi.org/10.1007/s11119-013-9305-x

Prabakaran G, Vaithiyanathan D, Ganesan M. 2018. Fuzzy decision support system for improving the crop productivity and efficient use of fertilizers. Computers and Electronics in Agriculture 150: 88–97. https://doi.org/10.1016/j.compag.2018.03.030

Rahman A, Singh A. 2014. A simple low-cost water sprinkling nozzle for field crop irrigation. Current Science 107 (1): 22–25.

Ranjan S, Sow S. 2021. Fertigation: An efficient means for fertilizer application to enhance nutrient use efficiency. Food and Scientific Reports 2 (5): 24–27.

Rogers D, Kisekka I, Lamm FR. 2017. Center pivot irrigation system losses and efficiency. *In* 29 Annual Central Plains Irrigation Conference. Burlengton, CO, USA, pp: 19–34.

Schultz B, Thatte CD, Labhsetwar VK. 2005. Irrigation and drainage. Main contributors to global food production. Irrigation and Drainage 54 (3): 263–278. https://doi.org/10.1002/ird.170

Semananda, NPK, Ward JD, Myers BR. 2018. A semi-systematic review of capillary irrigation: The benefits, limitations, and opportunities. Horticulturae 4 (3): 23. https://doi.org/10.3390/horticulturae4030023

Shankar MS, Ramanjaneyulu AV Neelima TL, Das A. 2018. Sprinkler irrigation–an asset in water scarce and undulating areas. *In* Rajkhowa DJ, Das A, Ngachan SV, Sikka AK, Lyngdoh M. (eds.), Integrated Soil and Water Resource Management for Livelihood and Environmental Security. Umiam, India, pp: 259–283.

Sheikhesmaeili O, Montero J, Laserna S. 2016. Analysis of water application with semi-portable big size sprinkler irrigation systems in semi-arid areas. Agricultural Water Management 163: 275–284. https://doi.org/10.1016/j.agwat.2015.10.004

Shukla M, Chinchmalatpure A, Prasad I, Kumar S. 2018. Fertigation - modern technique of fertilizer application. Indian Farmer 5 (9): 1062–1071.

Siebert S, Doll P. 2010. Quantifying blue and green virtual water contents in global crop production as well as potential production losses without irrigation. Journal of Hydrology 384 (3–4): 198–217. https://doi.org/10.1016/j.jhydrol.2009.07.031

Sobenko LR, de Camargo AP, Botrel TA, dos Santos JDM, Frizzone JA, de Oliveira MF, da Silva JVL. 2018. An iris mechanism for variable rate sprinkler irrigation. Biosystems Engineering 175: 115–123. https://doi.org/10.1016/j.biosystemseng.2018.09.009

Sui R, Yan H. 2017. Field study of variable rate irrigation management in humid climates. Irrigation and Drainage 66 (3): 327–339. https://doi.org/10.1002/ird.2111

Tang H, Wang J, Xu C, Zhou W, Wang J, Wang X. 2019. Research progress analysis on key technology of chemical fertilizer reduction and efficiency increase. Nongye Jixie Xuebao/Transactions of the Chinese Society for Agricultural Machinery 50 (4).

Threadgill ED. 1985. Chemigation via sprinkler irrigation: current status and future development. Applied Engineering in Agriculture 1 (1): 16–23. https://doi.org/10.13031/2013.26756

Tsaboula A, Papadakis EN, Vryzas Z, Kotopoulou A, Kintzikoglou K, Papadopoulou-Mourkidou E. 2016. Environmental and human risk hierarchy of pesticides: A prioritization method, based on monitoring, hazard assessment and environmental fate. Environment International 91: 78–93. https://doi.org/10.1016/j.envint.2016.02.008

Urrego-Pereira YF, Martínez-Cob A, Cavero J. 2013. Relevance of sprinkler irrigation time and water losses on maize yield. Agronomy Journal 105 (3): 845–853. https://doi.org/10.2134/agronj2012.0488

Wang X, Liu J, Zhang Q. 2022. Water–pesticide integrated micro-sprinkler design and influence of key structural parameters on performance. Agriculture 12 (10): 1532. https://doi.org/10.3390/agriculture12101532

Wang Y, Sun P, Sun W, Wang T, Chong B. 2015. Key components design and experiment of roll wheel line move sprinkling irrigation machine. Paiguan Jixie Gongcheng Xuebao/Journal of Drainage and Irrigation Machinery Engineering 33 (10): 915–920.

Xia J, Duan QY, Luo Y, Xie ZH, Liu ZY, Mo XG. 2017. Climate change and water resources: Case study of Eastern Monsoon Region of China. Advances in Climate Change Research, National Climate Center 8 (2): 63–67. https://doi.org/10.1016/j.accre.2017.03.007

Yan H, Hui X, Li M, Xu Y. 2020. Development in sprinkler irrigation technology in China. Irrigation and Drainage 69 (2): 75–87. https://doi.org/10.1002/ird.2435

Yan H, Ma J, Wang Z. 2015. Design and field experiment on fertilizer injection device in center pivot irrigation system. Nongye Jixie Xuebao/Transactions of the Chinese Society for Agricultural Machinery 46 (9): 100–106.

Zang W, Li J, Pei S, Li Y, Yan H. 2018. Effects of different water-nitrogen combinations on potato water consumption, yield and quality under sprinkler irrigation. Paiguan Jixie Gongcheng Xuebao/Journal of Drainage and Irrigation Machinery Engineering 36 (8): 773–778.

Zhang M, Zhao W, Li J, Li Y. 2018. Fertigation uniformity and evaporation drift losses of center pivot irrigation system. Paiguan Jixie Gongcheng Xuebao/Journal of Drainage and Irrigation Machinery Engineering 36 (11): 1125–1130.

Zhao WX, Li J, Yang RM, Li YF. 2017. Crop yield and water productivity responses in management zones for variable-rate irrigation based on available soil water holding capacity. Transactions of the ASABE 60 (5): 1659–1667. https://doi.org/10.13031/trans.12340

Zhu X, Peters T, Neibling H. 2016, Hydraulic performance assessment of Lesa at low pressure. Irrigation and Drainage 65 (4): 530–536. https://doi.org/10.1002/ird.1982

Zhu X, Yuan S, Liu J. 2012. Effect of sprinkler head geometrical parameters on hydraulic performance of fluidic sprinkler. Journal of Irrigation and Drainage Engineering 138 (11): 1019–1026. https://doi.org/10.1061/(asce)ir.1943-4774.0000495

Zou X, Li YE, Gao Q, Wan Y. 2012. How water saving irrigation contributes to climate change resilience- A case study of practices in China. Mitigation and Adaptation Strategies for Global Change 17 (2): 111–132. https://doi.org/10.1007/s11027-011-9316-8

Agrociencia

RURAL PIG FARMERS: A CASE STUDY ON WELL-BEING PERCEPTION IN TEPETLÁN, VERACRUZ, MEXICO

Miguel Ángel **Solís-Tejeda**[1], Octavio **Ruíz-Rosado**[1], Ponciano **Pérez-Hernández**[1*], Pablo **Díaz-Rivera**[1], Fabiola **Lango-Reynoso**[2], Jorge **Aguilar-Ávila**[3], Alberto **Asiain-Hoyos**[1]

[1]Colegio de Postgraduados Campus Veracruz. Carretera Xalapa-Veracruz km 88.5, Tepetates, Manlio Fabio Altamirano, Veracruz, Mexico. C. P. 91690.
[2]Tecnológico Nacional de México. Instituto Tecnológico de Boca del Río. Carretera Veracruz-Córdoba km 12, Boca del Río, Veracruz, Mexico. C. P. 94290.
[3]Universidad Autónoma Chapingo. Centro de Investigaciones Económicas, Sociales y Tecnológicas de la Agroindustria y la Agricultura Mundial. Carretera Mexico-Texcoco km 38.5, Chapingo, Texcoco, State of Mexico, Mexico. C. P. 56277.
* Author for correspondence: pperez@colpos.mx

Citation: Solís-Tejeda MA, Ruíz-Rosado O, Pérez-Hernández P, Díaz-Rivera P, Lango-Reynoso F, Aguilar-Ávila J, Asiain-Hoyos A. 2024. Rural pig farmers: A case study on well-being perception in Tepetlán, Veracruz, Mexico. **Agrociencia** 58(7): 817-830. https://doi.org/ 10.47163/agrociencia.v58i7.2821

Editor in Chief:
Dr. Fernando C. Gómez Merino

Received: May 31, 2022.
Approved: August 29, 2024.
Published in Agrociencia: October 28, 2024.

ABSTRACT

Rural pig farming (*Sus domesticus* Erxleben) is a major agricultural activity in Veracruz, Mexico. Given the controversies surrounding pig farming, the perception of well-being was studied along with the impact of this activity in Vicente Guerrero, in Tepetlán, Veracruz, Mexico. Twenty-six pig farms were characterized to understand their dynamics and profiles. Then, seven farmers were selected to conduct a case study on the location. A triangulation was carried out with other family members, local authorities, and a former farmer in the community. The segment interviewed was all female, with an average age of 48 years. Pig farming is the second most important economic activity in households and the main source of income for women. Production systems are traditional, with pared floors; 62.9 % are carried out in a space smaller than 1000 m^2. On average, each farmer has 21 animals and 53.9 m^2 of pigsties, and 96.2 % of farmers do not treat the waste generated by this activity. The interviewees relate well-being to the economy and health. The pig farming business does not currently satisfy the economic needs of the farmers. To generate more income, it is required to decrease the cost of pig feed and raise the sale price. Additionally, this activity affects the well-being of other members of the community.

Keywords: Subjective well-being, characterization of farmers, dimensions of well-being.

INTRODUCTION

Veracruz is the fifth largest state of pig production (*Sus domesticus* Erxleben) in Mexico (SIAP, 2021). This activity was incentivized in small-scale farmers through state programs such as *Fomento Ganadero* (Livestock Promotion) of the Secretariat of Agriculture, Livestock, Rural Development, Fishing, and Food (SAGARPA) (IICA, 2016). The municipal area of Tepetlán, located in the State´s, is a model of backyard

pig farming, carried out with basic infrastructure without waste treatment (Solís-Tejeda *et al*., 2021a). Pigs are fed on concentrated foods, which represents 70 % of total production costs (Cisneros-Saguilán *et al*., 2020). This is a challenge to reaching profitability, so alternatives that benefit this activity are required.

The World Health Organization defines personal well-being as the optimal state of mental health that makes people able to materialize their potential, overcoming the stress of everyday life and contributing to their community (WHO, 2018). It is possible to understand well-being as the satiation satiety that people achieve of their basic and complementary needs, as well as the possibility of reaching their aspirations in a particular timeframe (Duarte and Jiménez, 2007).

The Mexican government considers that to achieve well-being for rural families, it is necessary to generate income above the poverty line (DOF, 2020). This is equivalent to the value of the food basket plus the non-food basket, which in December 2021 was $2 343.5 MXN for rural areas and $3 542.14 MXN for urban areas per person (CONEVAL, 2022). Individual economic development has a greater influence on well-being than an increase in income for the entire population. Individuals strive for well-being. Income, professional development, and the acquisition of goods are all means of achieving it (Rojas, 2011). Well-being is used as a measure of progress, and it is useful in comparing societies over time and space, as well as defining good and bad aspects. Numerous factors influence well-being, including family, health, income, and employment.

Production and economic activities are important steps toward achieving well-being. Agriculture, has shown to improve the perception of well-being by creating community ties, contributing to environmental care, political influence, and positive aspects related to working the land (Molina-Posada *et al*., 2019). Pig farming can improve aspects of personal and family well-being, such as financial, physical, and social health. Understanding and measuring these aspects from the farmer's perspective is critical (Santos-Barrios *et al*., 2017), considering the damage to the social well-being that this activity generates, such as the effects on both human health and the environment due to the residues produced, while promoting systems that guarantee well-being in all dimensions (GreenPeace, 2020).

This article provides an insight into the perception of well-being generated by backyard pig farming. Given the controversy, it is critical to understand the perception of well-being produced by this activity and how it affects social and family well-being in the community, as demonstrated by the town of Vicente Guerrero in Tepetlán, Veracruz, Mexico. The information analyzed was obtained from the perspective of female pig farmers at a backyard level, family members, and other local participants of the community.

MATERIALS AND METHODS

The study was carried out in the town of Vicente Guerrero, in the municipality of Tepetlán, Veracruz, Mexico (19° 36′ 38′′ N and 96° 48′ 26′′ W, at an altitude of 900 m). This area is highly marginalized, with an index of 52.6. It has 935 inhabitants, of whom

456 are women. The weather is warm-humid, with a mean annual temperature of 19 °C and a mean annual rainfall of 1320 mm (SEFIPLAN, 2021).

Non-probabilistic sampling was used to identify 26 small pig farms. A structured survey was used to characterize them, which included questions about household characteristics as well as production and business systems. The characterization is presented using descriptive statistics. Following that, an exploratory and multiple case study was conducted, in which seven farmers from previously characterized farms, each with defined characteristics such as a backyard and a traditional production system, were interviewed.

To be considered, the subject of study must have had at least four years of experience as a pig farmer, with assets ranging from one to 15 sows, as well as the ability to sell finished animals. A semi-structured questionnaire was developed to interview farmers and prompt new questions. To confirm the information in the case study, a semi-structured questionnaire was applied for the triangulation process including family members, community authorities, and a former male pig farmer.

RESULTS AND DISCUSSION

Farm characterization

Characteristics of the farmers

All farms studied were run by women, who control the pig production system, which coincides with Valencia *et al*. (2007) and demonstrates their ability to direct these systems. Housewives are satisfied with this activity because it provides economic independence from their husbands and the possibility to contribute financially to the household. However, Chávez-Torres (2010) explains that it is common for women to work in small pig farms, despite the fact that their primary responsibility is to their homes.

The average age of these farmers is 48 years, with a minimum age of 30 (Table 1), which is lower than the 55 years reported by Jaramillo-Albuja *et al*. (2018) for backyard

Table 1. Economic activities of families of pig farmers in Tepetlán, Veracruz, Mexico.

Farmer	Age (years)	Economic activity (percentage of the family income)	Education
Martha	31	Pigs (100)	High school, complete
Reyna	62	Hourly employee (50), coffee (10), sugarcane (20), pigs (20)	Second grade
Magdalena	30	Butchery (70), pigs (30)	Bachelor's, incomplete
Elsa	46	Cheese-making (40), cooking (40), pigs (20)	Elementary school, complete
Estela	42	Cooking job (60), milking cows (20), pigs (20)	Elementary school, complete
Araceli	37	State transit job (60), pigs (30), limes (10)	Elementary school, complete
Carmela	53	Hourly employee (50), nixtamal mill (20), pigs (20), sells ice wholesale (10)	Fourth grade

farmers. These farmers have an average of eight years of pig farming experience and a low level of formal education (33.3 % incomplete elementary school, 40.7 % elementary, 14.8 % junior high school, 7.4 % high school, and 3.7 % bachelor's).

Characteristics of the households

The households are composed of two to seven members, with an average of three. All members contribute to production, though the heads of the families direct and run the households. The time dedicated to the activity is 3.5 h d^{-1} on average, seven days a week.

Production and business system

The farming systems are considered "backyard" activities according to their level of productivity and technology. However, only 38.5 % of farms are located on household land; the remainder are developed within the same town. Moreover, 65.4 % are located in plots smaller than 1000 m^2, whereas only 15.4 % are larger than one hectare. In terms of ownership, 80.8 % of the land is commonly owned (ejidos), 11.6 % is privately owned, and 7.7 % is rented. The average area to house the animals is 54 ± 27.5 m^2. On average, the area is divided into six pens, with a minimum of two and a maximum of 13.

All pens are built with block walls. The roofs are made of metal sheets, except one farm, where the roof is made of wood and nylon. The pens all have concrete floors and polyvinyl chloride (PVC) drainage, except for one, which has a dirt floor and wood shaving bedding. Of the farms studied, 38.5 % have maternity or gestation cages, 23 % have nipple drinkers, and the remainder use concrete water troughs. This description coincides with the scarce infrastructure reported by Santos-Barrios *et al*. (2017) for backyard farmers. However, this study observes a higher level of equipment, obtained through social and productive assistance programs. No farm with a traditional firm-floor system provides treatment for wastewater or the solids produced; 50 % directly discharge wastewater into municipal drainage; 34.6 % dispose of the water on the same land; 11.5 % have a septic tank; and 3.8 % produce no wastewater. These data are consistent with those by Solís-Tejeda *et al*. (2021a).

Pigs are the second most important economic activity for 57.7 % of the households surveyed, and the third for 19.6 %. Nonetheless, in 84.6 % of cases, it is the primary economic activity in which women participate. Out of all farmers, 57.7 % sell live pigs weighing 90 to 110 kg; 15.4 % sell 40-day-old weaned piglets; 19.2 % do both; and only 7.7 % transform the pigs through butcheries. This indicates an opportunity for farmer organizations to benefit from joint sales, thus improving technologies that help reach volumes that satisfy markets, produce more income, and increase well-being (Vargas-Prieto *et al*., 2019).

Out of the total number of farmers, 7.7 % consider their farm to be consolidated, 46.1 % consider it to be growing, 30.8 % consider it to be stagnant, and 15.4 % consider it to be declining. Farmers have access to providers in town. Providers sell animal feed,

medications, and veterinary services, resulting in a one-component network (Aguilar-Gallegos *et al*., 2017). The scheme shows that the provider is "P003," due to a credit policy that benefits the finance of farmers "T" (Figure 1).

The customer network is made up of eight components (Figure 2), and most farmers have only one single client for their products. "AC" clients are middlemen from outside the town. Clients labeled "CA1" and "CA2" are local butchers, and "I" represents diverse, indefinite, and occasional clients. "CA1" is known for being less demanding in terms of quality, whereas the other clients demand the provision of finishing feed to the animals. The farmers identify their incomes and health as key aspects of their family well-being (Figure 3).

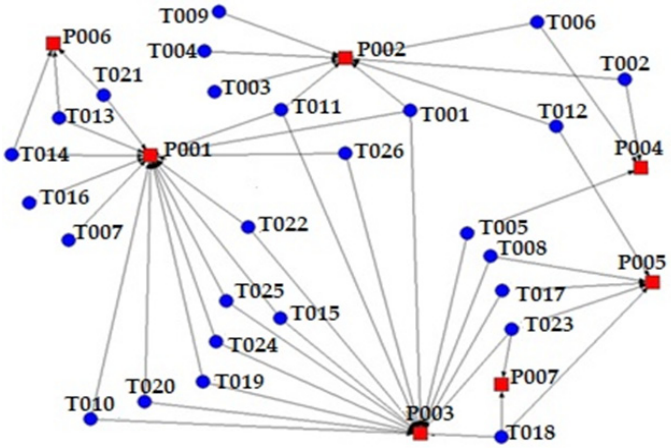

Figure 1. Provider network for pig farms in Tepetlán, Veracruz, Mexico.

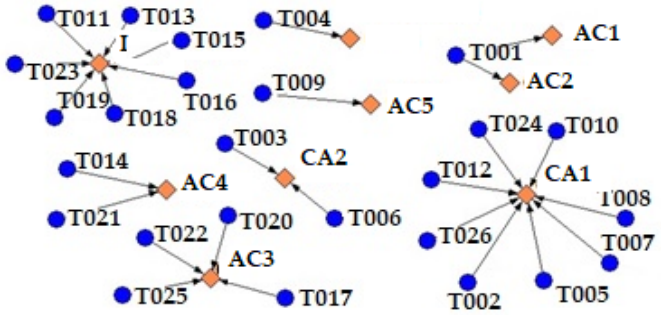

Figure 2. Customer network of the pig farmers surveyed in Tepetlán, Veracruz, Mexico.

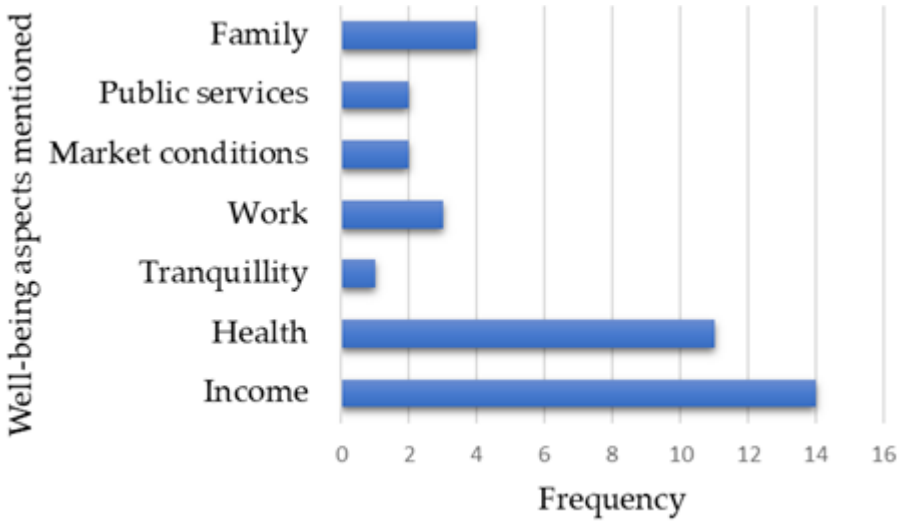

Figure 3. Aspects of family well-being and the frequency with which they were mentioned by farmers in Tepetlán, Veracruz, Mexico.

Case study on the perception of well-being

Interview conducted on farmers

Pig farming was started by 71 % of female producers to boost their family income. *"…Here in this town, I think it is one of the important activities, pig farming. Most families have their income like there, their savings, fattening forces them to save, in a way …"* Magdalena. Meanwhile, 14 % started in this activity by family inheritance. *"…For as long as I can remember, my mom and dad had one or two for their expenses, and then we just took over the job …"* Martha. When asked what economic activity they performed before raising pigs, 71 % responded that they did housework. *"…I have always done housework …"* On the other hand, 28 % had other economic activities as jobs. *"…I would work in the mill. I would start working at six in the morning …"* Carmela.

Currently, pigs are not the main source of income (Table 1). Pig farming provides interviewed families with an average yield of $20 420.00 MXN a year per farm. Surpassing the poverty line requires $26 444.28 MXN per person to satisfy the basic food and non-food baskets (CONEVAL, 2022). Therefore, other productive activities are needed to contribute to the family expenses.

To identify the perception of well-being, we asked what well-being is, and the answers were: *"To earn well and health"* (Martha), *"…To have a bit more income …"* (Reyna), *"…A good income, good quality of life, adequate services, that roads were well…"* (Magdalena), *"…That we were given some kind of help and health…"* (Elsa), *"…To be well, to have health and work…"* (Estela), *"…That we were well, with economic well-being to live better…"* (Araceli)

and *"…To have good health to be able to work. Having a market for the pigs…"* (Carmela).

Of all the people surveyed, 57 % believe that they are well off and that raising pigs has contributed to this, mainly through the resources obtained from their sale. *"…I have achieved well-being by working with them (the pigs) and investing to save a bit in case I need something. In case I need to, I'd sell the pigs, even if they aren't finished…"* Martha.

Out of the total of farmers who do not consider themselves to be well off, 43 % relate it to the drop in pork prices and the increase in prices of balanced foods; this situation causes them to become stressed. *"…A bit more income from the pigs would give me greater well-being because I would no longer be worried about what I'll do, or what I'll have to eat, or if there is anything to eat. Now I feel worried because I sold my pigs and made no profit. I feel depressed…"* Reyna. *"…Well-being becomes hard with the reduction in the price of pork, and then there is too much pork, and selling it gets complicated. Lots of pork is coming in from Puebla. I don't know how they sell it so cheap…"* Carmela.

The rise in the price of corn in the year 2020 persisted in 2021, causing an increase in the price of animal feed, including pig feed. The reaction is a reduction in worldwide production, leading up to a reduction in the grain reserves in the United States, along with the effects of the "La Niña" phenomenon in Brazil and Argentina. On top of this, China has increased its demand for grains. Other factors are the reduction in the supply of crude oil by Saudi Arabia and the COVID-19 (Aguilar-Gómez, 2021). In order to reduce the consumption of balanced foods, it is possible to provide pastures using the pig-to-field production system in one or all of the stages of development of the animal (Carballo-Sánchez *et al*., 2021). However, the farmers in our study do not know other pig farming technologies.

All the farmers surveyed wish to continue with the activity. *"…I am motivated to continue because it is something that can be done here, at home. You don't need as much space, and one can get things done in little time …"* Martha. In addition, 57 % mention that the activity has provided returns in other moments. *"…When they come, when pork goes up in other places, when buyers start coming to this area, prices go up. Now I'm paying $37.00, but if they come from elsewhere, it forces me to pay more…"* Magdalena's husband and local butcher.

The farmers agree that it is a critical moment for pig production due to the increase in the price of balanced feed and the drop in the price of pork. Hence the question, "What motivates you to continue to raise pigs?" to which 43 % responded that they continue because they like to work with animals, and 28 % explained that the little time they dedicate to the pigs helps them do other productive, recreational, or educational activities.

All interviewees consider that raising pigs is an adequate activity for them. When asked what the activity contributes to their well-being, the following answers were provided: *"…it gives us money…"* (Martha), *"…The pigs give me money to buy myself the things I need…"* (Reyna), *"…It's another source of income, we can't have only one source of income because we are a big family…"* (Magdalena), *"…For us it's like saving, and you know you are fattening them, you tighten your belts on some things, but you know you are going to*

get it back…" (Elsa), *"…They have helped me pay for my kids' school…"* (Estela), *"…My son is in university, and that's where we have taken money from for him to study…"* (Araceli), and *"…That's where I get money from to pay for the services for the house …"* (Carmela).

Interviews conducted on farmers' families

All the farmers interviewed consider that their families agree with their work raising pigs. Their family members were asked what they like about their relatives' raising pigs. The responses were: *"…However little, money does come in…"* (María, Martha's mother), *"…It's convenient for my wife to have these pigs because she buys whatever she wants and I don't move my money…"*. (Enrique, Reyna's husband), *"…I like it because when she has (pigs), I buy them, and the money stays here…"* (Jorge, Magdalena's husband), *"… When we sell, we get money for us, and that's what we use to buy things …"* (Julia, Elsa's daughter), *"…It doesn't take lots of our time, you just go tend to them and wash them twice a day and you come back …"* (Juan, Estela's husband), *"…I like animals, but I can't work on them anymore, so I say she goes on …"* (Clara, Araceli's mother-in-law), and *"…She's busy and helps me with expenses…"* (Federico, Carmela's husband).

The farmers' family members were asked about their perceptions of well-being (Table 2). 71 % believe they do not have a sense of well-being. *"…I think I lack in well-being because one has to work a lot to be well, and if we get sick, it costs a lot of money and we can't leave work; and if we go to the doctor, we waste many hours and have to leave work and make no money…"* Jorge. Only 14 % of the family members surveyed consider pig farming as the only source of their well-being. *"…The pigs do contribute to our well-being, that's what we feed off. That's why I try that my daughter doesn't get discouraged and goes on…"* María.

Table 2. Perception of well-being by the families of pig farmers in Tepetlán, Veracruz, Mexico.

Name	Relationship	Age (years)	Education	Economic activity	Perception of well-being
María	Martha's mother	64	Elementary school, complete	Housewife	*"…Health and support from the government…"*
Enrique	Reyna's husband	62	First grade	Farmer	*"…Earning enough for food and get cured when we get sick …"*
Jorge	Magdalena's husband	41	High school, complete	Butcher	*"…Having enough resources to continue working and to be able to eat …"*
Julia	Elsa's daughter	19	High school, complete	Student	*"…Having money to eat, feel good, being able to study …"*
Juan	Estela's husband	45	Elementary school, complete	Cow milker	*"…Having money for the home expenses, such as food and electricity, for the children …"*
Clara	Araceli's mother-in-law	69	Elementary school, complete	Mole vendor	*"…That they can assist you because I can't work anymore. That my family members have jobs …"*
Federico	Carmela's husband	57	Elementary school, complete	Laborer	*"…Having opportunities, earn more …"*

Although 86 % consider that pigs contribute to their well-being, it is not the activity that provides them the greatest well-being. *"…Pigs do give us a profit, and it helps. But I feel that we see money more often from cattle. Pigs are like savings …"* Juan.

We asked the family members what could be done so pigs could further promote the well-being of their families: *"…To have space to keep breeding and being able to feed them…"* (María), *"…We should be taught how to make the pig feed and get a better price for each pig…"* (Enrique), *"…Having more money for pigpens and fitting more animals in…"* (Jorge), *"…That the feed was cheaper, because it's expensive…" (Julia), "…To find a way to be paid more per pig and sell them faster…"* (Juan), *"…Well, we should get support to be able to produce more…"* (Clara), and *"…There's a lack of market opportunities here, pork is poorly paid…"* (Federico).

Neighbors complain to 28 % of the relatives due to smells related to pig farming, which is considered harmful to the health and well-being of the community. This has led to the search for places to move their farming facilities. *"…Almost all of us do this for a living, and that's why there are no problems with neighbors…"* Araceli.

Interview conducted on a former farmer

As part of the case study process triangulation was used with Martín (age 56), a five year former farmer who left pig farming one year ago. He was asked what well-being is. *"…It is that one that is relatively well economically. That you work but also see a profit …"* Do you think you have well-being? *"…Yes, but a low one; let's say 50 or 60 %; one has to make an effort to have well-being…"* What economic activities do you carry out to obtain well-being? *"…I have always worked with cattle, even before pigs. And that gives me a bit of well-being…"* Why did you decide to produce pigs? *"Sometimes you see that others are producing. And when you see that there is a bit higher price, you do get excited. But there comes a time in which food prices rise and the price of pork drops. We do try hard, but then the price drops and there are no buyers, and the pigs keep eating; that's why we stopped …"*

Do you consider that cows provide greater well-being than pigs? *"…Yeah, we also feed them, but only one portion, and we go to the sugarcane plantation and bring back the cane tip, and it doesn't incur any costs…"* Would you go back to raising pigs? *"…I would like to, but it would have to be economically a fixed amount to begin. I have pigpens there. The prices of the feed would have to improve because otherwise, why would I work if I won't make a profit…"*

Interview conducted with local authorities

A representative of the health sector, a municipal agent of the area, and the president of a farmers' association with influence on the municipality were interviewed. They were asked about their concept of well-being (Table 3) and some questions about well-being in the community (Table 4). In this regard, Solís-Tejeda *et al*. (2021a) report that 72.2 % of a sample of farms in Vicente Guerrero, Veracruz, Mexico, discharge their wastewater into the drainage system, including untreated feces.

Daniel was asked the following questions: What problems pig farms cause in the area? *"…People complain about the pigpens, the smell, and the flies. I go visit houses, and*

Table 3. Perception of the well-being by authorities in Tepetlán, Veracruz, Mexico.

Name	Age (years)	Job	Perception of well-being
José	49	Municipal agent	*"…That the community is better off, that the streets can be fixed, and that we all have the same quality of life in the economy. That there are more jobs …"*
Diego	38	Health promoter	*"…To be well physically, emotionally, to have a general stability in life and at work …"*
Deysi	38	President of a farmers' organization	*"…To have health, homes, and resources to be well-fed, dressed, and a possibility of thriving …"*

Table 4. Well-being in the community and the effect of pig farming in Vicente Guerrero, Veracruz, Mexico.

Name	What do you consider well-being in the community?	How does pig farming affect the community's well-being?
José	*"…What contributes most are sugarcane, coffee, and animals. But more economic activities are needed …"*	*"…The problem we have is with those who do it here, in the town. The drainage often gets blocked and they smell bad. But I think it helps the well-being of those who produce it; it's what they live off…"*
Diego	*"…There's a lack of action promotion, and for people to take action on what they are responsible for. Hard work is being done to change habits to avoid diseases…"*	*"…There are plenty of pigsties. Some adapted following municipal guidelines, but others are in backyards and cause certain diseases and annoyances to the people who don't do that for a living…"*
Deysi	*"…We need to work more for our well-being. There is a great demand for infrastructure for farms and equipment to help the farmers earn more and live better. There are currently no support programs for farmers…"*	*"…Pigs provide them with incomes, however little, because of a lack of investment. Families help each other to buy or improve their homes, and even for parties…"*

that's what people comment. But there haven't been any diseases…" What to do to avoid pigs from harming the community's well-being? *"…Most people have pigpens. It's good because those families get incomes. It's bad because it affects other families that don't do that, and that's why they think it's bad. It should be more regulated, so that they are better-kept and avoid troubles for others…"* Does it affect the consumption of pork in the area? *"… There are many people who are diabetic and hypertense and with other diseases, and so they shouldn't be eating pork. Our promotion activities include teaching them about healthy eating and following up on their doctors' recommendations…"*

José was asked: What is your opinion on the pig farming in the area? *"…It's fine, it's a source from which everyone helps each other. The problem is that we have many who have pigpens in the town. We should consider moving them out…"* What actions have you considered to improve the town's well-being in the face of the increase in pig farms*?*

"…Our biggest problem is that there are two huge pig farms, and two cheese factories as well. Everyone is willing to take the pig farms out of the town, but those people who have cheese factories, which are big farms, are the ones with the most money, and they do nothing to take them out. And now those with little money say, they should take them out, and then me…"

Solís-Tejeda *et al*. (2021b) explain that backyard pig farming is important for rural development, although it must be carried out sustainably. The increase of small-scale farms in rural areas rises the risk of soil, water, and air degradation. Nevertheless, there are affordable alternatives that can be adopted, such as the treatment of wastewater through constructed wetlands and the use of deep bedding made with inexpensive materials from the region (Solís-Tejeda *et al*., 2022) and pig farming in the field (Oyhantçabal *et al*., 2011), which is necessary to evaluate as alternatives to the problem of this study.

Deysi was asked: What actions have you taken to improve the well-being of unionized members of your organization in Vicente Guerrero? *"…For seven years now, we began providing metal sheets for rooves. We have projects for women in bakeries and tortilla shops. But what we people have asked for the most have been pigpens and equipment for pig farms. In this town, up to 15 projects of this type have been delivered per year, until the current government came in, and there is no more possibility of helping …"* What must be done for the pig farms to provide more well-being? *"…Not leaving pig farmers on their own. Counseling is urgent; there is no support for extension workers. Pigpens need to be improved and enlarged. An impactful project is necessary to transform the pork industry; I am always told that sales are hard…"*

Do you consider that the increase in the number of pig farms in Vicente Guerrero affects the town's inhabitants? *"…I suppose so. Many people are moving their farms to the outskirts of the town, but it's an important source of income. Pork moves the local economy; it brings money into the town, and food is produced. And while there is no work in the countryside, it's always a good option…"*

Opportunities to improve the well-being of pig farmers

The present study reflects the need to co-innovate in the current backyard pig farming systems. In these processes, the main actor must be integrated, and the co-innovations suggested must be evaluated according to the financial, technical, environmental, and social impact, as well as their contribution to the well-being of the farmers' families. It is suggested to evaluate the implementation of systems with constructed wetlands, deep beddings, and pigs in the fields, as per the particular characteristics of the farmers. For this, the productive area, the current infrastructure, and the resources of the region must be considered, among other aspects. It is necessary to create productive programs in favor of well-being, supported economically and environmentally, that promote a shift in the production methods of small-scale farmers.

CONCLUSIONS

Women participation in the family´s economy plays a decisive and undervalued role. Backyard pig farmers' well-being is closely related to the success of their economic activities, sometimes with a negative impact when expected returns are not met and when they do not have the health required to perform their economic activities. Backyard pig farming is an activity that provides economic resources to acquire goods and services. It allows the farmer getting money in a short time, acting as a savings fund. However, it cannot provide all the necessary resources to achieve well-being, as it is only a supplement to the family´s economy.

Backyard pig farming has become a challenge for the people of Vicente Guerrero, affecting the well-being of non-farmers. Pig farms cause discomfort due to their waste. There are verifiable impacts, such as the clogging of the community's drainage system. To increase the well-being of families, it is necessary to increase profitability in local pig farming. Key options include reducing costs and increasing sale prices, as well as continuous training. As a strategy for the first case, pig farmers consider learning how to make their feed locally.

REFERENCES

Aguilar-Gallegos N, Martínez-González EG, Aguilar-Ávila J. 2017. Análisis de redes sociales: conceptos clave y cálculo de indicadores. Universidad Autónoma Chapingo. Centro de Investigaciones Económicas, Sociales y Tecnológicas de la Agroindustria y la Agricultura Mundial. Chapingo, México. 145 p.

Aguilar-Gómez J de J. 2021. Maíz 2021: su precio aumenta y hace más caro el alimento de animales en granjas. Porcicultura.com. Tezuitlán, México. https://www.porcicultura.com/destacado/Maiz-2021%3A-su-precio-aumenta-y-hace-mas-caro-el-alimento-de-animales-en-granjas (Retrieved: May 2024).

Carballo-Sánchez CS, Espino-Martínez NS, Vodanovich-Possamai AL. 2021. Producción de cerdos al aire libre como estrategia productiva a escala familiar. *In* Palma-García JM, Cruz-Uribe JF. (compls.), Tecnologías Sociales en la Producción Pecuaria de América Latina y el Caribe. Universidad de Colima: Colima, México, pp: 175–184.

Chávez-Torres M. 2010. La familia, regazo de las unidades de producción pequeñas en el contexto de la globalización. *In* Jiménez-Hernández NE. (ed.), Familia y Tradición. Herencias Tangibles e Intangibles en Escenarios Cambiantes. El Colegio de Michoacán: Zamora, México, pp: 193–212.

Cisneros-Saguilán P, Aniano-Aguirre H, Martínez-Martínez R, Gómez-Vázquez A, Maldonado-Peralta M de los Á, Ayala-Monter MA. 2020. Forraje verde hidropónico en dietas de cerdos en crecimiento en Pinotepa Nacional, Oaxaca. Revista Mexicana de Ciencias Agrícolas 11 (24): 247–253. https://doi.org/10.29312/remexca.v0i24.2375

CONEVAL (Consejo Nacional de Evaluación de la Política de Desarrollo Social). 2022. Medición de la pobreza. Consejo Nacional de Evaluación de la Política de Desarrollo Social. Ciudad de México, México. https://www.coneval.org.mx/Medicion/MP/Paginas/Lineas-de-bienestar-y-canasta-basica.aspx (Retrieved: May 2024).

DOF (Diario Oficial de la Federación). 2020. ACUERDO por el que se emiten las reglas de operación del Programa Sembrando Vida, para el ejercicio fiscal 2021. Gobierno de México. Secretaría de Bienestar. Ciudad de México, México. https://www.dof.gob.mx/nota_detalle.php?codigo=5608917&fecha=28/12/2020 (Retrieved: May 2024).

Duarte T, Jiménez RE. 2007. Aproximación a la teoría del bienestar. Scientia et Technica 1 (13): 305–310.

GreenPeace. 2020. ¿Qué hay detrás de la industria porcícola en la península de Yucatán? La carne que está consumiendo al planeta. GreenPeace México. Ciudad de México, México. https://www.greenpeace.org/mexico/publicacion/8357/que-hay-detras-de-la-industria-porcicola-en-la-peninsula-de-yucatan-la-carne-que-esta-consumiendo-al-planeta/ (Retrieved: May 2024).

IICA (Instituto Interamericano de Cooperación para la Agricultura). 2016. Evaluación de diseño Programa de Fomento Ganadero. Secretaría de Agricultura, Ganadería, Desarrollo Rural, Pesca y Alimentación. Instituto Interamericano de Cooperación para la Agricultura. Ciudad de México, México. https://www.transparenciapresupuestaria.gob.mx/work/models/PTP/programas/sed/evaluaciones/2016/08s260pcdi16.pdf (Retrieved: May 2024).

Jaramillo-Albuja JG, Peña-Olvera BV, Hernández-Salgado JH, Díaz-Ruiz R, Espinosa-Calderón A. 2018. Caracterización de productores de maíz de temporal en Tierra Blanca, Veracruz. Revista Mexicana de Ciencias Agrícolas 9 (5): 911–923. https://doi.org/10.29312/remexca.v9i5.1501

Molina-Posada DV, Muñoz-Duque LA, Molina-Jaramillo AN. 2019. Agricultura urbana, bienestar subjetivo y actitudes ambientales en el colectivo Agroarte. Estudio de caso en la comuna 13, Medellín. Revista Virtual Universidad Católica del Norte 56: 89–108.

Oyhantçabal G, Tommasino H, Barlocco N. 2011. Sustentabilidad de la producción familiar de cerdos a campo: un estudio de caso múltiple. Agrociencia (Uruguay) 15 (2): 144–157.

Rojas M. 2011. El bienestar subjetivo: su contribución a la apreciación y a la consecución del progreso y el bienestar humano. Realidad, Datos y Espacio. Revista Internacional de Estadística y Geografía 1 (2): 64–77.

Santos-Barrios L, Martínez-Castañeda FE, Gómez-Demetrio W, Sánchez-Vera E, Ruiz-Torres M. 2017. Percepciones de bienestar social relacionadas con la producción de cerdos de traspatio en zonas peri-urbanas. Universidad Autónoma Chapingo. Colegio de Postgraduados. Texcoco, México. 13 p.

SEFIPLAN (Secretaría de Finanzas y Planeación). 2021. Cuadernillos municipales 2021, Tepetlán. Gobierno del Estado de Veracruz. Xalapa, México. http://ceieg.veracruz.gob.mx/2021/06/17/cuadernillos-municipales-2021/ (Retrieved: May 2024).

SIAP (Servicio de Información Agroalimentaria y Pesquera). 2021. Carne en canal porcino. Gobierno de México. Servicio de Información Agroalimentaria y Pesquera. Ciudad de México, México. http://infosiap.siap.gob.mx/repoAvance_siap_gb/pecAvanceProd.jsp (Retrieved: May 2024).

Solís-Tejeda MA, Lango-Reynoso F, Castañeda-Chávez M del R, Ruelas-Monjardin LC. 2021a. Analysis of the environmental impact generated by backyard swine production in Tepetlán, Veracruz, Mexico. Agro Productividad 14. https://doi.org/10.32854/agrop.v14i6.1875

Solís-Tejeda MA, Lango-Reynoso F, Díaz-Rivera P, Aguilar-Ávila J, Asiain-Hoyos A, Pérez-Hernández P. 2021b. Constructed wetlands as alternatives for swine sustainability. Agro Productividad 14 (12): 181–188.

Solís-Tejeda MA, Lango-Reynoso F, Díaz-Rivera P, Aguilar-Ávila J, Asiain-Hoyos A, Pérez-Hernández P. 2022. Deep litter pig production system as a sustainable alternative for small farmers. Agrociencia 56 (6): 1–14. https://doi.org/10.47163/agrociencia.v56i6.2755

Valencia E, Rejón M, Pech V, Chimal P. 2007. Factores organizacionales que influyen en la producción de cerdos manejados por grupos de mujeres con un enfoque microempresarial en la comunidad de Chumbec, Yucatán, México. Livestock Research for Rural Development 19 (10): 978–994.

Vargas-Prieto A, Fajardo-Rodríguez CL, Romero-Rodríguez YE, Nieves-Forero KY. 2019. La asociatividad para articular cadenas productivas en Colombia. El caso de los pequeños productores de papa criolla en Subachoque, Cundinamarca. Cooperativismo y Desarrollo 27 (115): 1–34. https://doi.org/10.16925/2382-4220.2019.02.10

WHO (World Health Organization). 2018. Mental health. World Health Organization. Geneva, Switzerland. https://www.who.int/es/news-room/fact-sheets/detail/mental-health-strengthening-our-response (Retrieved: May 2024).

Agrociencia

LABORATORY INFECTION COMPARISON OF THREE CATFISH SPECIES WITH *Ligictaluridus floridanus* (Monogenoidea: Dactylogyridae)

Flaviano **Benavides-González**[1], Victoria **González-Castillo**[1], Isidro Othoniel **Montelongo-Alfaro**[2], Jesús Alberto **de la Cruz-Cervantes**[1], Andrés **Zúñiga-Cortes**[2], Gaspar M. **Parra-Bracamonte**[4], Jaime Luis **Rábago-Castro**[1], Roberto **Pérez-Castañeda**[1], María de la Luz **Vázquez-Sauceda**[1], Zeferino **Blanco-Martínez**[1], Lorena **Garrido-Olvera**[3], Jesús Genaro **Sánchez-Martínez**[1*]

[1]Universidad Autónoma de Tamaulipas. Facultad de Medicina Veterinaria y Zootecnia. Carretera Victoria-Mante km 5, Ciudad Victoria, Tamaulipas, Mexico. C. P. 87000.
[2]Universidad Tecnológica del Mar de Tamaulipas Bicentenario. Carretera Soto La Marina-La Pesca km 46+400 S/N, La Pesca, Soto La Marina, Tamaulipas, Mexico. C. P. 87678.
[3]Universidad Autónoma de Tamaulipas. Instituto de Ecología Aplicada. División del Golfo 356, La Libertad, Ciudad Victoria, Tamaulipas, Mexico. C. P. 87019.
[4]Centro de Biotecnología Genómica del Instituto Politécnico Nacional. Boulevard del Maestro S/N, esq. Elías Piña, Colonia Narciso Mendoza, Reynosa, Tamaulipas, Mexico. C. P. 88710.
* Author for correspondence: jgsanchez@docentes.uat.edu.mx

Citation: Benavides-González E, González-Castillo V, Montelongo-Alfaro IO, de la Cruz-Cervantes JA, Zúñiga-Cortes A, Parra-Bracamonte GM, Rábago-Castro JL, Pérez-Castañeda R, Vázquez-Sauceda M de la L, Blanco-Martínez Z, Garrido-Olvera L, Sánchez-Martínez JG. 2024. Laboratory infection comparison of three catfish species with *Ligictaluridus floridanus* (Monogenoidea: Dactylogyridae). **Agrociencia** 58(7): 831-837. https://doi.org/ 10.47163/agrociencia.v58i7.3025

Editor in Chief:
Dr. Fernando C. Gómez Merino

Received: June 06, 2023.
Approved: October 04, 2024.
Published in Agrociencia: October 11, 2024.

ABSTRACT

This study looked at the prevalence, abundance, and mean intensity of the parasite *Ligictaluridus floridanus* (Monogenoidea: Dactylogyridae) in channel catfish (*Ictalurus punctatus*), hybrid catfish (*I. punctatus* x *I. furcatus*), and the striped catfish (*Pangasianodon hypophthalmus*), an exotic, non-local species. The channel catfish was the most susceptible to *L. floridanus* infection, followed by the hybrid catfish with a 100 % prevalence. The striped catfish was the least susceptible, and although the parasite was detected once, this species does not seem susceptible to long-term infection.

Keywords: non local fish, hybrid, infection, striped catfish.

INTRODUCTION

Ligictaluridus floridanus (Monogenoidea: Dactylogyridae) is a monogenean parasite that chronically infects the channel catfish (*Ictalurus punctatus*) (Rábago-Castro *et al*., 2014), a fish native to North America that is commercially cultured in the United States and Mexico (Lara-Rivera *et al*., 2015). Catfish crossbreeding is performed to induce hybrid vigor and positive heterosis. The cross of channel catfish x blue catfish (*I. punctatus* x *I. furcatus*) usually outperforms parental species in most environments (Argue *et al*., 2014).

The striped catfish (*Pangasianodon hypophthalmus*), a fish native to the Mekong River, is now a significant component of the global whitefish supply due to its ease

of production (Griffiths *et al*., 2010) and increased consumer popularity (Mendoza-Franco *et al*., 2018); however, it is considered an exotic species, and its introduction into new habitats may endanger local fish populations. Its parasites have also been found in places where it has been introduced, including Poland (Wiecaszek *et al*., 2009) and India (Chaudhary *et al*., 2014). Striped catfish were first introduced in Mexico for ornamental aquaria, and their culture is a source of concern for fish farmers because no study has been conducted on the environmental impact of their introduction and that of their parasites into local wild habitats (Mendoza-Franco *et al*., 2018). Many striped catfish found in the wild are escapees from ornamental ponds, fish farms, or aquarium fish waste dumps (Garcia *et al*., 2018).

Intensive channel catfish production in Tamaulipas, Mexico, is primarily done in cage culture systems (Lara-Rivera *et al*., 2015), where *L. floridanus* is prevalent (>85 %). This is problematic (Rábago-Castro *et al*., 2011), as the chronic parasite's damage to the gill lamellae reduces the mean weight of channel catfish. Many monogeneans have been described for the Pangasiidae family in Southeast Asia (Pariselle *et al*., 2003) and India (Tripathi *et al*., 2014), and monogenean transfaunation, i.e., the exchange of fauna from an introduced species to a native one and vice versa, has been reported in Mexico between cichlids (Jiménez-García *et al*., 2001), and even between different families in Cameroon (Bahanak *et al*., 2022). However, while *L. floridanus* is common in channel catfish, its infectivity in hybrid or the non-local striped catfish is unknown. Thus, the goal of this study was to compare the susceptibility of two local catfish species (channel catfish, hybrid catfish) and a non-local catfish species (striped catfish) to experimental infection with *L. floridanus* under identical laboratory conditions.

MATERIALS AND METHODS

The experimental animals were cared for and used in accordance with the local Bioethics Committee of the Faculty of Veterinary Medicine of the Autonomous University of Tamaulipas. Seventy-five healthy fingerlings of each catfish species (channel, hybrid, and striped) were obtained and transported to the Aquaculture Laboratory at the Autonomous University of Tamaulipas (Ciudad Victoria, Mexico). Channel catfish were obtained from a local hatchery in Soto La Marina, Mexico; hybrid catfish were produced at the Technological University of the Sea of Tamaulipas Bicentennial (Soto La Marina, Mexico); and striped catfish were obtained from a pet store ("Acuario fish club," Guadalajara, Mexico). Fish were examined for the presence of parasites (Hoffman, 1999) before being randomly assigned to nine 40 L aquaria (n = 25 per aquarium), forming three groups based on the fish species, with three replicates each.

All fish were acclimated for two weeks and grown for 16 additional weeks to increase their size and weight before the experiment. They were fed a commercial 32 % protein feed (Purina®, Mexico) *ad libitum* until satiation without waste twice a day, six days a week. The water temperature was kept constant at 25.17±1.93 °C, the pH was 7.15±0.21, and the dissolved oxygen averaged 4.05±0.38 mg L^{-1}, as measured with a freshwater

kit (La Motte®, Charlestown, MD, USA). Subsequently, all fish were anesthetized, weighed, and measured before the infection trial. The mean ± standard deviation (SD) weight and fork length of the catfish (CF) were as follows: channel CF (40.97 ± 5.83 g, 15.02 ± 0.55 cm), hybrid CF (8.90 ± 2.79 g, 8.90 ± 0.91 cm), and stripped CF (28.18 ± 4.47 g, 13.32 ± 0.51 cm).

In preparation for the experimental fish infection with *L. floridanus*, each 40 L aquarium was fitted with a mesh (0.5 cm^2) to create two compartments. Channel catfish infected with *L. floridanus* were obtained from a local farm (Abasolo, Tamaulipas, Mexico). Parasites on the infected fish were identified as *L. floridanus*, according to Hoffman (1999). Co-habitation was used to achieve monogenean infection (del Rio-Zaragoza *et al*., 2011), with four channel catfish naturally infected with *L. floridanus* placed on one side of the mesh-divided aquarium and healthy fish on the other. Infected fish had an initial mean infection of 11.67±8.69 parasites per gill arch and had no direct physical contact with the uninfected fish during the 14-day co-habitation.

The presence of parasites on healthy fish was monitored by sampling three fish from each aquarium every 48 h for a total of nine fish from each group during the 14-day co-habitation period. After euthanasia with an overdose (120 mg L^{-1}) of benzocaine and excision of the four left gill arches from each fish, parasite infection in the three groups was determined. Parasites were counted under a stereomicroscope with the gills placed in Petri dishes containing 0.65 % saline solution, and identification was confirmed. According to Bush *et al*. (1997) and Mladineo (2005), the mean parasite number per gill arch was determined, as well as the prevalence and mean intensity of *L. floridanus* (immature and adults).

Prevalence was assessed with the formula:

$$\text{Prev} = \frac{\text{Number of IF}}{\text{Number of EF}} \times 100$$

where Prev = prevalence; IF = infected fish; and EF = examined fish (infected and uninfected).

Mean abundance was calculated as:

$$\text{MA} = \frac{\text{Number of parasites found in EF}}{\text{Number of EF}} \times 100$$

where MA = Mean bbundance; and EF = Examined fish (infected and uninfected).

Mean Intensity was measured with the following formula:

$$\text{MI} = \frac{\text{Number of parasites found in EF}}{\text{Number of EF}}$$

where MI = Mean intensity; EF = Examined fish (infected and uninfected); and IF= Infected fish.

Mean abundance and mean intensity of parasites were standardized per unit of body weight. The commercial software Statistica® was used to statistically process all of the data (StatSoft Inc., Tulsa, OK, USA). To meet ANOVA assumptions, data were transformed to the fourth root function when necessary for the normality test (Kolmogorov-Smirnov) and variance homogeneity test (Bartlett) (Zar, 1999). With the data obtained, a one-way ANOVA was performed, followed by a Tukey honestly significant difference post hoc test. Additionally, to determine if there was an association between the mortality (proportion of live and dead fish) and the host type (i.e., ictalurid species), a chi-square analysis of a 2 x 3 contingency table was carried out. A significance level (α) of 0.05 was utilized in all statistical tests.

RESULTS AND DISCUSSION

Ligictaluridus floridanus was detected in both channel catfish and hybrid catfish from day 2 post-cohabitation. In striped catfish, *L. floridanus* was detected only once in two fish on day 8 post-cohabitation, similar to *Enterogyrus malmbergi*, a parasite of African cichlids reported in a native Mexican cichlid (Jiménez-García *et al*., 2021). Mortality rates for striped, channel, and hybrid catfish were 1.33, 7.11, and 10.66 %, respectively (Table 1). However, no significant association ($p > 0.05$) was found between fish mortality and the host type (i.e., ictalurid species).

The mean abundance of *L. floridanus* in channel catfish fluctuated throughout the experiment, ranging from 1.4 ± 0.41 to 2.8 ± 0.91 per g of fish body weight (fbw). In hybrid catfish, the abundance started low but increased at each sampling point, peaking at 10.19 ± 7.66 per g fbw on the last day. In striped catfish, mean parasite abundance was zero on all days except day 8, where it was 0.01 ± 0.02 per g fbw (Table 1). The mean abundance of parasites in striped catfish was significantly lower than in channel catfish and hybrid catfish, with no significant differences detected between the latter two species. This outcome was consistently observed throughout the experiment (from days 2 to 14 of the trial).

When analyzing the mean intensity of parasites, the channel catfish showed the highest mean intensity by day 2 (2.8 ± 0.91 per g fbw), while hybrid catfish had similar values to channel catfish during the first four days, increasing to 10.19 ± 7.66 per g fbw by day 14. However, no significant differences were observed throughout the experiment ($p > 0.05$). The striped catfish was excluded from this analysis due to the impossibility of calculating the parasite mean intensity, as the monogenean *L. floridanus* only infected a single fish throughout the experiment (particularly on day 8) (Table 1).

The preference of *L. floridanus* for channel catfish has been observed (Rábago-Castro *et al*., 2014), as most monogeneans are strict host-specific parasites (Bahanak *et al*., 2022). The observed infection rate appears to confirm the parasite's preference for channel

Table I. Average number of parasites per gill arch, prevalence, mean abundance, and mean intensity (± standard deviation) of *Ligictaluridus floridanus* during the infection trial in channel catfish (*Ictalurus punctatus*), hybrid catfish (*I. punctatus* x *I. furcatus*), and stripped catfish (*Pangasianodon hypophthalmus*) at different sampling days.

Parameter	Day 0	Day 2	Day 4	Day 6	Day 8	Day 10	Day 12	Day 14
Channel catfish								
Parasites per gill arch	0	13.89 ±2.83	13.64 ±2.56	11.69 ±5.88	7.49 ±0.99	10.61 ±6.38	7.17 ±2.09	13.47 ±9.00
Prevalence	0 %	100 %	100 %	100 %	100 %	100 %	100 %	100 %
Mean abundance per g fbw	0	2.80 ±0.91	2.73 ±0.84	2.27 ±1.43	1.58 ±0.32	2.02 ±1.16	1.40 ±0.41	2.52 ±1.33
Mean intensity per g fbw	N/A	2.80 ±0.91	2.73 ±0.84	2.27 ±1.43	1.58 ±0.32	2.02 ±1.16	1.40 ±0.41	2.52 ±1.33
Hybrid catfish								
Parasites per gill arch	0	2.08 ±1.42	3.25 ±1.24	4.47 ±1.25	5.39 ±3.86	4.86 ±0.74	6.97 ±5.29	9.56 ±3.88
Prevalence	0 %	89 %	100 %	100 %	100 %	100 %	100 %	100 %
Mean abundance per g fbw	0	2.31 ±2.28	2.95 ±0.64	4.07 ±0.36	6.19 ±6.45	4.53 ±0.91	8.07 ±8.80	10.19 ±7.66
Mean intensity per g fbw	N/A	2.40 ±2.18	2.95 ±0.64	4.07 ±0.36	6.19 ±6.45	4.53 ±0.91	8.07 ±8.80	10.19 ±7.66
Stripped catfish								
Parasites per gill arch	0	0	0	0	0.06 ±0.10	0	0	0
Prevalence	0 %	0 %	0 %	0 %	22 %	0 %	0 %	0 %
Mean abundance per g fbw	0	0	0	0	0.01 ±0.02	0	0	0
Mean intensity per g fbw	N/A	N/A	N/A	N/A	N/A	N/A	N/A	N/A

N/A: not available because the denominator in the mean intensity formula (i.e., infected fish) is zero in some cases. The mean abundance and intensity of *L. floridanus* are reported per g of fish body weight (g fbw).

catfish, as well as the fact that hybrid catfish are equally susceptible to infection with this parasite, whereas striped catfish appear to be immune to persistent infection.

Translocation of fish and their parasites from their original biotope may endanger natural fish populations in importing countries, with disastrous consequences for native communities (Tompkins *et al*., 2011). Transfaunation of parasites can occur from introduced to native species (Jiménez-García *et al*., 2001). Monogenea are considered least probable species switchers, although some transfers between clariid and non-clariid fish have been reported in Cameroon (Bahanak *et al*., 2022), while other transfers from African to American cichlids (and viceversa) have been reported in Mexico (Jiménez-García *et al*., 2001). Although new Monogenea species have been reported from Pangasiidae (Pariselle *et al*., 2001), as observed in this study, striped catfish does not appear susceptible to a sustained infection by *L. floridanus*, suggesting the non-transfaunation of this parasite from channel catfish to striped catfish. However, further studies are recommended.

CONCLUSIONS

The degree of infection among channel catfish, hybrid catfish, and striped catfish after experimental infection with *Ligictaluridus floridanus* varied greatly. The most susceptible

species is channel catfish, with a prevalence of infection of 100 % with medium to high intensity; in hybrid catfish, *L. floridanus* took slightly longer to reach 100 % prevalence, but once reached, it never decreased, exhibiting the highest abundance and mean intensity of parasites from six days after infection onwards. Striped catfish was the least susceptible to a sustained infection, and although *L. floridanus* was detected one time, had an infection prevalence of zero for the majority of the trial, and does not seem susceptible to long-term infection with *L. floridanus*.

ACKNOWLEDGEMENTS

The scholarship to J. A. de la Cruz-Cervantes was provided by Mexico's National Council of Science and Technology (CONACYT).

REFERENCES

Argue BJ, Kuhlers DL, Liu Z, Dunham RA. 2014. Growth of channel catfish (*Ictalurus punctatus*), blue catfish (*I. furcatus*), and their F1, F2, F3, and F1 reciprocal backcross hybrids in earthen ponds. Journal of Animal Science 92 (10): 4297–4305. https://doi.org/10.2527/jas.2013-7549

Bahanak DN, Mbondo JA, Bassock Bayiha ED, Pariselle A, Nack J, Bilong Bilong CF, Agnèse JF. 2022. Description of a new species from *Clarias maclareni* and phylogenetical analysis of *Quadriacanthus* (Monogenea, Dactylogyridae) species transfers between clariid and non-clariid fish hosts in Cameroon. Parasite 29 (37): 2022035. https://doi.org/10.1051/parasite/2022035

Bush AO, Lafferty KD, Lotz, JM, Shostak AW. 1997. Parasitology meets ecology on its own terms: Margolis *et al*. revisited. Journal of Parasitology 83 (4): 575–583. https://doi.org/10.2307/3284227

Chaudhary A, Verma C, Varma M, Singh H. 2014. Identification of *Thaparocleidus caecus* (Mizelle & Kritsky, 1969) (Monogenea: Dactylogyridae) using morphological and molecular tools: A parasite invasion in indian freshwater. BioInvasions Records 3 (3): 195–200. https://doi.org/10.3391/bir.2014.3.3.10

del Rio-Zaragoza OB, Fajer-Ávila EJ, Almazán-Rueda P. 2011. Influence of β-glucan on innate immunity and resistance of *Lutjanus guttatus* to an experimental infection of dactylogyrid monogeneans. Parasite Immunology 33 (9): 483–494. https://doi.org/10.1111/j.1365-3024.2011.01309.x

Garcia DAZ, Magalhães ALB, Vitule JRS, Casimiro ACR, Lima-Junior DP, Cunico AM, Brito MFG, Petrere-Junior M, Agostinho ÂA, Orsi ML. 2018. The same old mistakes in aquaculture: The newly-available striped catfish *Pangasianodon hypophthalmus* is on its way to putting Brazilian freshwater ecosystems at risk. Biodiversity and Conservation 27 (13): 2545–3558. https://doi.org/10.1007/s10531-018-1603-1

Griffiths D, Van Khanh P, Trong TQ. 2010. *Pangasianodon hypophthalmus* (Sauvage, 1878) [Pangasiidae]. Cultured aquatic species information program. United Nations Food and Agriculture Organization. Rome, Italy. 8 p.

Hoffman GL. 1999. Parasites of North American freshwater fishes. Cornell University Press: Ithaca, NY, USA. 539 p.

Jiménez-García MI, Vidal-Martínez VM, López-Jiménez S. 2001. Monogeneans in introduced and native cichlids in Mexico: Evidence for transfer. Journal of Parasitology 87 (4): 907–909. https://doi.org/10.1645/0022-3395(2001)087[0907:miianc]2.0.co;2

Lara-Rivera AL, Parra-Bracamonte GM, Sifuentes-Rincón AM, Gojón-Báez HH, Rodríguez-González H, Montelongo-Alfaro IO. 2015. El bagre de canal (*Ictalurus punctatus* Rafinesque, 1818): estado actual y problemática en México. Latin American Journal of Aquatic Research 43 (3): 424–434. https://doi.org/10.3856/vol43-issue3-fulltext-4

Mendoza-Franco EF, Caspeta-Mandujano JM, Osorio MT. 2018. Ecto-and endo-parasitic monogeneans (Platyhelminthes) on cultured freshwater exotic fish species in the state of Morelos, South-central Mexico. ZooKeys 776: 1–12. https://doi.org/10.3897/zookeys.776.26149

Mladineo I. 2005. Parasite communities of Adriatic cage-reared fish. Diseases of Aquatic Organisms 64 (1): 77–83. https://doi.org/10.3354/dao064077

Pariselle A, Lim LHS, Lambert A. 2003. Monogeneans from Pangasiidae (Siluriformes) in Southeast Asia: V. Five new species of *Thaparocleidus* Jain, 1952 (Ancylodiscoididae) from *Pangasius nasutus*. Parasite 10 (4): 317–323. https://doi.org/10.1051/parasite/2003104317

Rábago-Castro J, Sánchez-Martínez JG, Loredo-Osti J, Gomez-Flores R, Tamez-Guerra P, Ramírez-Pfeiffer C. 2011. Temporal and spatial variations of ectoparasites on cage-reared channel catfish, *Ictalurus punctatus*, in Tamaulipas, Mexico. Journal of the World Aquaculture Society 42 (3): 406–411. https://doi.org/10.1111/j.1749-7345.2011.00480.x

Rábago-Castro JL, Sánchez-Martínez JG, Pérez-Castañeda R, Vázquez-Sauceda ML, Ruiz-Orozco G. 2014. Chronic effects of a monogenean *Ligictaluridus floridanus* (Ancyrocephalidae) infection on channel catfish (*Ictalurus punctatus*) growth performance. Acta Veterinaria Brno 83 (2): 83–87. https://doi.org/10.2754/avb201483020083

Tompkins DM, Dunn AM, Smith MJ, Telfer S. 2011. Wildlife diseases: From individuals to ecosystems. Journal of Animal Ecology 80 (1): 19–38. https://doi.org/10.1111/j.1365-2656.2010.01742.x

Tripathi A, Rajvanshi S, Agrawal N. 2014. Monogenoidea on exotic Indian freshwater fishes. 2. Range expansion of *Thaparocleidus caecus* and *T. siamensis* (Dactylogyridae) by introduction of striped catfish *Pangasianodon hypophthalmus* (Pangasiidae). Helminthologia 51 (1): 23–30. https://doi.org/10.2478/s11687-014-0204-0

Wiecaszek B, Keszka S, Sobecka E, Boeger WA. 2009. Asian pangasiids-An emerging problem for European inland waters? Systematic and parasitological aspects. Acta Ichthyologica et Piscatoria 39 (2): 131–138. https://doi.org/10.3750/AIP2009.39.2.08

Zar JH. 1999. Biostatistical analysis. Prentice-Hall: Upper Saddle River, NJ, USA. 663 p.

Agrociencia

EFFECT OF PARTIALLY REPLACING SOYBEAN MEAL AND SOYBEAN OIL WITH DEHULLED SUNFLOWER SEEDS ON MEAT QUALITY AND OXIDATIVE STABILITY OF BROILERS

Ana Estela **Arcos-Hernández**[1], Arturo **Pro-Martínez**[1], Omar **Hernández-Mendo**[1*], Jaime **Gallegos-Sánchez**[1], Francisco Javier **Lazo-Bustamante**[1]

[1]Colegio de Postgraduados Campus Montecillo. Departamento de Ganadería. Carretera Mexico-Texcoco km 36.5, Montecillo, Texcoco, State of Mexico, Mexico. C.P. 56264.
* Author for correspondence: ohmendo@colpos.mx

Citation: Arcos-Hernández AE, Pro-Martínez A, Hernández-Mendo O, Gallegos-Sánchez J, Lazo-Bustamante FJ. 2024. Effect of partially replacing soybean meal and soybean oil with dehulled sunflower seeds on meat quality and oxidative stability of broilers. **Agrociencia** 58(7): 838-852. https://doi.org/ 10.47163/agrociencia.v58i7.3216

Editor in Chief:
Dr. Fernando C. Gómez Merino

Received: February 18, 2023.
Approved: October 28, 2024.
Published in Agrociencia: November 04, 2024.

ABSTRACT

Broiler chicken (*Gallus gallus domesticus* L.) production in Mexico is fundamental for contributing to food security since it is inexpensive and has a high nutritional value. However, given the insufficient national production of ingredients such as soybeans to obtain oil and make balanced foods, it has been necessary to import them, thus increasing the cost of raising broilers. In this context, sunflower seed (*Helianthus annuus* L.), due to its nutritional makeup, can be used to replace soybean meal and soybean oil in broiler diets. The purpose of this study was to evaluate the effect of partially replacing soybean meal and soybean oil in broilers' diets with dehulled sunflower seeds on the physicochemical properties, fatty acid profile, and antioxidant capacity of meat. The experimental design was completely randomized: basal diet (sorghum-soybean meal); diet with 5 % sunflower seed and soybean oil; diet with 5 % sunflower seeds without soybean oil; and diet with 10 % sunflower seeds without soybean oil. There was no effect of the diet on the physicochemical characteristics ($p > 0.05$), but there was an effect on the fatty acid profile, which was better ($p \leq 0.001$) in the treatments with sunflower seed, with or without soybean oil. The antioxidant activity in raw and cooked meat decreased after 9 and 6 days of refrigerated storage ($p \leq 0.05$), respectively, without diet effect. Therefore, soybean meal can be substituted at 10 %, and soybean oil can be partially or completely replaced by dehulled sunflower seed in broiler diets as long as production parameters are not negatively affected.

Keywords: Carcass quality, chicken, fatty acid profile, nutrition, rancidity, shelf life.

INTRODUCTION

Broiler chicken (*Gallus gallus domesticus* L.) production in Mexico is fundamental for contributing to food security since it is the cheapest meat and has a high nutritional value. However, the insufficient national production of ingredients has made it necessary to import soybeans for oil and feed production, increasing the cost of raising broilers. In this context, sunflower seeds (*Helianthus annuus* L.), given their nutritional composition, represent an alternative to substitute soybean meal and soybean oil in

broiler diets (Karkelanov *et al*., 2020). Sunflower is grown in Mexico, and the amount imported is smaller than soybean (Bye *et al*., 2009).

Research on the use of sunflower seeds and sunflower meal on broiler performance has shown positive results (Ciurescu *et al*., 2019; Sosa-Montes *et al*., 2021). Moreover, given that sunflower seeds have a high amount of polyunsaturated fatty acids (PUFA), their effect on the metabolism of broilers has been examined, concluding that it can decrease the ratio of saturated fatty acids in abdominal fat as well as breast and thigh meat (Kalakuntla *et al*., 2017) while increasing PUFA contents (Mahfoudh *et al*., 2016). The high fiber content of sunflower seeds is a disadvantage; therefore, it is recommended not to use in a proportion higher than 25 % (Sosa-Montes *et al*., 2021). Alternatively, dehulling the seed can improve its digestibility (Karkelanov *et al*., 2020). A 15 % inclusion level of sunflower meal in broiler diets has been proposed with no any negative effects on performance, or even higher levels with the addition of enzymes, which can improve body weight gain of broilers raised up to 35 days of age (Mbukwane *et al*., 2022).

This work hypothesized that using dehulled sunflower seeds can enhance the fatty acid profile in broiler meat. Nevertheless, it could potentially reduce chicken meat production, especially when considering the added value of the meat. Its shelf life could be negatively affected since polyunsaturated fatty acids are highly susceptible to oxidation, requiring the addition of antioxidants. Based on these facts, the present study evaluated the effect of partially replacing soybean meal and soybean oil by dehulled sunflower seeds on the physicochemical characteristics, fatty acid profile, and antioxidant activity of broiler breast meat.

MATERIALS AND METHODS

Study site

The study was conducted at the Poultry Research Unit of the Experimental Farm of the Colegio de Postgraduados, Montecillo Campus, located in Texcoco, State of Mexico, Mexico (19.3° N, 98.53° W, at an altitude of 2250 m), under the international, national, and institutional guidelines for the care and use of animals according to NOM-033-ZOO-1995 (DOF, 1995) (human slaughter of domestic and wild animals) and approved by the Animal Welfare Committee of the Colegio de Postgraduados (02.11.16).

Animals, treatments, and feeding

A total of 200 eighty-one-day-old broilers (Ross 308®) were used, which were distributed into 28 experimental units of 10 broilers each and fattened for 49 days. Four treatments were randomly assigned to the 28 experimental units, with seven replicates per treatment. The treatments were: DBSS, basal diet based on sorghum-soybean meal; D5SO, diet with 5 % dehulled sunflower seeds + soybean oil + soybean meal; D10WO, diet with 10 % dehulled sunflower seeds without soybean oil + soybean meal; and

D5WO, diet with 5 % dehulled sunflower seeds without soybean oil + soybean meal. The sunflower seeds were dehulled to improve their digestibility and were added to the diet to replace soybean meal and soybean oil, according to the experimental treatments. All diets had isoproteic and isoenergetic contents. The ingredient and chemical composition of the diets and dehulled sunflower seeds are shown (Tables 1 and 2). The broilers had *ad libitum* access to feed and water.

Sampling

Fourteen broilers were randomly selected from each treatment (n = 56) and slaughtered at 49 days of age. Breast meat samples (*Pectoralis major*) were collected and stored in hermetically sealed polyethylene bags at -10 °C for laboratory analysis 48 hours after slaughtering.

Table 1. Ingredient composition of the experimental diets.

Item	DBSS	D5SO	D10WO	D5WO
	Starter diet (0–21 days)			
Sorghum	53.09	53.88	54.53	56.72
Soybean meal	37.06	33.61	30.26	33.12
DSS	0.00	5.00	10.00	5.00
Dicalcium phosphate	2.08	2.05	2.03	2.04
Calcium carbonate	1.18	1.17	1.19	1.21
Biolys®	0.59	0.67	0.76	0.69
Methionine	0.45	0.45	0.44	0.44
Threonine	0.18	0.19	0.20	0.19
Salt (NaCl)	0.30	0.30	0.30	0.30
Vitamin/mineral premix	0.30	0.30	0.30	0.30
Oil	4.79	2.38	0.00	0.00
	Finishing diet (22–49 days)			
Sorghum	60.62	61.64	62.36	64.5
Soybean meal	30.13	26.64	23.20	26.14
DSS	0.00	5.00	10.00	5.00
Dicalcium phosphate	0.94	0.93	0.98	0.97
Calcium carbonate	1.58	1.56	1.54	1.55
Biolys®	0.37	0.46	0.55	0.47
Methionine	0.34	0.33	0.32	0.33
Threonine	0.08	0.09	0.11	0.09
Salt (NaCl)	0.30	0.30	0.30	0.30
Vitamin/mineral premix	0.30	0.30	0.30	0.30
Oil	5.00	2.41	0.00	0.00
Coccidiostat	0.05	0.05	0.05	0.05
Pigment	0.30	0.30	0.30	0.30

DBSS: basal diet based on sorghum-soybean meal; D5SO: diet with 5 % dehulled sunflower seeds + soybean oil; D10WO: diet with 10 % dehulled sunflower seeds without soybean oil; D5WO: diet with 5 % dehulled sunflower seeds without soybean oil; DSS: dehulled sunflower seeds.

Table 2. Chemical composition of the experimental diets and dehulled sunflower seeds.

Item	DBSS	D5SO	D10WO	D5WO	DSS
Dry matter (%)	93.44	93.06	93.45	93.51	97.69
Metabolizable energy (kcal kg^{-1})†	3149	3148	3158	3019	4250
Crude protein (%)	21.68	21.69	21.70	21.69	28.34†
Ether extract (%)	5.96	4.46	6.30	3.67	48.72
Ash (%)	5.71	5.33	6.01	5.82	4.69
NDF (%)	14.72	15.99	16.64	15.79	34.03
ADF (%)	14.39	15.28	16.32	15.60	29.09
Fatty acid profile (g 100 g^{-1} fatty acids)					
Caproic acid (C6:0)	8.72	0.59	0.37	NI	NI
Tridecanoic acid (C13:0)	5.32	NI	NI	NI	NI
Palmitic acid (C16:0)	11.40	11.27	13.86	7.61	5.83
Stearic acid (C18:0)	2.60	3.55	2.52	3.71	6.88
Oleic acid (C18:1n9)	22.13	26.72	27.58	21.04	21.52
Linoleic acid (C18:2n6)	45.62	56.86	52.03	51.14	63.90
Arachidonic acid (C20:4n6)	NI	NI	NI	NI	0.42
Linolenic acid (C18:3n3)	NI	0.81	3.62	NI	NI
Eicosenoic acid (C20:1n9)	NI	NI	NI	16.48	NI
DGLA (20:3n6)	4.17	NI	NI	NI	NI
Behenic acid (C22:0)	NI	NI	NI	NI	0.98
Lignoceric acid (C24:0)	NI	NI	NI	NI	0.26
∑SFA	28.07	15.44	16.75	11.32	13.97
∑MUFA	22.13	26.77	27.58	27.52	21.56
∑PUFA	49.79	57.78	55.65	51.14	64.45
∑n-3	NI	0.81	3.62	NI	NI
∑n-6	49.79	56.97	52.03	51.14	64.45
Antioxidant activity (mmol TroloxEq kg^{-1} sample)	15.24	13.93	23.07	21.20	9.45¶

DBSS: basal diet based on sorghum-soybean meal; D5SO: diet with 5 % dehulled sunflower seeds + soybean oil; D10WO: diet with 10 % dehulled sunflower seeds without soybean oil; D5WO: diet with 5 % dehulled sunflower seeds without soybean oil; DSS: dehulled sunflower seeds; NDF: neutral detergent fiber; ADF: acid detergent fiber; NI: not identified; DGLA: dihomo-gamma linolenic acid; SFA: saturated fatty acids; MUFA: monounsaturated fatty acids; PUFA: polyunsaturated fatty acids; n-3: omega 3 acids; n-6: omega 6 acids. †Datum provided by EVONIK (Evonik Industries de México, S.A. de C.V.). ¶Seeds treated with BHA (butylated hydroxyanisole) and BHT (butylated hydroxytoluene) at a ratio of 1 g kg^{-1} sunflower seeds.

pH and color

The pH of the breast meat was measured 30 min after bleeding and 24 h post-mortem by inserting the electrode of a HI 99163 portable potentiometer (HANNA Instruments, Mexico) to a depth of 1 cm in the muscle. Immediately after, the color was measured in the internal part of the breasts using a Konica-Minolta colorimeter (CR-410 Sensing Inc.,

Tokyo, Japan). The results were reported using the color system of the International Commission on Illumination (CIE) for the trichromatic coordinates: lightness (L*), red index (a*), and yellow index (b*).

Texture

The texture of raw and cooked breast meat was measured through shear force using a Warner-Bratzler blade and the TA-XT2i stable texture analyzer (Microsystems, Godalming, England) (Honikel, 1998). To do this, 10 rectangular prisms were cut (4 x 2 x 0.7 cm) parallel to the muscle fibers in each breast sample at an average temperature of 5 °C. Five of these prisms were kept raw, and the others were cooked in water at 75 °C for 30 min. The meat samples were refrigerated at 4 °C until analysis. The evaluation conditions were: pre-essay speed of 4 mm s^{-1}, essay speed of 1 mm s^{-1}, post-essay speed of 5 mm s^{-1}, and 30 mm of distance. The shear force was expressed in newtons (N).

Water holding capacity

Five grams of finely chopped meat with 8 mL of sodium chloride solution 0.6 M were placed in ice for 30 min and centrifuged (Beckman Coulter J2-HS, CA, USA) (Honikel, 1998) for 15 min at 10 000 rpm. The released water was poured out and its volume was measured, and the difference was reported in millimeters of NaCl (0.6 M) solution retained per 100 g of meat.

Proximal analysis

The proximal and cellulosic fractions of the dehulled sunflower seeds and diets (Table 2) were determined according to the Association of Official Analytical Chemists (AOAC, 2003) and van Soest *et al*. (1991) methodologies. The contents of protein, fat, moisture, and collagen of each breast sample were determined using the FoodScanTM (FOSS, MN, USA) near infrared (NIR) spectrophotometer (Analytical AB, Sweden), according to the Official Method 2007.04 (AOAC, 2003). To do so, 200 g of meat were ground and homogenized in a food processor for 30 s, so the fat, connective tissue, and muscle fibers were distributed uniformly. The ground meat sample was placed in the glass cup inside the support of the instrument, and three readings were taken per sample.

Fatty acid profile

To measure the fatty acid profile of the lyophilized samples (Labconco Free Zone 6, Kansas City, KS, USA), the methylation technique proposed by Palmquist and Jenkins (2003) was used, where the fatty acids are shown as methyl esters. The fatty acids were determined with a gas chromatograph (Hewlett-Packard 6890, USA) with automatic injector and capillary column (100 m x 0.25 mm x 0.20 μm width, Sp-2560, Supelco). To identify the fatty acids, the standard retention times were compared (Supelco 37 FAME Components) against those of the samples. The results were expressed in g of fatty acids contained in 100 g of fatty acids.

Antioxidant activity

The antioxidant activity of the raw and cooked broiler breast meat was determined using the conventional 2,2-diphenyl-1-picrylhydrazyl (DPPH) method described by Brand-Williams *et al*. (1995). This was evaluated at 0, 3, 6, and 9 days of refrigeration storage. All the samples were kept at 4 °C in hermetically sealed polyethylene bags. The amount of DPPH (Sigma Aldrich, USA) was determined using a visible UV light spectrophotometer (Cary 1-E Varian, USA) at 517 nm. To determine the antioxidant activity or free radical scavenging, a standard curve was used (absorbance reduction vs. Trolox concentration). Trolox ((S)-(−)-6-hydroxy-2,5,7,8-tetramethylchroman-2-carboxylic, Sigma Aldrich, USA) reacts with DPPH, a stable free radical. The results were expressed as mmol of TroloxEq kg^{-1} meat sample. The higher the TroloxEq, the higher the antioxidant activity of the sample (Normah and Hanapi, 2019).

Statistical analysis

The data were analyzed through analysis of variance (ANOVA) under a completely randomized experimental design. The Tukey test for mean comparison was performed at a $p \leq 0.05$ significance level. The data of the antioxidant activity were analyzed through the PROC MIXED procedure in SAS 9.4 (SAS Institute). The Schwarz and Akaike Bayesian information criteria were obtained to determine the most appropriate covariance structure for each variable. The variance components procedure was used for the repeated measures design.

RESULTS AND DISCUSION

Physicochemical characteristics of the meat

The physicochemical characteristics of the breast meat samples were not significantly altered ($p > 0.05$) by the treatments (Table 3 and 4).

Although there was no effect of the treatments on the physicochemical characteristics of the meat, according to Cavitt *et al*. (2005), the texture of both raw and cooked meat in this study (19.6 and 26.6 N, respectively) is classified as extremely soft. In their study, these authors found an increase in broiler meat tenderness as post-mortem hours increased, from 0.25 to 24 h, with values from 78.9 to 35.9 N, classifying them as slightly tough to moderately tough. Those values are highly related to the ease of chewing and palatability (Jiang *et al*., 2018).

Color, whose mean L* and a* values were 45.5 and 5.94, respectively, correspond to dark meat according to the classification by Soares *et al*. (2009) and Oda *et al*. (2009), which might be influenced by the composition of the diet (Wideman *et al*., 2016), particularly by the contents of flavonoids, tocopherols, carotenoids, and chlorogenic acid that sunflower seeds contain (Velasco and Ruiz-Mendez, 2015; Pajak *et al*., 2014). Wildermuth *et al*. (2016) point out that chlorogenic acid reacts oxidatively with proteins, forming greenish colorations that affect the color of meat, although the present study did not support this idea.

Table 3. Physical characteristics of breast meat of broilers (*Gallus gallus domesticus* L.) fed with or without dehulled sunflower seeds in their diet.

Attribute	Treatments				SEM	*p*
	DBSS	D5SO	D10WO	D5WO		
Shear force cooked meat (N)	27.07	27.66	28.15	23.54	0.163	0.079
Shear force raw meat (N)	19.81	21.48	19.12	18.05	0.384	0.210
Lightness L^* value	45.17	44.57	45.88	46.38	7.296	0.317
Color a^* value	6.09	5.97	5.67	6.04	1.526	0.817
Color b^* value	19.70	18.41	18.33	18.10	3.740	0.169
pH (30 min post-mortem)	6.26	6.28	6.17	6.23	0.030	0.404
pH (24 h post-mortem)	5.26	5.17	5.25	5.46	0.080	0.140
WHC (%)	25.10	31.65	30.19	32.46	1.161	0.323

DBSS: basal diet based on sorghum-soybean meal; D5SO: diet with 5 % dehulled sunflower seeds + soybean oil; D10WO: diet with 10 % dehulled sunflower seeds without soybean oil; D5WO: diet with 5 % dehulled sunflower seeds without soybean oil; SEM: standard error of the mean; WHC: water holding capacity; L^*: lightness; a^*: red index; b^*: yellow index ($p \leq 0.01$). All attributes, except shear force, were measured in raw meat.

Table 4. Chemical composition of raw breast meat from broilers (*Gallus gallus domesticus* L.) fed partially with or without dehulled sunflower seeds in their diet.

Fraction (%)	Treatments				SEM	*p*
	DBSS	D5SO	D10WO	D5WO		
Collagen	0.75	0.70	0.71	0.68	0.007	0.229
Protein	23.20	23.35	23.31	22.92	0.772	0.534
Fat	2.00	2.10	2.09	2.00	0.008	0.727
Moisture	74.80	74.88	74.81	74.99	0.625	0.919
Ash[†]	1.19	1.02	1.24	0.96	0.021	0.315

DBSS: basal diet based on sorghum-soybean meal; D5SO: diet with 5 % dehulled sunflower seeds + soybean oil; D10WO: diet with 10 % dehulled sunflower seeds without soybean oil; D5WO: diet with 5 % dehulled sunflower seeds without soybean oil; SEM: standard error of the mean ($p \leq 0.01$). [†]Determined directly according to AOAC (2003). The other fractions were indirectly determined by near infrared (NIR) spectrophotometry, according to AOAC (2003).

The water holding capacity (WHC) values found in this study were lower than those obtained by other authors (Barbin *et al*., 2015; Carvalho *et al*., 2017). This is presumably due to the pH value close to the isoelectric point of meat at 24 h post-mortem, when the WHC was measured. Zhao *et al*. (2017b) reported an isoelectric point of 5.5 for pale soft exudative meat of broilers. This value was very close to the average pH

at 24 h post-mortem (5.29) (Table 3). At that point, the net charge of the protein is zero, meaning that the numbers of positive and negative charges on the proteins are essentially equal. Consequently, there is a reduction in the amount of water that can be attracted and held by those proteins (Ghimire and Parajuli, 2020). All treatments produced very similar pH of the breast meat ($p > 0.05$); however, from 30 min to 24 h post-mortem, these pH values decreased on average from 6.24 to 5.29 ($p \leq 0.05$). To this regard, Veeramuthu and Sams (1999) found that pH values decreased from 6.67 to 5.65 after 24 h postmortem in broiler carcasses.

The fact that the chemical composition of the breast meat samples was not different between treatments could indicate that the experimental broilers have the capacity to regulate their feed intake and therefore the nutrient intake, especially energy, whose levels are equaled when access is *ad libitum* and, consequently, protein and fat deposition in the muscle tend to be similar, independently of the diet. Kalakuntla *et al*. (2017) evaluated diets containing different polyunsaturated fatty acid sources and found no differences in the chemical composition of thighs and breasts. This is concordant with the fact that including dehulled sunflower seeds did not modify the chemical composition of the meat (Table 4).

Fatty acid profile

The fatty acid profile of the breast meat samples was influenced by the experimental diets (Table 5). Treatments D5SO, D10WO, and D5WO showed similar contents of polyunsaturated fatty acids (PUFA) ($p > 0.05$), which were higher than the content of meat samples under the DBSS treatment ($p \leq 0.05$). Contrarily, treatments D5SO, D10WO, and D5WO showed similar contents ($p > 0.05$) of saturated fatty acids (SFA), which were lower than the content of meat samples under the DBSS treatment ($p \leq 0.05$). The first trend with PUFA was also observed with the omega-6 fatty acids and the PUFA:SFA ratio. However, the MUFA content of meat under the D5WO diet was higher than the corresponding content under the other diets.

The addition of 5 and 10 % dehulled sunflower seeds with or without soybean oil caused higher concentrations of polyunsaturated fatty acids, as well as higher omega-3 and omega-6 content and lower levels of saturated fatty acids in the meat than the corresponding values of the DBSS diet. Consequently, these meat samples showed a higher PUFA:SFA ratio. It is important to point out that C18:3n3 is the fatty acid that is most used as an energy source throughout the muscle β-oxidation pathway (Smink *et al*., 2010). The treatments had no effect on the concentrations of C18:0, C20:4n6, C20:2n6, and 20:3n6 fatty acids of the breast meat samples ($p > 0.05$). The C18:2n6 acid was the most abundant under treatments D5SO, D10WO, and D5WO ($p \leq 0.05$), since soybean oil and sunflower oil (Kalakuntla *et al*., 2017) provide high amounts of polyunsaturated fatty acids, mainly C18:2n6 (Table 2).

Very long chain omega-3 fatty acids are a result of the lengthening and desaturation of 18:3n-3 acid, like the correspondent omega-6 fatty acids are formed from 18:2n6 acid. In this study, there was a higher concentration ($p \leq 0.05$) of omega-6 acids than

Table 5. Fatty acid profile of raw breast meat of broilers (*Gallus gallus domesticus* L.) fed partially with or without dehulled sunflower seeds in their diet.

Fatty acid (g 100 g^{-1} fatty acids)	Treatments				SEM	*p*
	DBSS	D5SO	D10WO	D5WO		
Myristic acid (C14:0)	0.53 a	0.45 b	0.43 b	0.44 b	0.003	0.001
Palmitic acid (C16:0)	22.73 a	19.22 b	19.10 b	18.59 b	0.001	0.001
Palmitoleic acid (C16:1n7)	1.90 b	2.62 b	2.53 b	4.32 a	0.689	0.001
Stearic acid (C18:0)	7.17	7.04	7.85	7.54	1.606	0.406
Oleic acid (C18:1n9)	25.35 c	27.68 b	27.71 b	32.25 a	5.84	0.001
Linoleic acid (C18:2n6)	26.00 b	34.56 a	34.77 a	34.83 a	8.30	0.001
α-linolenic acid (C18:3n3)	0.30 c	1.78 a	1.56 a	0.53 b	0.158	0.001
Arachidonic acid (C20:4n6)	2.80	3.27	3.55	2.77	1.791	0.403
Eicosadienoic acid (C20:2n6)	0.60	0.68	0.68	0.50	0.042	0.108
DGLA (20:3n6)	0.52	0.53	0.52	0.60	0.043	0.740
∑SFA	31.56 a	27.38 b	27.53 b	28.22 b	4.540	0.001
∑MUFA	28.44 b	30.92 b	30.85 b	37.33 a	7.510	0.001
∑PUFA	34.01 c	41.68 ab	40.91 b	41.10 ab	6.50	0.001
∑n-3	0.45 b	1.82 a	1.58 a	0.54 b	0.152	0.001
∑n-6	30.55 b	39.86 a	40.33 a	40.55 a	6.30	0.001
PUFA:SFA	0.98 b	1.52 a	1.60 a	1.46 a	0.024	0.001

Means in a row with different letters indicate differences ($p \leq 0.01$). DBSS: basal diet based on sorghum-soybean meal; D5SO: diet with 5 % dehulled sunflower seeds + soybean oil; D10WO: diet with 10 % dehulled sunflower seeds without soybean oil; D5WO: diet with 5 % dehulled sunflower seeds without soybean oil. DGLA: dihomo-gamma linolenic acid; SFA: saturated fatty acids; MUFA: monounsaturated fatty acids; PUFA: polyunsaturated fatty acids; n-3, omega-3 acids; n-6, omega-6 acids; SEM: standard error of the mean.

omega-3 acids in the breast samples under treatments with dehulled sunflower seeds. The deposition and distribution of fatty acids in the meat depend on absorption, *de novo* synthesis, and β-oxidation of fatty acids, processes that in turn depend on the concentrations and types of fatty acids contained in the diet (Villaverde *et al*., 2006). To this regard, Smink *et al*. (2010) found that diets with high concentrations of polyunsaturated fatty acids inhibit lipogenic enzymes (Δ9 desaturase) and decrease the *de novo* synthesis of saturated and monounsaturated fatty acids in chickens.

Additionally, during absorption, there is a greater affinity of fatty acid-linking proteins in intestinal cells for polyunsaturated fatty acids (Ravindran *et al*., 2016). The low percentage of polyunsaturated fatty acids in the breast meat samples of the DBSS treatment could be caused by the reduced concentration of unsaturated fatty acids in the diet. The Δ-5 and Δ-6 desaturase and elongase enzymes break the bonds of saturated fatty acids, insert double bonds, and elongate the chains of C18:2n6 and C18:3n3 acids (Wood and Enser, 2017). The DBSS treatment did not have enough substrate to carry out these functions. The acids C18:3n3 and C18:2n6 compete for the same enzymes and interfere in the elongation and desaturation processes (Betti *et al*.,

2009); at the same time, the β-oxidation pathway decreases their availability (Smink *et al*., 2010).

It is important to point out that the diet of the D5WO treatment had a lower concentration of metabolizable energy compared with the other treatments. According to Villaverde *et al*. (2006), this promotes the synthesis of saturated and monounsaturated fatty acids to maintain an adequate ratio of saturated to unsaturated fatty acids in the cell membranes. As noted above, sunflower seed oil has a high concentration of polyunsaturated fatty acids. This fact was confirmed by Crespo and Esteve-García (2002), who found that the main acids resulting from hepatic lipogenesis are C16:0, C18:0, C18:1n9, and C16:1n7. For this reason, the breast meat samples under the D5WO treatment had a higher amount of monounsaturated fatty acids. Comparing the results of the breast samples under treatment D5SO against DBSO, it is deduced that soybean oil mixed with sunflower seed oil can improve (increase the polyunsaturated acids) of the meat.

Antioxidant activity

The antioxidant activity of the raw or cooked breast meat samples (Figures 1 and 2) was not different between treatments ($p > 0.05$), although it did vary throughout the time ($p \leq 0.01$). The antioxidant activity of meat, measured as the activity of free radical

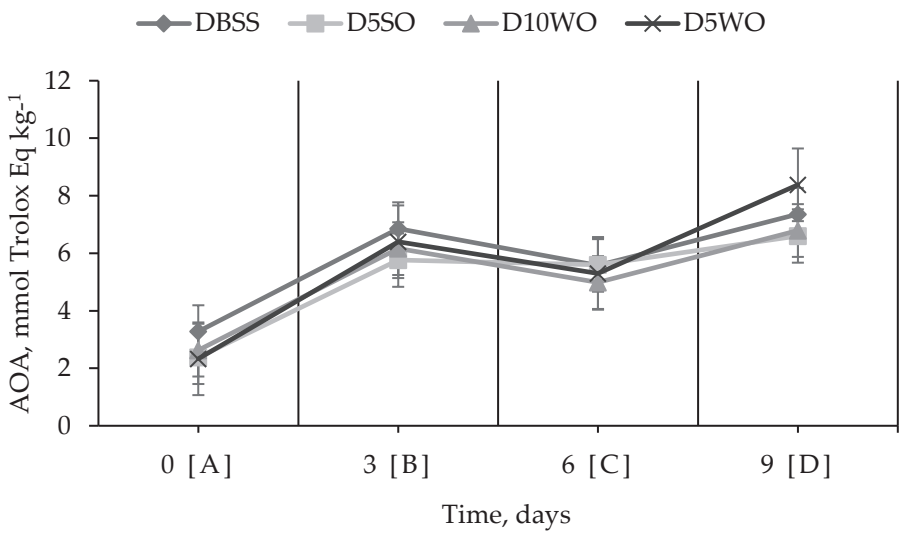

Figure 1. Antioxidant activity of raw breast meat of broilers (*Gallus gallus domesticus* L.) partially fed with dehulled sunflower seeds in the diet. DBSS: basal diet based on sorghum-soybean meal; D5SO: diet with 5 % dehulled sunflower seeds + soybean oil; D10WO: diet with 10 % dehulled sunflower seeds without soybean oil; D5WO: diet with 5 % dehulled sunflower seeds without soybean oil; AOA: antioxidant activity or free radical scavenging as Trolox equivalents. Means with different letters indicate differences ($p \leq 0.01$).

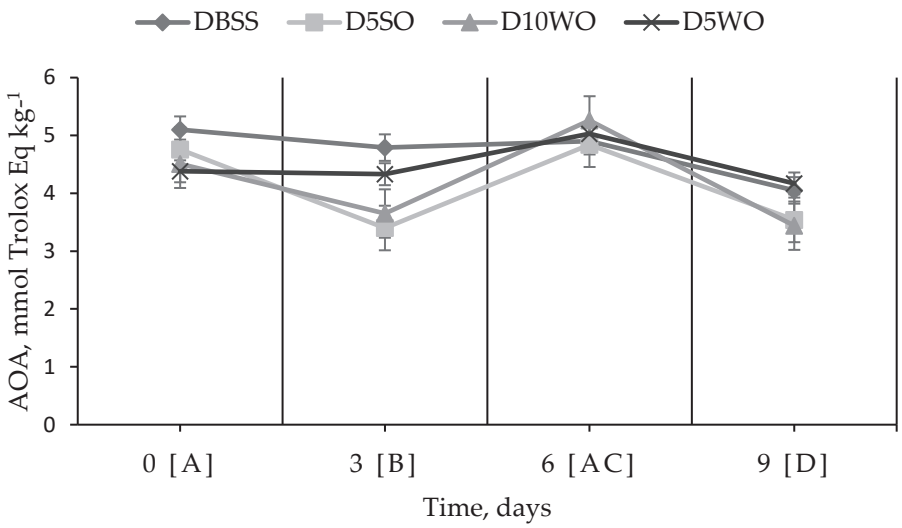

Figure 2. Antioxidant activity of cooked breast meat of broilers (*Gallus gallus domesticus* L.) partially fed with dehulled sunflower seeds in the diet. DBSS: basal diet based on sorghum-soybean meal; D5SO: diet with 5 % dehulled sunflower seeds + soybean oil; D10WO: diet with 10 % dehulled sunflower seeds without soybean oil; D5WO: diet with 5 % dehulled sunflower seeds without soybean oil; AOA: antioxidant activity or free radical scavenging as Trolox equivalents. Means with different letters indicate differences ($p \leq 0.01$).

scavenging, was only different over time. This could be attributed to the sunflower seed used in the experimental diets, which was treated with BHA (butylated hydroxyanisole) and BHT (butylated hydroxytoluene) at a ratio of 1 g kg^{-1} sunflower seeds, as was the commercial soybean oil, which also contained synthetic antioxidants. This suggests that the diets contributed significantly to the antioxidant activity of the meat due to their content of exogenous antioxidants (Sampaio *et al*., 2012). To this regard, it has been reported that sunflower seeds contain phenolic acids, flavonoids, tocopherols, and carotenoids that function as potent natural antioxidants (Velasco and Ruiz-Mendez, 2015), although their effect on chicken meat is still unknown.

Oxidative rancidity is one of the main causes of food deterioration, measured by the low free radical scavenging activity in mmol TroloxEq kg^{-1}; this technique is used to predict the optimum storage time or shelf life of foods for humans and animals. According to the results, raw meat loses its oxidative stability on day 9 of storage in refrigeration (4 °C), while cooked meat does so on day 6. This result is probably because the heat treatment causes structural and functional changes in the meat. For example, heat denatures proteins, breaks cell membranes, and begins the degradation of endogenous antioxidants like vitamin C and vitamin E (Serpen *et al*., 2011; Sampaio *et al*., 2012).

When the meat contains high levels of polyunsaturated fatty acids, heat can produce lipid oxidation due to the susceptibility and instability of their double bonds. Lipid oxidation increases free radicals, which in turn decreases antioxidants (Zhao *et al*., 2017a). Therefore, antioxidant activity or free radical scavenging activity decreases due to the excess of free radicals. These results agree with Serpen *et al*. (2011), who found a decrease in the antioxidant capacity of chicken meat as an effect of heat treatment. As time passes, the concentration of fatty acids in the meat decreases (Sampaio *et al*., 2012), and secondary and tertiary compounds increase as a consequence of the oxidation processes. Cooked meat, unlike raw meat (Figures 1 and 2), shows lower free radical scavenging activity as time progresses because heat decreases the initial concentration of fatty acids (Serpen *et al*., 2011), increasing the production of free radicals.

CONCLUSION

Including dehulled sunflower seeds in the diets of broilers did not modify the physicochemical characteristics of the meat but improved the fatty acid profile. Soybean meal can be substituted by 10 %, and soybean oil can be substituted partially or completely by dehulled sunflower seeds in the diet of broilers as long as the production parameters are not negatively affected.

ACKNOWLEDGEMENTS

We greatly thank to CONAHCyT (National Council of Humanities, Sciences, and Technologies, Mexico) for the degree scholarship granted to the first author. We also thanks to the LGAC of the *Colegio de Postgraduados: Innovación Tecnológica y Seguridad Alimentaria en Ganadería* for its support.

REFERENCES

AOAC (Association of Official Analytical Chemists). 2003. Official methods of analysis of AOAC International (17th edition). Association of Official Analytical Chemists: Arlington, VA, USA.

Barbin DF, Kaminishikawahara CM, Soares AL, Mizubuti IY, Grespan M, Shimokomaki M, Hirooka EY. 2015. Prediction of chicken quality attributes by near infrared spectroscopy. Food Chemistry 168: 554–560. https://doi.org/10.1016/j.foodchem.2014.07.101

Betti M, Zuidhof M, Renema R. 2009. Omega-3-enriched broiler meat: 3. Fatty acid distribution between triacylglycerol and phospholipid classes. Poultry Science 88 (8): 1740–1754. https://doi.org/10.3382/ps.2008-00449

Brand-Williams W, Cuvelier ME, Berset C. 1995. Use of a free radical method to evaluate antioxidant activity. Food Science and Technology 28 (1): 25–30. https://doi.org/10.1016/S0023-6438(95)80008-5

Bye R, Linares E, Lentz DL. 2009. México: centro de origen de la domesticación del girasol. Revista Especializada en Ciencias Químico-Biológicas 12 (1): 5–12.

Carvalho RH, Ida EI, Madruga MS, Martínez SL, Shimokomaki M, Estévez M. 2017. Underlying connections between the redox system imbalance, protein oxidation and impaired quality traits in pale, soft and exudative (PSE) poultry meat. Food Chemistry 215: 129–137. https://doi.org/10.1016/j.foodchem.2016.07.182

Cavitt L, Meullenet J, Xiong R, Owens C. 2005. The relationship of razor blade shear, Allo-Kramer shear, Warner-Bratzler shear and sensory tests to changes in tenderness of broiler breast fillets. Journal Muscle of Foods 16 (3): 223–242. https://doi.org/10.1111/j.1745-4573.2005.00001.x

Ciurescu G, Vasilachi A, Grigore D, Grosu H. 2019. Growth performance, carcass traits, and blood biochemistry of broiler chicks fed with low-fibre sunflower meal and phytase. South African Journal of Animal Science 49 (4): 735–745. https://doi.org/10.4314/sajas.v49i4.15

Crespo N, Esteve-García E. 2002. Nutrient and fatty acid deposition in broilers fed different dietary fatty acid profiles. Poultry Science Journal 81 (10): 1533–1542. https://doi.org/10.1093/ps/81.10.1533

DOF (Diario Oficial de la Federación). 1995. NORMA Oficial Mexicana NOM-033-ZOO-1995., Sacrificio humanitario de los animales domésticos y silvestres. Gobierno de México. Secretaría de Agricultura, Ganadería, Desarrollo Rural, Pesca y Alimentación. Ciudad de México, México. 10 p.

Ghimire A, Parajuli P. 2020. Effect of frozen storage on the water-holding capacity and pH of broiler chicken cut-up parts (*Gallus gallus domesticus*). Himalayan Journal of Science and Technology 1 (3–4): 8–15. https://doi.org/10.3126/hijost.v4i0.33860

Honikel KO. 1998. Reference methods for the assessment of physical characteristics of meat. Meat Science 49 (4): 447–457. https://doi.org/10.1016/S0309-1740(98)00034-5

Jiang H, Yoon S, Zhuang H, Wang W, Lawrence K, Yang Y. 2018. Tenderness classification of fresh broiler breast fillets using visible and near-infrared hyperspectral imaging. Meat Science 139: 82–90. https://doi.org/10.1016/j.meatsci.2018.01.013

Kalakuntla S, Nagireddy N, Panda A, Jatoth N, Thirunahari R, Vangoor R. 2017. Effect of dietary incorporation of n-3 polyunsaturated fatty acids rich oil sources on fatty acid profile, keeping quality and sensory attributes of broiler chicken meat. Animal Nutrition 3 (4): 386–391. https://doi.org/10.1016/j.aninu.2017.08.001

Karkelanov N, Chobanova S, Dimitrova K, Whiting IM, Rose SP, Pirgozliev V. 2020. Feeding value of de-hulled sunflower seed meal for broilers. Acta Agrophysica 27: 31–38. https://doi.org/10.31545/aagr/126566

Mahfoudh M, Trabelsi H, Sebei K, Boukhchina S. 2016. Effects of adding different proportions of sunflower seeds on fatty acid composition of chicken tissues. Journal of Food Processing and Technology 7 (3): 569. https://doi.org/10.4172/2157-7110.1000569

Mbukwane MJ, Nkukwana TT, Plumstead PW, Snyman N. 2022. Sunflower meal inclusion rate and the effect of exogenous enzymes on growth performance of broiler chickens. Animals 12 (3): 253. https://doi.org/10.3390/ani12030253

Normah H, Hanapi MJ. 2019. Antioxidant capacity of the green leafy vegetables using oxygen radical antioxidant capacity (orac), 2,2'-azino-bis(3-ethylbenzothiazoline-6-sulphonic acid) (abts) and 2,2-diphenyl-1-picrylhydrazyl (dpph) assays. Science Heritage Journal 3 (1): 1–7. http://doi.org/10.26480/gws.01.2019.01.07

Oda S, Nepomuceno A, Ledur M, Oliveira M, Marin S, Ida E, Shimokomaki M. 2009. Quantitative differential expression of alpha and beta ryanodine receptor genes in PSE (Pale, Soft,

Exudative) meat from two chicken lines: broiler and layer. Brazilian Archives of Biology and Technology 52 (6): 1519–1525. https://doi.org/10.1590/S1516-89132009000600024

Pajak P, Socha R, Galkowska D, Roznowski J, Fortuna T. 2014. Phenolic profile and antioxidant activity in selected seeds and sprouts. Food Chemistry 143 (15): 300–306. https://doi.org/10.1016/j.foodchem.2013.07.064

Palmquist D, Jenkins T. 2003. Challenges with fats and fatty acid methods. Journal of Animal Science 81 (12): 3250–3254. https://doi.org/10.2527/2003.81123250x

Ravindran V, Tancharoenrat P, Zaefarian F, Ravindran G. 2016. Fats in poultry nutrition: Digestive physiology and factors influencing their utilisation. Animal Feed Science and Technology 213: 1–21. https://doi.org/10.1016/j.anifeedsci.2016.01.012

Sampaio GR, Saldanha T, Soares RAM, Torres EAFS. 2012. Effect of natural antioxidant combinations on lipid oxidation in cooked chicken meat during refrigerated storage. Food Chemistry 135 (3): 1383–1390. https://doi.org/10.1016/j.foodchem.2012.05.103

Serpen A, Gökmen V, Fogliano V. 2011. Total antioxidant capacities of raw and cooked meats. Meat Science 90 (1): 60–65. https://doi.org/10.1016/j.meatsci.2011.05.027

Smink W, Gerrits W, Hovenier R, Geelen M, Verstengen M, Beynen A. 2010. Effect of dietary fat sources on fatty acid deposition and lipid metabolism in broiler chickens. Poultry Science 89 (11): 2432–2440. https://doi.org/10.3382/ps.2010-00665

Soares AL, Marchi D, Matsushita M, Guarnieri P, Droval A, Ida E, Shimokomaki M. 2009. Lipid oxidation and fatty acid profile related to broiler breast meat color abnormalities. Brazilian Archives of Biology and Technology 52 (6): 1513–1518. https://doi.org/10.1590/S1516-89132009000600023

Sosa-Montes E, Martínez-Martínez U, Pro-Martínez A, González-Cerón F, Gallegos-Sánchez J, Rodríguez-Ortega LT. 2021. Nutritive value of full-fat dehulled sunflower seeds in diets for broiler chickens. South African Journal of Animal Science 51 (4): 542–549. https://doi.org/10.4314/sajas.v51i4.15

van Soest PJ, Robertson JB, Lewis BA. 1991. Methods for dietary fiber, neutral detergent fiber, and nonstarch polysaccharides in relation to animal nutrition. Journal of Dairy Science 74 (10): 3583–3597. https://doi.org/10.3168/jds.S0022-0302(91)78551-2

Veeramuthu GI, Sams AR. 1999. Postmortem pH, myofibrillar fragmentation, and calpain activity in *Pectoralis* from electrically stimulated and muscle tensioned broiler carcasses. Poultry Science 78 (2): 272–276. https://doi.org/10.1093/ps/78.2.272

Velasco L, Ruiz-Méndez M. 2015. Sunflower oil minor constituents. *In* Martínez-Force E, Dunford N, Salas J. (eds.), Sunflower. Chemistry, Production, Processing, and Utilization. AOCS Press: Urbana, IL, USA, pp: 297–329. https://doi.org/10.1016/b978-1-893997-94-3.50017-9

Villaverde C, Baucells M, Cortinas L, Barroeta A. 2006. Effects of dietary concentration and degree of polyunsaturation of dietary fat on endogenous synthesis and deposition of fatty acids in chickens. British Poultry Science 47 (2): 173–179. https://doi.org/10.1080/00071660600610898

Wideman N, O'bryan CA, Crandall PG. 2016. Factors affecting poultry meat colour consumer preferences – A review. World's Poultry Science Journal 72 (2): 353–366. https://doi.org/10.1017/S0043933916000015

Wildermuth SR, Young EE, Were LM. 2016. Chlorogenic acid oxidation and its reaction sunflower proteins to gorm green-colored complexes. Comprehensive Reviews in Food Science and Food Safety 15 (5): 829–843. https://doi.org/10.1111/1541-4337.12213

Wood J, Enser M. 2017. Manipulating the fatty acid composition of meat to improve nutritional value and meat quality. *In* Purslow PP. (ed.), New Aspects of Meat Quality, From Genes to Ethics. Woodhead Publishing: Tandil, Argentina, pp: 501–535. https://doi.org/10.1016/B978-0-08-100593-4.00023-0

Zhao H, He Y, Li S, Sun X, Wan Y, Shao Y, Hou Z, Xing M. 2017a. Subchronic arsenism-induced oxidative stress and inflammation contribute to apoptosis through mitochondrial and death receptor dependent pathways in chicken immune organs. Oncotarget 8 (25): 40327–40344. https://doi.org/10.18632/oncotarget.16960

Zhao X, Xing T, Chen X, Han M, Li X, Xu X, Zhou G. 2017b. Precipitation and ultimate pH effect on chemical and gelation properties of protein prepared by isoelectric solubilization/precipitation process from pale, soft, exudative (PSE)-like chicken breast meat. Poultry Science 96 (5): 1504–1512. https://doi.org/10.3382/ps/pew412

Agrociencia

DOES RESIN TAPPING AFFECT THE TAPERING AND ACCUMULATION OF MERCHANTABLE TIMBER VOLUME IN PINE TREES?

Mayra Rocío **Ramírez-Vargas**[1], Héctor Manuel d**e los Santos-Posadas**[1*], José René **Valdez-Lazalde**[1], Valentín José **Reyes-Hernández**[1], J. Carmen **Ayala-Sosa**[2]

[1]Colegio de Postgraduados Campus Montecillo. Posgrado en Ciencias Forestales. Carretera México-Texcoco km 36.5, Montecillo, Texcoco, State of Mexico, Mexico. C. P. 56264.
[2]Universidad Autónoma Chapingo. División de Ciencias Forestales. Carretera México-Texcoco km 38.5, Chapingo, Texcoco, State of Mexico, Mexico. C. P. 56227.
* Author for correspondence: hmsantos@colpos.mx

Citation: Ramírez-Vargas MR, de los Santos-Posadas HM, Valdez-Lazalde JR, Reyes-Hernández VJ, Ayala-Sosa JC. 2024. Does resin tapping affect the tapering and accumulation of merchantable timber volume in pine trees?. **Agrociencia** 58(7): 853-868. https://doi.org/ 10.47163/agrociencia.v58i7.2964

Editor in Chief:
Dr. Fernando C. Gómez Merino

Received: July 01, 2022.
Approved: September 04, 2024.
Published in Agrociencia: October 28, 2024.

ABSTRACT

Form factors and taper functions are used for the quantitative and qualitative description of tree stem shape. In southeastern Mexico, there are plantations of *Pinus caribaea* var. *hondurensis* (Sénécl.) W.H. Barrett & Golfari, *Pinus elliottii* var. *elliottii* Engelm., and hybrids between these species to simultaneously produce resin and wood. Farmers need to know whether the practice of resin tapping to death has a negative impact on tree shape and volume of the wood produced. To answer these questions, this study compared the shape, taper, and volume of resin-tapped and untapped trees from three *P. caribaea* origins. A total of 198 trees (99 resin-tapped and 99 untapped) were measured in all diameter categories of the plantation. Total volume models, along with a compatible taper system and variable merchantable timber volume, were fitted using linear and nonlinear regression analyses. To compensate for the lack of initial tree size data prior to tapping, indicator variables (dummies) and an additive structure were used to parameterize volume and taper models. Untapped trees accumulated greater volume than tapped trees. In contrast, the form factor (*ff*) of resin-tapped trees (*ff* = 0.51) was greater than that of untapped trees (*ff* = 0.45). The form factor increased due to tapping between 4 and 7 % depending on the origin, although the hybrid *P. caribaea* × *P. elliottii* presented the most desirable stem geometry in tapped and untapped trees. Based on the Demaerschalk model, the variability is estimated at 99 and 97 % of the merchantable and taper volumes, respectively.

Keywords: *Pinus caribaea* var. *hondurensis*, *Pinus caribaea* × *Pinus elliottii*, shape factor, compatible system, dummy variables, resin.

INTRODUCTION

Pine resin is a valuable non-timber industrial product (Vázquez-González *et al*., 2021), whose components are used as additives in different food products, pharmaceuticals, agrochemicals, and medicines (Lai *et al*., 2020). In recent years, its derivatives have

gained importance to replace fuels and chemicals obtained from petroleum (Neis *et al*., 2019; Vázquez-González *et al*., 2021), making resin a renewable natural alternative in the industrial sector. In 2011, plantations of *Pinus caribaea* var. *hondurensis* (Sénécl.) W.H. Barrett & Golfari and *Pinus elliottii* var. *elliottii* Engelm. of different geographical origin were established in Las Choapas, Veracruz, Mexico, to produce resin as part of the Uumbal Agroforestry Project (Torres-Ávila *et al*., 2020). These species are used in the timber industry and for resin extraction due to their adaptability and the low crystallization rate and high turpentine content of their resin (Lai *et al*., 2020).

Research on the effect of resin tapping on tree shape and volume accumulation is limited. There has been work analyzing growth patterns through dendrochronological studies on tapped and untapped trees to determine growth in normal diameter, resin accumulation in wood, and tree sensitivity to climatic conditions due to resin tapping (Chen *et al*., 2015; van der Maaten *et al*., 2017; Zeng *et al*., 2021). Recent studies have addressed the impact of resin tapping on wood properties, the partitioning of nonstructural carbohydrates between resin extraction and wood production, and the growth of forest stands subjected to resin tapping to provide a reference for genetic improvement in *P. elliottii* (Du *et al*., 2022; Wu *et al*., 2022). Other research has focused on the study of wood mechanical properties in resin-tapped trees, as well as the feasibility of a combined resin-wood production in plantations of *P. caribaea* var. *hondurensis* (Reyes *et al*., 2015).

The geometry and the stem profile can be evaluated through mathematical models that describe the form factor and taper (Tlaxcala-Méndez *et al*., 2016). The form factor is described as the ratio between the volume of a tree and that of a cylinder with the same diameter and the same height; knowing this factor makes it easy to calculate the individual volume of the stem. Taper refers to the variation of the stem diameter along its length, which can be estimated using equations that simulate the profile of the tree stem (Hussain *et al*., 2020).

Given that not all of the trees in Agroforestal Uumbal's plantations are resin-tapped, it is important to understand how the tapped trees are selected. Initially, two reference criteria are established: minimum age of six years and minimum normal diameter of 12 cm. In addition, shape and size play a role, as tapped trees are not considered suitable for high-value timber production (sawmilling). However, tapping can occur before the age of six years if the trees have reached a certain diameter. Tapping can last from 3.5 to 4 years, always trying to leave half of the trees in the stand for timber production only.

The present study initially focused on collecting samples from different sources to construct specific volume models for tapped and untapped trees. This research hypothesizes that stem geometry and shape factor are affected by the resin-tapping that was applied to the trees, and that this in turn modifies the potential accumulation of total volume and product distribution. The objective of this study was to evaluate the potential effect of resin-tapping on the tapering and accumulation of commercial wood volume of trees of *P. caribaea* var. *hondurensis* and the hybrid *P. caribaea* × *P.*

elliottii in commercial plantations in Las Choapas, Veracruz, Mexico, based on the variation in the form factor and its tapering-commercial volume.

MATERIALS AND METHODS

Study area

The study was conducted in commercial forest plantations for resin production in Las Choapas, Veracruz, Mexico (17° 49′ 50.59″ N, 94° 6′ 11.84″ W, average altitude of 100 m), belonging to the Uumbal Agroforestry Project. The climate is warm-humid, with year-round, abundant summer rainfalls, annual precipitation of 2400 to 3100 mm, and average minimum and maximum temperatures of 22 and 30 °C (CONABIO, 2001). The physiography includes alluvial plains with hills, flooded coastal alluvial plains, and open valleys with hills. Luvisol and Cambisol soils predominate (INEGI, 2009).

Field data and timber volume estimation

Information was obtained from 198 trees, of which 99 were resin-tapped (*r*) and 99 were untapped (*nr*). Thirty-three trees for each origin group were considered: L1 (*P. caribaea* var. *hondurensis)* from Brazil, L4 (*P. caribaea* var. *hondurensis*) from Australia, and L5 (hybrid *P. caribaea* × *P. elliottii*) from Australia, aged 8, 9, and 8 years, respectively. Trees were resin-tapped on both sides using the American method beginning at six years of age, from stump height (0.1 m) to 2.6 to 3 m high at the stem. The tapping time varied by origin, using 3.5 years for L5 and 4 years for L1 and L4.

The selected trees were felled to obtain accurate diameter data at different stem heights using the stem analysis methodology (Torres-Ávila *et al*., 2020). A total of 3030 diameter-height pairs of observations were obtained (Figure 1A). The behavior in relative height against relative diameter per stem section of each tree within the

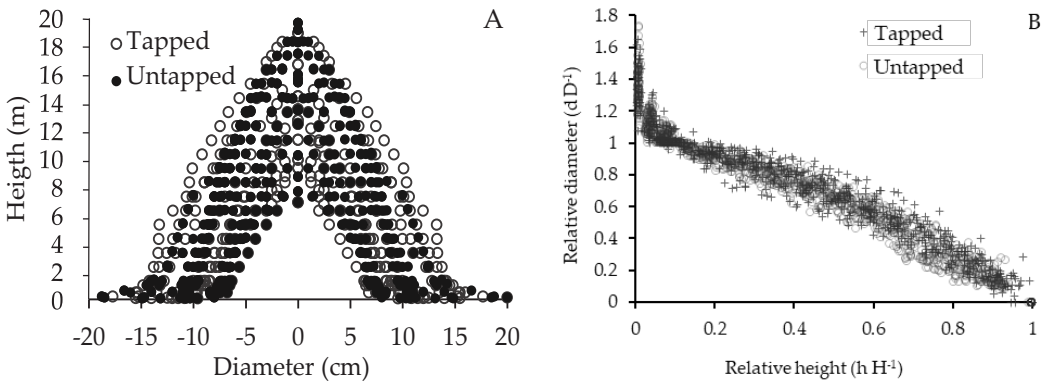

Figure 1. A: Partial heights as a function of partial diameters; B: dispersion of relative heights against relative diameters of the 198 resin-tapped and untapped trees used to adjust the taper and merchantable timber volume functions.

sample followed a logical behavior (Figure 1B). Because no data were available for the trees prior to tapping, the total diameter-height ranges were distributed evenly across origins and tapping conditions.

The Newton formula and the centroid method (Wiant *et al*., 1992) were used to calculate the volume of the lower and middle sections of the stem, and the cone formula was used for the tip of the tree. This way, the accumulated merchantable timber volume of the sampled trees was obtained (Figure 2A). Total stem volume was calculated using the overlapping log method developed by Bailey (1995) due to its accuracy (Torres-Ávila *et al*., 2020). The resin-tapped trees were concentrated in categories of 15 to 20 cm of normal diameter, while the untapped trees were grouped in categories of 15 to 35 cm (Figure 2B).

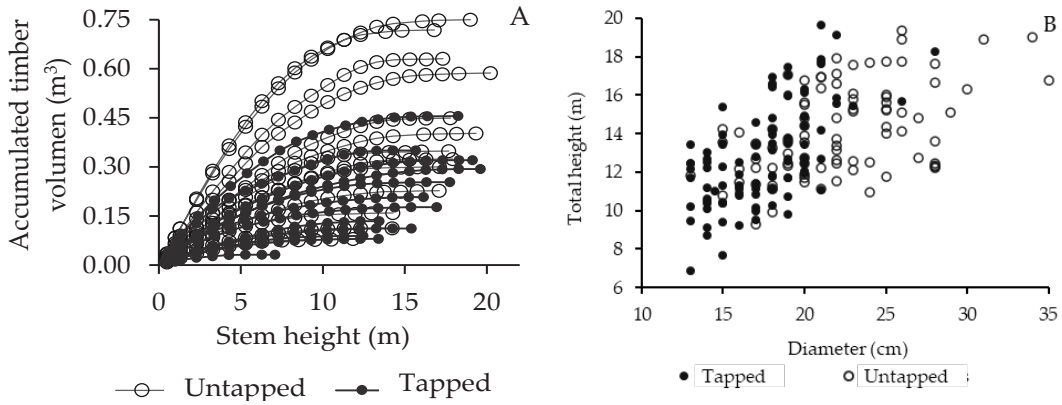

Figure 2. A: Accumulated merchantable timber volume as a function of stem height for the overall sample; B: dispersion of normal diameter-total height observations for the sampled trees.

Effect of resin-tapping and origin on shape and volume factor

Based on the results obtained by Torres-Ávila *et al*. (2020), to estimate the shape factor, a combined variable type total shaft volume model is considered (Bruce and Schumacher, 1942), given by the expression:

$$V = \alpha + \beta \cdot D^2 H$$

where the parameter a (i.e., intercept) is interpreted as the minimum inventoried volume, β is the implicit form factor of the function, D represents the normal diameter (cm), H the total height (m), and V the total timber volume of the stem with bark (m^3). Since $\beta = ff\frac{\pi}{40\,000}$, the form factor compared to the cylinder is $ff = \frac{\beta}{(\pi/40\,000)}$.

Indicator variables (dummies) were used in the statistical analysis to determine if the differences in shape resulting from origin and tapping are statistically significant. These variables have the characteristic of generating categories, taking values of zero or one depending on whether the observation belongs to a certain origin and whether it is resin-tapped (*r*) or not (*nr*). The *nr* trees were taken as the basis for estimating the other parameters in the regression analysis, including the indicator variables in the β parameter as follows:

$$V = \alpha + (\beta_{10} + X_1 \beta_{11}) D^2 H$$

where $X_1 = \begin{cases} 1, if\ it\ belongs\ to\ a\ resin\ tapped\ tree \\ 0, otherwise \end{cases}$

The hypothesis test evaluating the tapping effect was H_0: $\beta_{11} = 0$ *vs.* H_A: $\beta_{11} \neq 0$.

A single regression model was developed considering all trees (*r* and *nr*) of the three origins (L) to test the hypothesis of the shape factor among them. Thus, there were six categories: L1*r* (*P. caribaea* from Brazil, tapped), L1*nr* (*P. caribaea* from Brazil, untapped), L4*r* (*P. caribaea* from Australia, tapped), L4*nr* (*P. caribaea* from Australia, untapped), L5*r* (hybrid from Australia, tapped), and L5*nr* (hybrid from Australia, untapped). To make the parameters estimable, L5*nr* was considered as a reference in the regression analysis. The rest of the parameters are additive to this model, so that the overall function including the indicator variables is defined as:

$$V = \alpha + (\beta_{10} + X_1\beta_{11} + Z_1\beta_{20} + Z_1X_1\beta_{21} + Z_2\beta_{30} + Z_2X_1\beta_{31})D^{\prime}H$$

where:

$$Z_1 = \begin{cases} 1, if\ it\ belongs\ to\ origin\ L1 \\ 0, otherwise \end{cases}$$

$$Z_2 = \begin{cases} 1, if\ it\ belongs\ to\ origin\ L4 \\ 0, otherwise \end{cases}$$

The hypothesis test ($\beta_{10} = 0$) is trivial in this case since there is a general regression function described by a and β_{10}. What is relevant is to identify whether there is significant additionality on the part of the parameters representing the tapping and origin effect. Therefore, the relevant null hypothesis is H_0: $\beta_{11} = \beta_{20} = \beta_{21} = \beta_{30} = \beta_{31} = 0$ *vs.* H_A: at least one of them is different from zero.

To extend the test, in addition to the suggested constant shape volume model, the Spurr (1952) model, which is of variable shape $V = \alpha_0 (D^2 H)^{\beta_1}$, has goodness of fit, and was fitted nonlinearly (Husch, 1963). To detect changes in total volume between *r* and

nr, the parameters α_0 and b_1 ($\alpha_0 = \alpha_{01} + X_1\,\alpha_{02}$ and $\beta_1 = \beta_{11} + X_1\beta_{12}$) were redefined using the *nr* as a reference to estimate the other parameters showing the effect of tapping, testing the hypothesis H_0: $\alpha_{02} = \beta_{12} = 0$ against H_A: at least one of them is different from zero.

Evaluation of the effect of resin-tapping and origin on tapering

Initial tests with several taper models identified the Demaerschalk (1972) model, adjusted by Torres-Ávila *et al*. (2020) for data from the plantations and origins studied, as the most efficient due to its goodness of fit. This model is stated as follows:

$$\left(\frac{d}{D}\right)^2 = \theta_0\left(\frac{1}{D^2H}\right)X^{\theta_1} + \theta_2 X^{\theta_3},$$

where d is the diameter (cm) with bark of the i-th section at height h (m), D is the normal diameter (cm), H the total height (m), $X = (H - h) / H$, and θ_i represents the parameters to be estimated from the model.

The equations that make up the compatible system of taper total volume and merchantable timber volume generated from integration are as follows (Torres-Ávila *et al*., 2020):

$$\mathrm{V} = k\left(-\frac{\theta_0\left(\frac{H-h}{H}\right)^{\theta_1+1}}{\theta_1+1} - \frac{\theta_2 D^2 H\left(\frac{H-h}{H}\right)^{\theta_3+1}}{\theta_3+1}\right)\Bigg|_{h_1=0}^{h_2=H} = \frac{k\theta_0}{\theta_1+1} + \frac{k\theta_2}{\theta_3+1}D^2H$$

$$V_{merchantable} = k\left(-\frac{\theta_0}{\theta_1+1}\left(\left(\frac{H-h_c}{H}\right)^{\theta_1+1} - \left(\frac{H-h_t}{H}\right)^{\theta_1+1}\right)\frac{\theta_2 D^2 H}{\theta_3+1}\left(\left(\frac{H-h_c}{H}\right)^{\theta_3+1}\left(\frac{H-h_t}{H}\right)^{\theta_3+1}\right)\right)$$

where k is the constant used when diameters are expressed in cm and lengths in m; h, h_1, and h_2 are heights (m) of the i-th section at a certain diameter (cm); h_c is the height (m) above the stump at which the merchantable timber volume is given; and h_t is the height (m) of the stump.

The implied total volume model is of the combined variable type (constant form):

$$V = \frac{k\theta_0}{\theta_1+1} + \frac{k\theta_2}{\theta_3+1}D^2H$$

To test the hypotheses, the model is rewritten based on the parameters θ_2 and θ_3, taking the L5*nr* group as a reference:

$$\theta_2 = \theta_{20} + X_1\,\theta_{21} + Z_1\,\theta_{22} + X_1Z_1\,\theta_{23} + Z_2\,\theta_{24} + X_1Z_2\,\theta_{25}$$

$$\theta_3 = \theta_{30} + X_1\,\theta_{31} + Z_1\,\theta_{32} + X_1Z_1\,\theta_{33} + Z_2\,\theta_{34} + X_1Z_2\,\theta_{35}$$

Analogous to the shape factor and total volume hypothesis tests, the null hypothesis for taper was tested on the parameters indicating the effects of origin and tapping, so H_0: $\theta_{21} = \theta_{22} = \theta_{23} = \theta_{24} = \theta_{25} = \theta_{31} = \theta_{32} = \theta_{33} = \theta_{34} = \theta_{35} = 0$ *vs*. H_A: at least one of them is different from zero.

Similarly, the parameters θ_0 and θ_1, which represent the intercept in this taper equation, were tested on whether they are different between tapped and untapped trees, taking the *nr* trees as the basis for estimating the other parameters in the regression analysis, including the indicator variables in θ_0 and θ_1:

$$\theta_0 = \theta_{00} + X_1\,\theta_{01}$$

$$\theta_1 = \theta_{10} + X_1\,\theta_{11}$$

where:

$$X_1 = \begin{cases} 1, \text{if it belongs to a resin tapped tree} \\ 0, \text{otherwise} \end{cases}$$

The null hypothesis test evaluating the resin-tapping effect is H_0: $\theta_{01} = \theta_{11} = 0$ *vs*. H_A: $\theta_{01} \neq \theta_{11} \neq 0$.

Fitting strategy

Parameter estimation of the linear combined variable and total Spurr volume models was performed using the ordinary least squares method with the MODEL procedure of SAS® 9.0 (SAS Institute Inc, 2004), including simultaneous estimation with full information maximum likelihood (FIML) for the compatible system fit of taper-merchantable timber volume. The residuals were analyzed graphically to ensure compliance with homoscedasticity and autocorrelation assumptions in the regression analysis (Ramírez-Martínez *et al*., 2018).

A power function of the variance of the residual $\sigma_i^2 = (D^2H)^{\Phi}$ was used to correct for the heteroscedasticity associated with the total and merchantable timber volume. The Φ value was estimated using the method proposed by Harvey (1976), which considers the unweighted errors as the dependent variable in the potential error variance model. The estimation of these functions was performed using the weighted function with the SAS® 9.0 procedure option *resid*. *VT* = *resid*. *VT* / $((D^2H)^{\Phi})^{0.5}$.

Autocorrelation was corrected using a second-order continuous autoregressive structure (CAR 2) in the fit of the Demaerschalk taper and taper-merchantable timber volume models. The adjusted coefficient of determination (R^2_{Adj}), sum of squares of error (SCE), and root mean square of error (RMSE) (Torres-Ávila *et al*., 2020) were used to choose the models with the best goodness of fit.

RESULTS AND DISCUSSION

Effect of resin-tapping on form factor and total tree volume

The Spurr model showed a slightly higher fit than the Bruce and Schumacher model; however, it did not detect an effect of resin-tapping with parameters α_{11} and β_{11} ($p > 0.05$) in contrast to parameter β_{11} ($p < 0.01$) of the Bruce and Schumacher model, which indicates positive additionality due to resin-tapping (Table 1).

Table 1. Total volume models fitted for resin-tapped and untapped pines in forest plantations in Las Choapas, Veracruz, Mexico.

Model	P	Value	EE	*t* value	Pr > |*t*|	SCE	RMSE	R^2_{Adj}
Spurr	α_{10}	7.200E-05	3.092E-06	23.37	<.0001	0.119	0.0173	0.98
	α_{11}	1.300E-05	1.100E-05	1.17	0.2446			
	β_{10}	0.923	5.160E-03	179.10	<.0001			
	β_{11}	-0.011	0.016	-0.70	0.4869			
Bruce and Schumacher	α	2.917E-03	1.770E-04	16.46	<.0001	0.167	0.0206	0.97
	β_{10}	3.700E-05	2.519E-07	148	<.0001			
	β_{11}	3.317E-06	4.373E-07	7.59	<.0001			

P: parameters; EE: standard error; SCE: error sum of squares; RMSE: root mean square error; R^2_{Adj}: adjusted coefficient of determination; α: intercept in common; α_{10} and β_{10}: regression parameters of the reference group (L5*nr*); α_{11} and β_{11}: parameters of the indicator variables due to tapping.

After detecting the effect of resin-tapping on total volume with the Bruce and Schumacher model, a comparison was made on the form factor for the three origins, including the effect of tapping (Table 2).

For the untapped trees, the reference group origin (L5*nr*) had the largest form factor. The parameters associated with the effect of resin-tapping always indicate an increase in the form factor compared to the reference trees (L5*nr*). This effect extends between origins, although for L4, the specific effect of tapping is not statistically significant to the effect of tapping in L5 (Table 2).

Table 2. Results of the linear combined variable model fit with indicator variables to differentiate between origins and resin-tapped and untapped trees.

Group	P	Value	A	*ff*	EE	t value	Pr > |*t*|	SCE	RMSE	R^2_{Adj}
Intercept	α	2.715E-03	2.715E-03	----	1.480E-04	18.35	<.0001			
L5*nr*	β_{10}	3.900E-05	3.900E-05	0.5	3.649E-07	106.6	<.0001			
L5*r*	β_{11}	1.908E-06	4.100E-05	0.52	5.847E-07	3.26	0.0012			
L1*nr*	β_{20}	-1.040E-06	3.800E-05	0.48	5.587E-07	-1.86	0.0631	0.14	0.019	0.98
L1*r*	β_{21}	2.700E-06	4.300E-05	0.54	9.084E-07	2.97	0.0031			
L4*nr*	β_{30}	-3.150E-06	3.600E-05	0.46	5.083E-07	-6.19	<.0001			
L4*r*	β_{31}	1.178E-06	3.900E-05	0.5	8.416E-07	1.4	0.1623			

P: parameters; A: additionality; *ff*: form factor; EE: standard error; SCE: error sum of squares; RMSE: root mean square error; L1: *Pinus caribaea* from Brazil; L4: *P. caribaea* from Australia; L5: *P. caribaea* × *P. elliottii* from Australia; R^2_{Adj}: adjusted coefficient of determination; α: intercept in common; β_{10}: regression parameter of the reference group (L5*nr*); β_{11}, β_{20}, β_{21}, β_{30} and β_{31}: parameters showing the effect of tapping and origin.

Effect of resin-tapping and origin on the taper-merchantable timber volume system

In the parameters that refer to the intercept θ_0 and θ_1, additionalities were detected from resin-tapping ($p < 0.01$), so that the values should be considered to differentiate the equations between *r* (tapped) and *nr* (untapped) trees. Likewise, parameters $\theta_{21–25}$ and $\theta_{31–35}$ ($p < 0.01$) suggest additionalities by origin and by the effect of resin-tapping compared to the reference trees (L5*nr*) (Table 3).

The behavior of the residuals for taper (Figure 3A) and merchantable timber volume (m^3) (Figure 3B) showed compliance with homoscedasticity and error independence.

The results of the fitting indicate that there are differences in taper and merchantable timber volume between resin-tapped and untapped treated trees in all groups (Table 3). Therefore, the parameters obtained from the fitting of the compatible system were used to develop specific equations for each origin under study, and the constant form factor was obtained. The resin-tapped trees presented a larger form factor than the untapped trees in the three origins (Table 4).

The form factor for the *nr* trees of L5 origin had a 0.45 value, while for the *r* trees it was 0.51, which represents an increase of 6 % (Table 4). Similarly, increases of 4 and 7 % can be estimated for the L4 and L1 origins.

Assessment of the effect of tree size on tapering and commercial volume

The results obtained from the total volume and taper-merchantable timber volume models suggest that resin-tapping modifies the geometry of the trunk; specifically, it increases the form factor in all three origins. However, it is necessary to incorporate the average tree size into the analysis to make a more effective comparison. This is

Table 3. Results of the fitting with indicator variables in the compatible taper-merchantable timber volume system based on the Demaerschalk model (1972) for pine plantations in Las Choapas, Veracruz, Mexico.

Group	P	Value	EE	*t* value	Pr > |t|	SCE	RMSE	R^2_{Adj}	Model
nr	θ_{00}	6630.31	206.70	32.08	<.0001	0.3469	0.0106	0.99	Merchantable timber volume
r	θ_{01}	-2498.86	288.40	-8.67	<.0001				
nr	θ_{10}	40.8910	2.1428	19.08	<.0001				
r	θ_{11}	11.7011	4.7097	2.48	0.0130				
L5*nr*	θ_{20}	1.2505	0.0071	175	<.0001				
L5*r*	θ_{21}	0.0493	0.0162	3.05	0.0023				
L1*nr*	θ_{22}	-0.0724	0.0089	-8.07	<.0001				
L1*r*	θ_{23}	0.1152	0.0176	6.56	<.0001				
L4*nr*	θ_{24}	-0.1345	0.0071	-18.94	<.0001				
L4*r*	θ_{25}	0.0656	0.0162	4.05	<.0001				
L5*nr*	θ_{30}	1.7550	0.0154	114.14	<.0001	6284.9	1.4232	0.97	Taper volume
L5*r*	θ_{31}	-0.2196	0.0201	-10.91	<.0001				
L1*nr*	θ_{32}	-0.2665	0.0223	-11.96	<.0001				
L1*r*	θ_{33}	0.2344	0.0283	8.28	<.0001				
L4*nr*	θ_{34}	-0.2913	0.0179	-16.25	<.0001				
L4*r*	θ_{35}	0.2896	0.0248	11.67	<.0001				

P: parameters; EE: standard error; L1: *Pinus caribaea* from Brazil; L4: *P. caribaea* from Australia; L5: *P. caribaea* × *P. elliottii* from Australia; *nr*: untapped tree; *r*: tapped tree; θ_{00} and θ_{10}: base regression parameters for the intercept of untapped trees; θ_{01} and θ_{11}: parameters indicating additionality due to tapping on the intercept; θ_{20} and θ_{30}: regression parameters of the reference group (L5*nr*); θ_{21}, θ_{22}, θ_{23}, θ_{24}, θ_{25}, θ_{31}, θ_{32}, θ_{33}, θ_{34}, θ_{35}: parameters of the indicator variables due to origin and tapping effects; SCE: error sum of squares; RMSE: root mean square error; R^2_{Adj}: adjusted coefficient of determination.

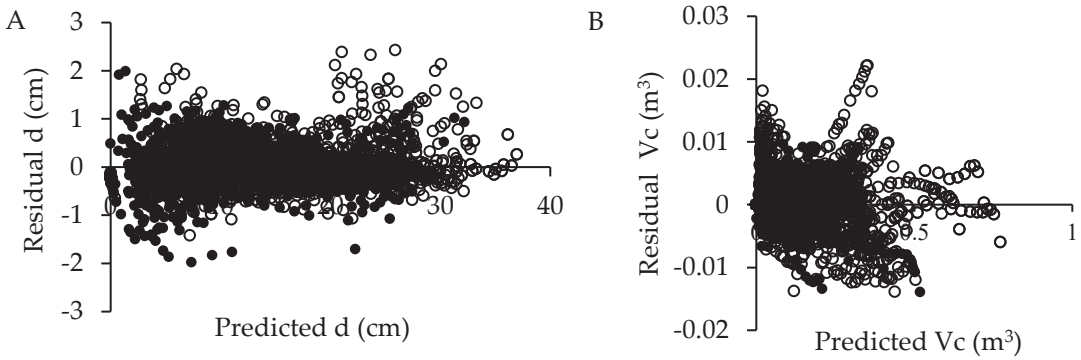

Figure 3. A: Plot of residuals versus predicted taper with diameter (d, cm); B: plot of residuals versus predicted merchantable timber volume (Vc, m^3) for the Demaerschalk (1972) model.

Table 4. Estimated parameters for the Demaerschalk (1972) simultaneous taper-merchantable timber volume model and form factor in commercial pine plantations for resin and timber production in Las Choapas, Veracruz, Mexico.

Parameters	Origin	*nr*	*R*	ff_{nr}	ff_r
θ_0	L5	6630.3150	4131.4550	0.45	0.51
θ_1		40.8910	52.5922		
θ_2		1.2505	1.2998		
θ_3		1.7550	1.5354		
θ_0	L4	6630.3150	4131.4550	0.45	0.49
θ_1		40.8910	52.5922		
θ_2		1.1159	1.2309		
θ_3		1.4637	1.5338		
θ_0	L1	6630.3150	4131.4550	0.47	0.54
θ_1		40.8910	52.5922		
θ_2		1.1781	1.3427		
θ_3		1.4885	1.5034		

L1: *Pinus caribaea* from Brazil; L4: *P. caribaea* from Australia; L5: *P. caribaea* × *P. elliottii* from Australia; θ_i: parameters of Demaerschalk commercial taper-volume model; *nr*: untapped trees; *r*: tapped trees; *ff*: form factor.

because, in general, resin-tapped trees have smaller diameter and total height than untapped-treated trees.

The company that owns the plantations carries out thinning (i.e., selecting suppressed and intermediate trees); therefore, the accumulated merchantable timber volume is greater in the sample of untapped trees, substantially increasing its value in timber products (Figure 2A). To illustrate the effect of resin-tapping on taper and cumulative merchantable timber volume for each origin, graphs were constructed from the average values of normal diameters and total heights of the sample taken in the plantation (Figure 4), using the specific values of the parameters obtained in the fitting (Table 4). In all origins, the resin-tapped trees showed a tendency to decrease the neiloid shape at the base of the stem and became more like a paraboloid (with relative height from 0 to 0.8), focusing where the tapping began, which ended in a conical shape (relative height from 0.8 to 1). On the other hand, untapped trees presented a neiloid form at the base (0 to 0.2), whose shape is truncated to take a paraboloid shape (0.2 to 0.8) and conical shape at the tip of the tree (0.8 to 1) (Figure 4). In terms of accumulated merchantable timber volume (m^3), the resin-tapped of the three origins accumulated less volume than their untapped counterparts.

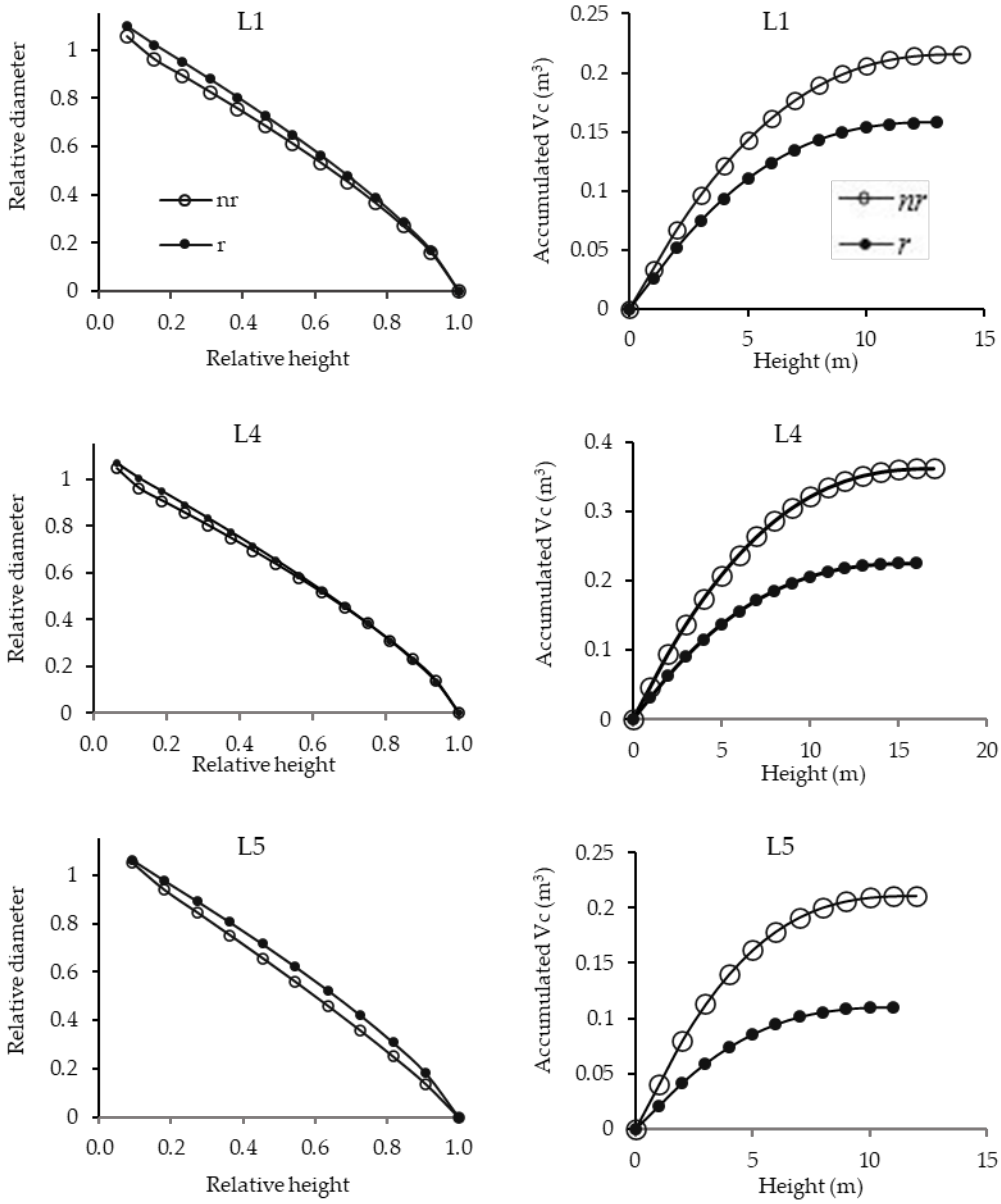

Figure 4. Taper behavior in height and diameter (relative or percentage scale) and cumulative merchantable timber volume (Vc, m³) in resin-tapped (*r*) and untapped (*nr*) trees. L1: *Pinus caribaea* from Brazil; L4: *P. caribaea* from Australia; L5: *P. caribaea* × *P. elliottii* from Australia.

Effect of resin-tapping on the form factor

From the taper-merchantable timber volume models, it is possible to detect differences in the shape and taper factors between resin-tapped and untapped trees and between origins since there are more observations per tree compared to the total volume models, where only one observation per tree is available (Tlaxcala-Méndez *et al*., 2016). Of the three origins analyzed (Table 4), the hybrid (L5) presented the best behavior in its shape factor, being the least tapered and with a geometry close to the paraboloid. Torres-Ávila *et al*. (2020) mentioned that this behavior can change in situations of water stress in geographical areas where rainy and dry seasons are marked.

Better-shaped trees are desirable in the sawmilling industry because more wood processing options can be obtained (Torres-Ávila *et al*., 2020). Resin-tapped trees presented a significant increase in their form factor compared to untapped trees (Table 4). The form factor is considered an observable characteristic or trait of each origin, affected by the environment in which it develops, its genetic potential, and other management factors. For example, the incidence of borer pests in juvenile stages favors more cylindrical stems (Tlaxcala-Méndez *et al*., 2016) of Spanish cedar (*Cedrela odorata* L.), as well as resin-tapping in *P. caribaea*, as suggested by the results of this study. Torres-Ávila *et al*. (2020) reported similar values for *nr* trees from these same plantations: 0.48 for L5, 0.44 for L4, and 0.45 for L1. These results indicate that the stem geometry of resin-tapped trees changed in the three origins. For L4, the shape factor is barely close to 0.5, whereas for L1 and L5, this value is higher.

Effect of resin-tapping on taper

Since the stem geometry of the three origins is close to a paraboloid, the Demaerschalk model is the most appropriate to describe it (Torres-Ávila *et al*., 2020). This model showed that there are differences in the shape and taper factors due to origin and the effect of resin-tapping. Tlaxcala-Méndez *et al*. (2016) mention that this is attributed to the fact that the taper models have more observations per tree, whereas in the total volume models, such as the combined variable and Spurr, there is one observation per tree. Taper models tend to be more sensitive to hypothesis testing. Having more observations allows for more degrees of freedom in the error, and this makes it possible to experiment more successfully with the hypotheses in the taper parameters.

The results show that L4*nr*, L4*r*, L1*nr*, L1*r*, and L5*r* express different taper. This is because, when performing the additionality test for the effect of tapping (X) and origin (Z) on the parameters, the effects of the indicator variables X and Z and their interactions are significant. This methodology was used by Tlaxcala-Méndez *et al.* (2016) to find differences in taper, using indicator variables to differentiate between seven geographical origins of *Cedrela odorata* L. in Mexico, where all presented different taper due to genotype-environment interaction and stress caused by borer incidence.

Effect of resin-tapping on wood volume

Studies have been aimed at evaluating the effect of resin production on tree growth, mostly using the dendrochronological approach. However, there are still no studies

on the effect of resin-tapping on tree stem thinning. For example, the effect of resin-tapping on radial growth of *P. massoniana* in southern China showed that growth is greater in tapped trees than untapped trees, with no significant differences (Williams *et al*., 2017). Du *et al*. (2021) mentioned that the effect of tapping is focused and that grooving had no significant effect on annual radial increment in *P. elliottii*.

Wu *et al*. (2022) found that tapping inhibits stand growth when harvesting is intensive, while Chen *et al.* (2015) indicated that the negative effect on radial growth occurred especially in old trees. On the other hand, van der Maaten *et al*. (2017) showed that in *P. sylvestris*, resin-tapping has a positive effect on tree growth at normal diameter height, suggesting that this is because wood formation is concentrated in the live part of the stem (i.e., after fluting there is no growth on the resin face due to mechanical damage caused to the cambium); however, resin-tapped trees presented slightly higher growth levels 30 years after resin extraction.

In a larger study, conducted from 1967 to 2017 in *P. tubuliformis* in China, tapped trees were shown to have interannual variations consistent with those of untapped trees, although they presented significantly lower values after resin extraction (Zeng *et al*., 2021). In the present study, it should be considered that the resin-tapped trees are those that are suppressed or co-dominant, which influenced the accumulation of merchantable timber volume, presenting approximately 35 % less accumulated volume at 15 m total height than the untapped trees.

CONCLUSIONS

Resin-tapping did not have a negative effect on the shape factor in trees from the three geographical origins. The best-shaped group is the hybrid (L5), both in tapped and untapped trees, presenting a more cylindrical shape, followed by L1 and L4 being the most tapered. Resin-tapping changed the shape of the stem at the base of the tree, making it resemble a paraboloid. The untapped trees of the three groups accumulated higher merchantable timber volume compared to the tapped ones. This is because the trees selected for tapping correspond to the suppressed and intermediate trees and not to the resin-tapping activity.

The fitted models with indicator variables (dummy) allowed finding differences in the form factor using the taper methodology for resin-tapped and untapped trees of the three origins analyzed. This is because there were more observations per tree in contrast to the total volume models, where there was only one observation per tree. The compatible system of taper and merchantable timber volumes helped improve the sensitivity of the hypothesis tests and find the differences resulting from tapping and origins in the group under study in taper and shape factors.

It is important to emphasize that in order to use the parameters obtained in these analyses, compliance with the assumptions of the regression analysis must be taken into account, and if they are not met, to resort to methodologies that allow improving the behavior of the residuals, such as the autoregressive structure and power functions of the residual variance.

REFERENCES

Bailey RL. 1995. Upper stem volumes from stem analysis data: An overlapping bolts method. Canadian Journal of Forest Research 25 (1): 170–173. https://doi.org/10.1139/x95-020

Bruce D, Schumacher F. 1942. Forest mensuration. McGraw-Hill: New York, NY, USA. 483 p.

Chen F, Yuan YJ, Yu SL, Zhang TW. 2015. Erratum to: Influence of climate warming and resin collection on the growth of Masson pine (*Pinus massoniana*) in a subtropical forest, southern China. Trees 30 (3): 1017. https://doi.org/10.1007/s00468-015-1313-1

Demaerschalk JP. 1972. Converting volume equations to compatible taper equations. Forest Science 18 (3): 241–245. https://doi.org/10.1093/forestscience/18.3.241

Du B, Luan Q, Ni Z, Sun H, Jiang J. 2022. Radial growth and non-structural carbohydrate partitioning response to resin tapping of slash pine (*Pinus elliottii* Engelm. var. *elliottii*). Journal of Forestry Research 33 (2): 423–433. https://doi.org/10.1007/s11676-021-01357-1

CONABIO (Comisión Nacional para el Conocimiento y Uso de la Biodiversidad). 2001. Climas (clasificación de Köppen, modificado por García). Escala 1:1000000. México. Gobierno de México. Comisión Nacional para el Conocimiento y Uso de la Biodiversidad. Ciudad de México, México.

Harvey AC. 1976. Estimating regression models with multiplicative heteroscedasticity. Econometrica 44 (3): 461–465. https://doi.org/10.2307/1913974

Husch B. 1963. Forest mensuration and statistics. Canadian Journal of Forest Research 26 (1): 51–65.

Hussain A, Shahzad MK, He P, Jiang L. 2020. Stem taper equations for three major conifer species of Northeast China. Scandinavian Journal of Forest Research 35 (8): 562–576. https://doi.org/10.1080/02827581.2020.1843703

INEGI (Instituto Nacional de Estadística y Geografía). 2009. Prontuario de información geográfica municipal de los Estados Unidos Mexicanos. Ciudad de México, México. 120 p.

Lai M, Zhang L, Lei L, Liu S, Jia T, Yi M. 2020. Inheritance of resin yield and main resin components in *Pinus elliottii* Engelm. at three locations in southern China. Industrial Crops and Products 144: 112065. https://doi.org/10.1016/j.indcrop.2019.112065

Neis FA, de Costa F, de Almeida MR, Colling LC, de Oliveira Junkes CF, Fett JP, Fett-Neto AG. 2019. Resin exudation profile, chemical composition, and secretory canal characterization in contrasting yield phenotypes of *Pinus elliottii* Engelm. Industrial Crops and Products 132: 76–83. https://doi.org/10.1016/j.indcrop.2019.02.013

Ramírez-Martínez A, Santiago-García W, Quiñonez-Barraza G, Ruiz-Aquino F, Antúnez P. 2018. Modelación del perfil fustal y volumen total para *Pinus ayacahuite* Ehren. Madera y Bosques 24 (2): e2421496. https://doi.org/10.21829/myb.2018.2421496

Reyes C, Will EC, Molina VS, Betancourt LY. 2015. Propiedades mecánicas de la madera de *Pinus caribaea* var. *hondurensis* resinados y no resinados de las plantaciones de Uverito, Estado Monagas, Venezuela. Revista Forestal Venezolana 59 (1): 63–75.

SAS Institute Inc. 2004. SAS/ETS 9.1 User's Guide. Cary, NC, USA.

Spurr SH. 1952. Forest inventory. John Wiley and Sons: New York, NY, USA. 472 p.

Tlaxcala-Méndez RM, de los Santos-Posadas HM, Hernández-de la Rosa P, López-Ayala JL. 2016. Variación del factor de forma y el ahusamiento en procedencias de cedro rojo (*Cedrela odorata* L.). Agrociencia 50 (1): 89–105.

Torres-Ávila D, de los Santos-Posadas HM, Velázquez-Martínez A, Tamarit-Urias JC. 2020. Ahusamiento y volumen comercial de tres procedencias de pinos tropicales en plantaciones forestales de Veracruz, México. Madera y Bosques 26 (3): e2631890. https://doi.org/10.21829/myb.2020.2631890

van der Maaten E, Mehl A, Wilmking M, van der Maaten-Theunissen M. 2017. Tapping the tree-ring archive for studying effects of resin extraction on the growth and climate sensitivity of Scots pine. Forest Ecosystems 4 (1): 1–7. https://doi.org/10.1186/s40663-017-0096-9

Vázquez-González C, López-Goldar X, Alía R, Bustingorri G, Lario FJ, Lema M, de la Mata R, Sampedro L, Touza R, Zas R. 2021. Genetic variation in resin yield and covariation with tree growth in maritime pine. Forest Ecology and Management 482: 118843. https://doi.org/10.1016/j.foreco.2020.118843

Wiant HV, Wood GB, Furnival GM. 1992. Estimating log volume using the centroid position. Forest Science 38 (1): 187–191. https://doi.org/10.1093/forestscience/38.1.187

Williams R, Nauman C, Zhu J. 2017. The effects of resin tapping on the radial growth of Masson pine trees in South China - a case study. Agricultural Research and Technology 8 (2): 555732. https://doi.org/10.19080/artoaj.2017.08.555732

Wu H, Fan Y, Niu X, Luan Q, Li Y, Jiang J, Jin J. 2022. Effects of resin-tapping year on wood properties of living *Pinus elliottii*. Forest Research 35 (1): 31–39.

Zeng X, Sun S, Wang Y, Chang Y, Tao X, Hou M, Wang W, Liu X, Zhang L. 2021. Does resin tapping affect the tree-ring growth and climate sensitivity of the Chinese pine (*Pinus tabuliformis*) in the Loess Plateau, China? Dendrochronologia 65: 125800. https://doi.org/10.1016/j.dendro.2020.125800

Agrociencia

EDIBLE COATINGS BASED ON BEESWAX AND SHELLAC EFFECTIVELY PRESERVE CHAYOTE (*Sechium edule* (Jacq.) Sw. var. *virens levis*) FRUITS DURING STORAGE

Érika María **Cortés-Huerta**[1], Adriana **Contreras-Oliva**[1]*, José Andrés **Herrera-Corredor**[1], Juan Valente **Hidalgo-Contreras**[1], Josafhat **Salinas-Ruiz**[1], Fernando Carlos **Gómez-Merino**[2], Diana Patricia **Uscanga-Sosa**[1]

[1]Colegio de Postgraduados Campus Córdoba. Carretera Córdoba-Veracruz km 348, Manuel León, Amatlán de los Reyes, Veracruz, Mexico. C. P. 94953.
[2]Colegio de Postgraduados Campus Montecillo. Carretera México-Texcoco km 36.5, Montecillo, Texcoco, State of Mexico, Mexico. C. P. 56264.
*Author for correspondence: adricon@colpos.mx

Citation: Cortés-Huerta ÉM, Contreras-Oliva A, Herrera-Corredor JA, Hidalgo-Contreras JV, Salinas-Ruiz J, Gómez-Merino FC, Uscanga-Sosa DP. 2024. Edible coatings based on beeswax and shellac effectively preserve chayote [*Sechium edule* (Jacq.) Sw. var. *virens levis*] fruits during storage. **Agrociencia** 58(7): 869-880. https://doi.org/ 10.47163/agrociencia.v58i7.3203

Editor in Chief:
Dr. Fernando C. Gómez Merino

Received: April 10, 2024.
Approved: November 05, 2024.
Published in Agrociencia: November 08, 2024.

ABSTRACT

Edible coatings are used to maintain overall quality and extend the shelf-life of fruit after harvest. The objective of this research was to evaluate the effect of edible coatings based on beeswax and shellac on the postharvest quality of fresh chayote [*Sechium edule* (Jacq.) Sw. var. *virens levis*] stored for 0, 8, 16, 24, and 32 days at 7 °C. The experiment was conducted with a completely randomized design with mixed effects and three replicates. Physicochemical analyses were carried out for color, texture, acidity, pH, weight loss, and CO_2 concentration. The applied coatings stabilized the physicochemical properties and reduced the weight loss percentage (1.8 to 3.4 %) of the chayotes during the storage period without creating an adverse effect compared to the control (4.1 %). The most effective coating (treatment 6) had the highest concentration of beeswax and the lowest concentration of shellac, forming an effective barrier against gases and water vapor.

Keywords: color, weight loss, respiration rate, Hydroxypropyl methylcellulose.

INTRODUCTION

Mexico is one of the world's leading exporting countries of chayote (*Sechium edule* (Jacq.) Sw.), along with Costa Rica, Brazil, and the Dominican Republic (Rojas-Sandoval, 2018). Veracruz is the Mexican state with the largest chayote production (156 519.53 Mg annually) (SIAP, 2016). The commercial exploitation of this fruit is affected by microorganisms, mechanical damage, and natural decay processes such as dehydration, weight loss, wilting, and sprouting symptoms (del Ángel-Coronel *et al*., 2018). These factors lead to economic losses and increased prices for the fruit.

During postharvest, chayote fruits may present defects and undergo natural deterioration processes. Dehydration is reflected in weight loss and changes in

appearance. To delay this, it is recommended to process at low temperatures ranging from 8 to 10 °C. However, temperatures below 7 °C can cause chilling injury, resulting in pitting, dark depressions in the skin, dehydration, and necrosis (Cadena-Iñiguez *et al*., 2006). Additionally, exposure to ethylene can promote vivipary and premature senescence (Khan *et al*., 2024). Common problems in fruit production include lack of color or sheen in the epidermis, white spots from shading, twin-fused fruit, bruising (mechanical damage), sunburn, improper shape and size, and leaf spotting (GISeM, 2011).

Chayote fruit is susceptible to rubbing, compression, and impact during postharvest and transport due to its thin epidermis. These wounds make the fruit vulnerable to attack by microorganisms such as *Didymella bryoniae*, *Fusarium oxysporum*, *F. solani*, and *Chaetomium globosum*, which cause rotting symptoms in the epidermis and mesocarp (Romero-Velazquez *et al*., 2015).

A common preservation technique in packing houses is to individually wrap chayote fruits in a polyethylene bag to prevent mechanical damage and extend their shelf-life. However, brokers have rejected the product due to the presence of fungal diseases caused by the high humidity conditions inside the plastic packaging. Furthermore, the use of this material significantly contributes to environmental pollution. An alternative to polyethylene bags is the use of edible coatings (ECs) that adhere to and wrap around the product, creating a semi-permeable barrier to gases (O_2 and CO_2) and water vapor (Mohamed *et al*., 2020).

After harvest, horticultural products undergo metabolic processes such as respiration, transpiration, growth, ripening, and senescence. Edible coatings can be used to partially or completely halt these processes, including the application of natural preservatives that do not harm the health of consumers (García-García and Searle, 2016) or the environment. These preservation techniques allow obtaining good-quality products and extending the shelf-life of the fruit. ECs are mainly based on proteins, lipids, and polysaccharides; these additives are biodegradable, food-grade products, and are considered safe for human consumption (Nawab *et al*., 2017).

Polysaccharides provide structure to the fruit (exocarp) and allow gas permeability (O_2 and CO_2). They are flexible film formers, do not emit odor, and are tasteless, colorless, biodegradable, and water-soluble. However, they are considered inefficient against fruit moisture (Arnon *et al*., 2014; Danalache *et al*., 2016). On the other hand, lipids confer resistance to water vapor and provide greater gloss in coated fruits (Nawab *et al*., 2017). Both compounds provide ECs with good functional properties for the product and contribute to extending the shelf-life of the fruits. Among the most commonly used ingredients for the production of ECs are beeswax and shellac; the former forms a good barrier against moisture, and the latter provides firmness and improves gas permeability (Byun *et al*., 2012).

The objective of this study was to evaluate the effect of edible coatings based on beeswax-shellac on the postharvest quality of fresh chayote (*S. edule* var. *virens levis*). The hypothesis is that edible coatings based on beeswax and shellac will effectively

stabilize the physicochemical properties of fresh chayote and reduce weight loss during cold storage, with higher concentrations of beeswax providing better preservation of quality and shelf-life by forming a more effective barrier against gas exchange and water vapor loss.

MATERIALS AND METHODS

Chayote (*Sechium edule* (Jacq.) Sw. var. *virens levis*) samples were collected from the producing area of the municipality of Coscomatepec, Veracruz, Mexico. The criteria for selecting fruit samples were uniformity in maturity, green color, and size, in accordance with the NMX-FF-047-SCFI-2003 Standard (DOF, 2003). The fruits were stored in a refrigerator with a transparent glass door at 7 °C and 60 % relative humidity, indirectly exposed to natural light.

United States Pharmaceutical (USP) grade beeswax, USP grade oleic acid, E-904 shellac, USP grade glycerol, and sugarcane alcohol were obtained from "Droguería Cosmopolita S.A." (Mexico City, Mexico). Hydroxypropyl methylcellulose (HPMC) was donated by "Química Carayani S.A. de C.V." (Mexico City, Mexico). Food-grade reagents were used.

Coating formulations

The edible coating (EC) treatments were formulated using glycerol and oleic acid as a plasticizer and emulsifier, respectively. The beeswax-shellac ratios were 3:1 and 1:3 (dry basis) (Table 1), while the remaining ingredients were kept constant throughout the treatments. **T**he aqueous solutions were prepared using beeswax and shellac at 2 and 4 % solids content (v/v), respectively, following the Fagundes *et al*. (2014) method with some modifications. HPMC was hydrated in hot water at 90 °C for 15 min, then cooled to 20 °C before adding beeswax, shellac, glycerol, oleic acid, and alcohol. The solutions were heated again to 90 °C with stirring.

Table 1. Formulations of edible coatings based on beeswax and shellac applied to chayote fruits (*Sechium edule* (Jacq.) Sw. var. *virens levis*).

Treatment (T)- coating formulation	Beeswax (BW) (% w/w)	Shellac (S) (% w/w)	Solids content (SC) (%)
T1- without coating (control)	-	-	-
T2- polyethylene bag	-	-	-
T3- 1:3 BW-S_2 % SC	1	3	2
T4- 1:3 BW-S_4 % SC	1	3	4
T5- 3:1 BW-S_2 % SC	3	1	2
T6- 3:1 BW-S_4 % SC	3	1	4

To successfully mix the shellac with the other ingredients, the Byun *et al*. (2012) technique was used, which involves dissolving shellac in alcohol and stirring for 24 h. The mixture was then filtered using Whatman® #5 filter paper and mixed for 1 min at 12 000 rpm, followed by 3 min at 22 000 rpm using an Ultra Turrax® dispersing instrument (IKA® T10 basic, China). The samples were then cooled to 30 °C for 25 min with gentle stirring to ensure complete hydration. Finally, the ECs were stored at 5 °C for one day to verify the stability of the formulations.

Coating application

The application of each coating formulation (Table 1) was carried out by immersion for 1 min (Moalemiyan and Ramaswamy, 2012). Distilled water was used as a control solution, and a batch of uncoated fruits was left placed inside a polyethylene bag. All treated fruits were cold-stored at 7 °C for 0, 8, 16, 24, and 32 d (Poverenov *et al*., 2014). At the end of each storage period, the corresponding physicochemical analyses were carried out in triplicate. Each treatment involved a total of 63 chayote fruits.

Fruit evaluation

Color

Color was measured using a KONICA MINOLTA® colorimeter (model CR-400, Japan), where L*, a*, and b* values were obtained on the CIELAB scale. Each measurement was taken at three different sites in each chayote fruit, and data were reported as chroma (C*), lightness (L*), and color index (CI) (Moalemiyan and Ramaswamy, 2012).

Acidity and pH

The titratable acidity (TA) was determined according to Montecinos-Pedro *et al*. (2019), with slight modifications. Juice was extracted from the fruits of each treatment. Then, 15 mL were taken from each sample and titrated with 0.1 N NaOH using two drops of phenolphthalein as an indicator. TA was expressed as % of citric acid per L. The pH of the juice was determined using a potentiometer (Thermo Scientific®, Orion Star, Singapore) (Islam *et al*., 2018).

Weight loss

Weight loss was determined gravimetrically using an analytical balance (OHAUS® RANGER, Germany) (Poverenov *et al*., 2014), and the results were expressed as a percentage of weight loss compared to the initial weight of the fresh fruit:

$$\%\ Physiological\ weight\ loss = \left(\frac{Pi - Pf}{Pf}\right) * 100$$

where Pi = initial weight of the fresh fruit; and Pf = final weight of the coated fruit.

Firmness

Firmness was determined using a texture analyzer (SHIMADZU® EZ-S 500 N, Japan) equipped with a 3 mm diameter cylindrical punch. Results were expressed as the maximum force (N) needed to penetrate the fruit with skin (penetration) and without skin (puncture), as described by Aung *et al*. (1996) with some modifications. The distance traveled for both determinations was 10 mm at a speed of 5 mm s^{-1}.

Respiration rate

The respiration rate was determined as described by Márquez *et al*. (2009). Two fruits from each treatment were weighed and placed in hermetically sealed containers for 24 h. Data was collected using a CO_2 sensor (MQ-135 gas sensor, OKstar brand, Guangdong, China) and expressed as μg of CO_2 kg^{-1} h^{-1}.

Statistical analysis

The experiment was conducted using a completely randomized design with mixed effects and three replicates. The treatment followed a 6 x 5 factorial structure. The sample size consisted of 63 chayote units per treatment. The distribution of chayotes, according to the response variables measured, was as follows: for color, acidity, pH, and firmness, 45 chayotes were used per treatment across five time points (nine for each time); for the respiration variable, 10 chayotes were used; and for the weight loss variable, eight chayotes were used. The statistical model of the experiment was as follows:

$$y_i k_j = \mu + \alpha_i + \beta_j + (\alpha\,\beta)_{ij} + e_{ijk}$$

with $i = 1, 2, 3, 4, 5, 6$; $j = 1, 2, 3, 4, 5$ and $k = 1, 2, 3$

where y_{ijk} is the response variable of the ith treatment at the jth time and the kth replicate; μ is the global mean; α_i is the fixed effect of the ith treatment; β_j is the random effect of the jth time; $(\alpha\beta)_{ij}$ is the combined effect of the interaction of the ith treatment with the jth time; and e_{ijk} is the random experimental error, which is assumed to be independent, identically, and normally distributed with zero mean and variance $\sigma^2_{\alpha\beta}$. The analysis was carried out with the GLIMMIX procedure of the SAS version 9.4 statistical package (SAS Institute, Cary, NC, USA). Means were compared using the Tukey test.

RESULTS AND DISCUSSION

Color

The values of C*, L*, and CI remained constant after day 8 in all treatments. No significant difference was found among treatments (Table 2). All treatments exhibited

Table 2. Color parameters of chayote fruit (*Sechium edule* (Jacq.) Sw. var. *virens levis*) stored at 7 °C for 32 days, evaluated with and without coatings.

Treatments	Color index	Lightness (L*)	Chroma (C*)
T1- without coating (control)	-8.45 ± 0.36 a	60.23 ± 1.98 a	39.00 ± 1.21 a
T2- polyethylene bag	-9.22 ± 0.36 a	57.28 ± 1.98 a	37.60 ± 1.21 a
T3- 1:3 BW-S_2 % SC	-9.22 ± 0.36 a	54.44 ± 1.98 a	35.30 ± 1.21 a
T4- 1:3 BW-S_4 % SC	-9.20 ± 0.36 a	55.46 ± 1.98 a	36.82 ± 1.21 a
T5- 3:1 BW-S_2 % SC	-9.38 ± 0.36 a	55.84 ± 1.98 a	35.88 ± 1.21 a
T6- 3:1 BW-S_4 % SC	-9.35 ± 0.36 a	55.55 ± 1.98 a	36.04 ± 1.21 a

Means with the same letters are not statistically different ($p \leq 0.05$). BW: beeswax; S: shellac; SC: solids content.

a decrease in color over time. These findings show that none of the coatings had an adverse effect on the color of the chayote fruit.

The color index is considered a quality control variable. The evolution in the ripening of the chayote fruits was measured by the color index (CI), and it was also used to describe the color of the chayote epicarp. In most cases, skin color changes as the fruit ripens or matures, making it a useful ripening index for producers to establish the harvest date. Color charts are available for different cultivars for this purpose (FAO, 2003).

The CI ranges from -8.45 to -9.38 (Table 2). According to Machado-Molina *et al*. (2015), this indicates that the colors go from deep green to yellowish green. Fagundes *et al*. (2014) reported that the use of HPMC and beeswax in different concentrations reduces the respiration rate, leading to a slight increase in the color of some fruits, but with the treatments used in this research, this increase was not achieved. Similar results were observed by Li *et al*. (2018), who applied commercial wax to pineapple fruits and found no significant differences compared to the control.

Acidity and pH

The pH and TA variables (expressed as the percentage of citric acid) were determined for all coated and uncoated treatments stored at 7 °C (Table 3). The TA and pH values ranged from 0.21 to 0.36 % and 6.5 to 6.7, respectively. However, the control (T1) had small differences, showing from day 16 a progressive decrease in TA, while pH levels remained constant throughout the study period. Andrade *et al.* (2013) and Fagundes *et al.* (2014) point out that the TA and pH parameters are not usually affected by ECs because the internal quality of the fruit depends not only on the coating, but also on the harvest process, the ripening index, the variety, and the weather conditions.

These results coincide with those reported by Li *et al*. (2018), who found that the higher the amount of wax, the higher the TA inhibition. Wax maintains the respiration rate and therefore limits the excessive consumption of citric acid with respiration. Cadena-

Table 3. Acidity and pH of chayote fruit (*Sechium edule* (Jacq.) Sw. var. *virens levis*) with and without coating, stored at 7 °C for 32 days.

Treatments	pH	Acidity (% of citric acid per L)
T1- without coating (control)	6.47±0.06 b	0.28±0.02 ab
T2- Polyethylene bag	6.50±0.06 b	0.36±0.02 a
T3- 1:3 BW-S_2 % SC	6.58±0.06 ab	0.29±0.02 ab
T4- 1:3 BW-S_4 % SC	6.63±0.06 ab	0.28±0.02 ab
T5- 3:1 BW-S_2 % SC	6.65±0.06 ab	0.24±0.02 b
T6- 3:1 BW-S_4 % SC	6.70±0.06 a	0.21±0.02 b

Means with the same letters are not statistically different ($p \leq 0.05$). BW: beeswax; S: shellac; SC: solids content.

Iñiguez *et al*. (2006, 2011) found values between 0.039 and 0.041 % of citric acid at different temperatures, and there were no significant differences between treatments. It is thus confirmed that the use of beeswax-shellac-based ECs improved the citric acid percentage and stabilized pH values in chayote fruits.

All ECs applied to the fruits were effective in maintaining the metabolic process during the storage period. According to Nawab *et al*. (2017), citric acid and malic acid are the substrates involved in the respiration process of climacteric fruits, so a decrease during the storage period is to be expected, but these authors observed that the amount of TA and pH in the different treatments remained constant during the test period. Fagundes *et al*. (2014), on the other hand, observed a relationship between pH increase and citric acid loss, whereas in the present investigation the results obtained for TA remained constant during the analysis period, as did pH.

Weight loss

The weight loss percentage of the different treatments, with and without coating, ranged from 1.8 to 3.4 % and 2.6 to 4.1 %, respectively (Figure 1A). In relation to the T3, T4, T5, and T6 treatments (with coating) and the T2 treatment (polyethylene bag), no significant differences were found. In general, the treatment that created the best barrier against moisture was the 3:1 BW-S coating with 4 % SC (T6). This treatment significantly reduced the weight loss of the coated chayote fruits during storage compared to the control.

However, the coatings with the addition of beeswax prevented weight loss of the chayote fruits to a lesser extent than the control treatment (T1) but still presented more significant weight loss than the 3:1 BW-S coating with 4 % SC (T6) (Figure 1A). This indicates that the weight loss percentage decreased as the content of hydrophobic compounds increased. This coincides with Navarro-Tarazaga *et al*. (2008), who report that an increase in beeswax content creates a more effective barrier to weight loss by providing greater resistance to water movement through the fruit epicarp.

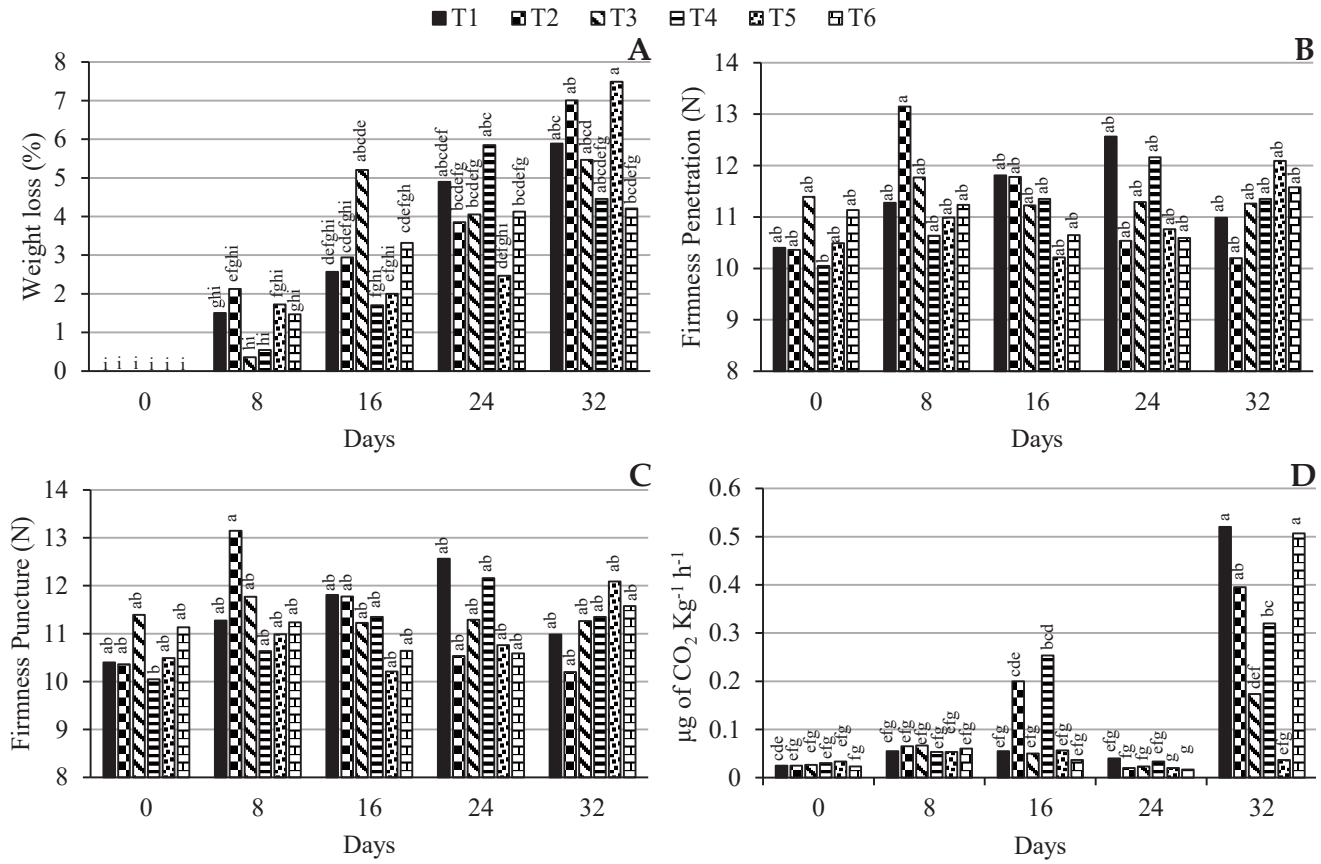

Figure 1. Fruit parameter values in chayote fruits with and without edible coatings stored at 0, 8, 16, 24, and 32 days at 7 °C. A: Weight loss; B: peel firmness (penetration); C: pulp firmness (puncture); D: respiration rate. Means with the same letters are not statistically different ($p \leq 0.05$). T1: control, fruits without any coating; T2: polyethylene bag; T3: 1:3 BW-S_2 % SC; T4: 1:3 BW-S_4 % SC; T5: 3:1 BW-S_2 % SC; T6: 3:1 BW-S_4 % SC.

Similar results were reported by Cadena-Iñiguez *et al*. (2006), who used ECs and commercial waxes and found weight loss values of 3.7 to 13.6 %. Also, the Interdisciplinary Research Group on *S. edule* in Mexico (GISeM, 2011) reported that the weight loss of fresh uncoated chayotes of the *virens levis* variety ranged between 8 and 10 % after harvest. Aung *et al*. (1996) indicated that the weight loss percentage in chayote fruits covered with edible films ranged from 0.02 to 40 %. It is thus confirmed that the use of beeswax and shellac as additives creates a more effective barrier against moisture loss in chayote fruits compared to commercial waxes. Additionally, seed germination did not occur at any point during the experiment, as the storage temperature of 7 °C prevented sprouting.

Firmness

The penetration (Figure 1B) and puncture tests (Figure 1C) in chayote fruit samples with and without EC indicated that all treatments maintained the firmness of the samples during the storage period. There were no significant differences among treatments with and without EC, since the coatings used did not affect the fruit epicarp over time. Similar results were found by Aung *et al*. (1996), who reported a pulp (puncture) value of 12.8 N and a skin firmness (penetration) of 19 N. In our research, the firmness of the chayote peel ranged from 12.7 to 13.5 N and the firmness of the pulp varied from 10.8 to 11.8 N; the little difference from our texture values not only depends on the EC applied but also on other factors such as the chayote variety, weather conditions, and storage time. Fagundes *et al*. (2014) indicated that ECs based on beeswax and shellac show high water vapor permeability during storage time due to the permanence of a saturated internal atmosphere, which controls enzymatic activities that improve fruit firmness.

Respiration rate

According to the classification proposed by GISeM (2011), chayote is a fruit with a low respiration rate, having values of 5–10 mg CO_2 kg^{-1} h^{-1} (1.389 μg CO_2 kg^{-1} h^{-1}) at 5 °C. The results obtained show that, until day 24, all treatments stored at 7 °C kept the emitted CO_2 levels stable, that is, the metabolic activity of the chayote fruit remained stable. However, on day 32, it was observed that all treatments drastically increased CO_2 levels except for T5 (3:1 BW-S_2 % SC), which, in addition to stabilizing CO_2 levels throughout the analysis period, also showed a significant difference compared to the other treatments (Figure 1D).

Cadena-Iñiguez *et al.* (2006) reported CO_2 values between 0.86 and 1.3 μg kg^{-1} s^{-1} of CO_2 (3096 and 4680 μg kg^{-1} h^{-1} of CO_2) in chayotes coated with commercial waxes and plastic films and stored at 10 °C for 28 days. For comparison, in our results, the respiration rate of chayote fruits with and without EC was 0.006 to 0.014 and 0.007 to 0.144 μg kg^{-1} s^{-1} (21.6 to 50.4 and 25.2 to 518.4 μg kg^{-1} h^{-1}), respectively.

Based on these results, the EC formulations applied to chayote fruits were effective in reducing the respiration rate. Degradation of organic reserves (proteins, carbohydrates, and fats) leads to the release of metabolic energy from the fruits. The formulations based on beeswax and shellac modified the internal atmosphere of the fruits, slowing the senescence process, respiration, and transpiration of the coated fruits. Chitravathi *et al*. (2014) reported that fruits with low gas emissions reduce enzymatic activities that cause deterioration of fruit tissues, thereby retaining firmness during storage.

CONCLUSIONS

The physicochemical properties of chayote fruits were retained after the application of edible coatings, and no adverse effects were observed compared to the control group. All of the edible coatings reduced the weight loss percentage of the fruits while

maintaining stable titratable acidity and pH. The T5 coating, which consisted of a 3:1 mixture of beeswax and shellac with 2 % solids content, was the most effective in reducing the respiration rate. The T6 coating (3:1 beeswax-shellac with 4 % solids content) was the most effective, creating a barrier against gases and water vapor due to its high proportion of beeswax and low amount of shellac. Edible coatings formulated with beeswax-shellac can preserve chayote fruits without compromising their quality.

ACKNOWLEDGEMENTS

The authors thank the Consejo Nacional de Humanidades, Ciencias y Tecnologías (CONAHCYT) for the support grant awarded to EMCH. They are also grateful for the support provided by the LGAC-2: Innovation and Development of Agrifood Processes for Social Welfare, a component of the Sustainable Agrifood Innovation Program of the Postgraduate College Cordoba Campus, and by the chayote producers and packers in the producing area of the Municipality of Coscomatepec, Veracruz.

REFERENCES

Andrade J, Acosta D, Bucheli M, Luna GC. 2013. Elaboración y evaluación de un recubrimiento comestible para la conservación postcosecha del tomate de árbol *Cyphomandra betacea* Cav. Sendt. Revista de Ciencias Agrícolas 30 (2): 60–72.

Arnon H, Zaitsev Y, Porat R, Poverenov E. 2014. Effects of carboxymethyl cellulose and chitosan bilayer edible coating on postharvest quality of citrus fruit. Postharvest Biology and Technology 87: 21–26. https://doi.org/10.1016/j.postharvbio.2013.08.007

Aung LH, Harris CM, Rij RE, Brown JW. 1996. Postharvest storage temperature and film wrap effects on quality of chayote, *Sechium edule* Sw. Journal of Horticultural Science 71 (2): 297–304. https://doi.org/10.1080/14620316.1996.11515408

Byun Y, Ward A, Whiteside S. 2012. Formation and characterization of shellac-hydroxypropyl methylcellulose composite films. Food Hydrocolloids 27 (2): 364–370. https://doi.org/10.1016/j.foodhyd.2011.10.010

Cadena-Iñiguez J, Arévalo-Galarza MDL, Ruiz-Posadas LM, Aguirre-Medina JF, Soto-Hernández M, Luna-Cavazos M, Zavaleta-Mancera HA. 2006. Quality evaluation and influence of 1-MCP on *Sechium edule* (Jacq.) Sw. fruit during postharvest. Postharvest Biology and Technology 40 (2): 170–176. https://doi.org/10.1016/j.postharvbio.2005.12.013

Cadena-Iñiguez J, Soto-Hernández M, Arévalo-Galarza ML, Avendaño-Arrazate CH, Aguirre-Medina JF, Ruiz-Posadas LM. 2011. Caracterización bioquímica de variedades domesticas de chayote *Sechium edule* (Jacq.) Sw. comparadas con parientes silvestres. Revista Chapingo Serie Horticultura 17 (2): 45–55.

Chitravathi K, Chauhan OP, Raju PS. 2014. Postharvest shelf-life extension of green chillies (*Capsicum annuum* L.) using shellac-based edible surface coatings. Postharvest Biology and Technology 92: 146–148. https://doi.org/10.1016/j.postharvbio.2014.01.021

Danalache F, Carvalho CY, Alves VD, Moldão-Martins M, Mata P. 2016. Optimisation of gellan gum edible coating for ready-to-eat mango (*Mangifera indica* L.) bars. International Journal of Biological Macromolecules 84: 43–53. https://doi.org/10.1016/j.ijbiomac.2015.11.079

del Ángel-Coronel OA, León-García E, Vela-Gutiérrez G, Rojas-Reyes JO, Gómez-Lim MA, García HS. 2018. Lipoxygenase activity associated to fruit ripening and senescence in chayote (*Sechium edule* Jacq. Sw. cv. "*virens levis*"). Journal of Food Biochemistry 42 (1): e12438. https://doi.org/10.1111/jfbc.12438

DOF (Diario Oficial de la Federación). 2003. Norma Mexicana NMX-FF-047-SCFI-2003. Productos alimenticios no industrializados para consumo humano, hortalizas frescas-chayote (*Sechium edule*). Gobierno de México. Secretaría de Economía. Ciudad de México, México.

Fagundes C, Palou L, Monteiro AR, Pérez-Gago MB. 2014. Effect of antifungal hydroxypropyl methylcellulose-beeswax edible coatings on gray mold development and quality attributes of cold-stored cherry tomato fruit. Postharvest Biology and Technology 92: 1–8. https://doi.org/10.1016/j.postharvbio.2014.01.006

FAO (Food and Agriculture Organization of the United Nations). 2003. Handling and preservation of fruits and vegetables by combined methods for rural areas. FAO Agricultural Services Bulletin 149. Rome, Italy. https://www.fao.org/3/y4358E/y4358e00.htm#Contents (Retrieved: September 2024).

García-García R, Searle SS. 2016. Preservatives: Food use. *In* Caballero B, Finglas PM, Toldrá F. (eds.), Encyclopedia of Food and Health. Academic Press: Cambridge, MA, USA, pp: 505–509. https://doi.org/10.1016/B978-0-12-384947-2.00568-7

GISeM (Grupo Interdisciplinario de Investigación en *Sechium edule* en México). 2011. Rescatando y aprovechando los recursos fitogenéticos de Mesoamérica, Volumen 3. Chayote: manejo postcosecha. Colegio de Postgraduados: Montecillo, México. 29 p.

Islam S, Kumar A, Kumar Dash K, Alom S. 2018. Physicochemical analysis and nutritional properties of fresh, osmo-dehydrated and dried chayote (*Sechium edule* L.). Journal of Postharvest Technology 6 (2): 49–56.

Khan S, Alvi, AF, Khan NA. 2024. Role of ethylene in the regulation of plant developmental processes. Stresses 4 (1): 28–53. https://doi.org/10.3390/stresses4010003

Li X, Zhu X, Wang H, Lin X, Lin H, Chen W. 2018. Postharvest application of wax controls pineapple fruit ripening and improves fruit quality. Postharvest Biology and Technology 136: 99–110. https://doi.org/10.1016/j.postharvbio.2017.10.012

Machado-Molina, García-Pereira A, Machado-García N. 2015. Sistema automatizado para la determinación del estado de maduración en fruta bomba. Revista Ciencias Técnicas Agropecuarias 24: 56–61.

Márquez CJC, Cartagena JRV, Pérez-Gago MB. 2009. Efecto de recubrimientos comestibles sobre la calidad en poscosecha del níspero japonés (*Eriobotrya japonica* T.). VITAE, Revista de la Facultad de Química Farmacéutica 16 (3): 304–310.

Moalemiyan M, Ramaswamy HS. 2012. Quality retention and shelf-life extension in Mediterranean cucumbers coated with a pectin-based film. Journal of Food Research 1 (3): 159–168. https://doi.org/10.5539/jfr.v1n3p159

Mohamed SAA, El-Sakhawy M, El-Sakhawy MAM. 2020. Polysaccharides, protein and lipid-based natural edible films in food packaging: A review. Carbohydrate Polymers 238: 116178. https://doi.org/10.1016/j.carbpol.2020.116178

Montecinos-Pedro LA, Arévalo-Galarza ML, García-Osorio C, Cadena-Iñiguez J, Ramírez-Guzmán ME. 2019. Calidad poscosecha de frutos de chayote almacenados a baja temperatura. Revista Mexicana de Ciencias Agrícolas 10 (5): 1157–1166. https://doi.org/10.29312/remexca.v10i5.1437

Navarro-Tarazaga ML, Sothornvit R, Pérez-Gago MB. 2008. Effect of plasticizer type and amount on hydroxypropyl methylcellulose-beeswax edible film properties and postharvest quality of coated plums (Cv. *Angeleno*). Journal of Agricultural and Food Chemistry 56 (20): 9502–9509. https://doi.org/10.1021/jf801708k

Nawab A, Alam F, Hasnain A. 2017. Mango kernel starch as a novel edible coating for enhancing shelf-life of tomato (*Solanum lycopersicum*) fruit. International Journal of Biological Macromolecules 103: 581–586. https://doi.org/10.1016/j.ijbiomac.2017.05.057

Poverenov E, Zaitsev Y, Arnon H, Granit R, Alkalai-Tuvia S, Perzelan Y, Weinberg T, Fallik E. 2014. Effects of a composite chitosan–gelatin edible coating on postharvest quality and storability of red bell peppers. Postharvest Biology and Technology 96: 106–109. https://doi.org/10.1016/j.postharvbio.2014.05.015

Rojas-Sandoval J. 2018. *Sechium edule* (chayote). CABI Compendium 49493. https://doi.org/10.1079/cabicompendium.49493

Romero-Velazquez SD, Tlapal-Bolaños B, Cadena-Iñiguez J, Nieto-Ángel D, Arévalo-Galarza ML. 2015. Hongos causantes de enfermedades postcosecha en chayote (*Sechium edule* (Jacq.) Sw.) y su control *in vitro*. Agronomia Costarricense 39 (2): 19–32.

SIAP (Servicio de Información Agroalimentaria y Pesquera). 2016. Anuario estadístico de la producción agrícola. Gobierno de México. Servicio de Información Agroalimentaria y Pesquera. Ciudad de México, México. https://nube.siap.gob.mx/cierreagricola/ (Retrieved: September 2024).

Agrociencia

DEVELOPMENT AND EVALUATION OF A MULTI-CHAMBER ENVIRONMENTAL CONTROL SYSTEM

Raúl Alfonso **Rodriguez-Ruelas**[1], José Alfredo **Carrillo-Salazar**[1*], Juan Manuel **González-Camacho**[1], Nicacio **Cruz-Huerta**[1], Reyna Isabel **Rojas-Martínez**[1], Manuel **Livera-Muñoz**[1], Francisco **Carrasco-Hernández**[2], Noé **López-Martínez**[3]

[1]Colegio de Postgraduados Campus Montecillo. Carretera México-Texcoco km 36.5, Montecillo, Texcoco, State of Mexico, Mexico. C. P. 56264.
[2]Universidad Tecnológica de Durango. Carretera Durango–Mezquital km 4.5, Gabino Santillán, Durango, Mexico. C. P. 34308.
[3]Universidad Autónoma Chapingo. Departamento de Fitotecnia. Carretera México-Texcoco km 38.5, Chapingo, Texcoco, State of Mexico, Mexico. C. P. 56227.
* Author for correspondence: asalazar@colpos.mx

Citation: Rodriguez-Ruelas RA, Carrillo-Salazar JA, González-Camacho JM, Cruz-Huerta N, Rojas- Martínez RI, Livera-Muñoz M, Carrasco-Hernández F, López-Martínez N. 2024. Development and evaluation of a multi-chamber environmental monitoring system.
Agrociencia 58(7): 881-895. https://doi.org/ 10.47163/agrociencia.v58i7.3122

Editor in Chief:
Dr. Fernando C. Gómez Merino

Received: November 28, 2023.
Approved: September 04, 2024.
Published in Agrociencia: October 22, 2024.

ABSTRACT

Growth chambers are control devices used in plant research. However, their high costs limit their application to a single environment, which compromises their efficiency for the generation of experimental data. The objective of this research was to design, construct, and assess the performance of a multi-chamber environmental control system capable of regulating both air temperature (*AT*) and relative humidity (*RH*). The evaluation was carried out using *Syngonium podophyllum* Schott plants. Three constant target temperature values (18, 23, and 40 °C) were established, together with a target RH value of 60 %. *AT* and *RH* data were recorded every 4 min for three days. The system was built with 15 growth chambers and the following devices: output (*AT*, *RH*, and lighting control), input (sensors), and central control managed by two Arduino® Mega 2560 based microcontrollers, plus a programmable logic controller. Programming was done in open-source languages such as Arduino® and Python®. Results indicate that the absolute error (*AE*) and standard deviation (*SD*) in *AT* were higher when the target temperature was lower (*AE* = 0.59 °C and *SD* = 0.93 °C) compared to the other higher target temperatures (*AE* = 0.31 °C and *SD* = 0.43 °C at 23 °C, and *AE* = 0.25 °C and *SD* = 0.51 °C at 40 °C). On the other hand, the *AE* in *RH* increased as temperature increased, going from *AE* = 3.75 % and *SD* = 5.12 % at 18 °C, to *AE* = 9.23 % and *SD* = 10.77 % at 40 °C. The use of open-source technologies allowed the construction of a multi-chamber environmental control system capable of replicating controlled environments.

Keywords: growth chamber, controlled environments, open source, control, *Syngonium podophyllum* Schott.

INTRODUCTION

Growth chambers are useful devices in basic and applied research, as they allow the regulation of the growth and development environment of plants (Mitchell, 2022).

These control variables include relative humidity, temperature, CO_2 level, and the quality and quantity of electromagnetic radiation, as well as photoperiod (Grindstaff *et al*., 2019). In addition, they are critical in intensive crop production infrastructure, such as in vertical farms within the framework of controlled environment agriculture (Mitchell, 2022).

In the field of agricultural research, agencies such as the National Aeronautics and Space Administration (NASA) have invested in the development of growth chambers to grow plants under extreme conditions (Reed and Vanden Bosch, 2023). They are also used in speed breeding research and in various areas of plant physiology, such as climate change, as well as in molecular biology (Bhatta *et al*., 2021; Jarvis *et al*., 2021; Dasgupta and Robinson, 2022; He *et al*., 2022). However, they are expensive (Cazzola *et al*., 2020), and usually only one growth chamber can be controlled at a time, whereas it would be desirable to be able to experiment with them in a more affordable, efficient, and extensive manner.

In response to this problem, some researchers have designed and built environmental control systems based on open-source technologies. For example, Padmanabha and Streif (2019) propose a low-cost programmable system for studies on organisms such as plants, fungi, and insect larvae using open-source technology. This system consists of modular units with sensors to measure gases and environmental properties, as well as relays to control lighting. On the other hand, Arunachalam and Andreasson (2022) present a remote monitoring system designed for plant experimentation. This system uses low-cost hardware components and open-source software, allowing data storage and automatic reconfiguration.

This work describes the physical components that make up a multi-camera environmental control system, including the structure, input, output, and control devices, as well as the programs used (user interface and code in Arduino®), based on open-source platforms. The objectives of this research were to design, construct, and evaluate a multiple environmental control system and to determine the accuracy and precision of the system for controlling the temperature and relative humidity of each growth chamber. The hypothesis was that technology based on open-source code such as Arduino® and Python® enables the design, construction, and operation of devices following the "do it yourself" concept. These tools make it possible to incorporate control algorithms from other authors easily and without copyright infringement issues (Fuller *et al.*, 2021; Marchus *et al*., 2022).

MATERIALS AND METHODS

The multi-chamber environmental control system was built inside a warehouse located in the facilities of the Postgraduate College Campus Montecillo, in Texcoco, State of Mexico, Mexico. The materials required for the construction of the system are available at the following link: https://github.com/Rodriguez-Ruelas/SISTEMA-DE-CONTROL-AMBIENTAL-MULTICAMARA

Design of the device

The system was designed to simultaneously control air temperature (*AT*, °C), relative humidity (*RH*, %), and photoperiod in 15 growth chambers, taking into account four of the six components required in environmental control systems for agricultural projects (Vatistas *et al*., 2022): thermal insulation, air conditioning (A/C) equipment, lighting, and the environmental control unit. However, control of CO_2 concentration and nutrient supply was not included in this design. Unlike other environmental control equipment, our approach provides air flow in each chamber using a single A/C source.

Physical components

The system is made up of four physical components: structure, control devices, input devices, and output devices (Figure 1).

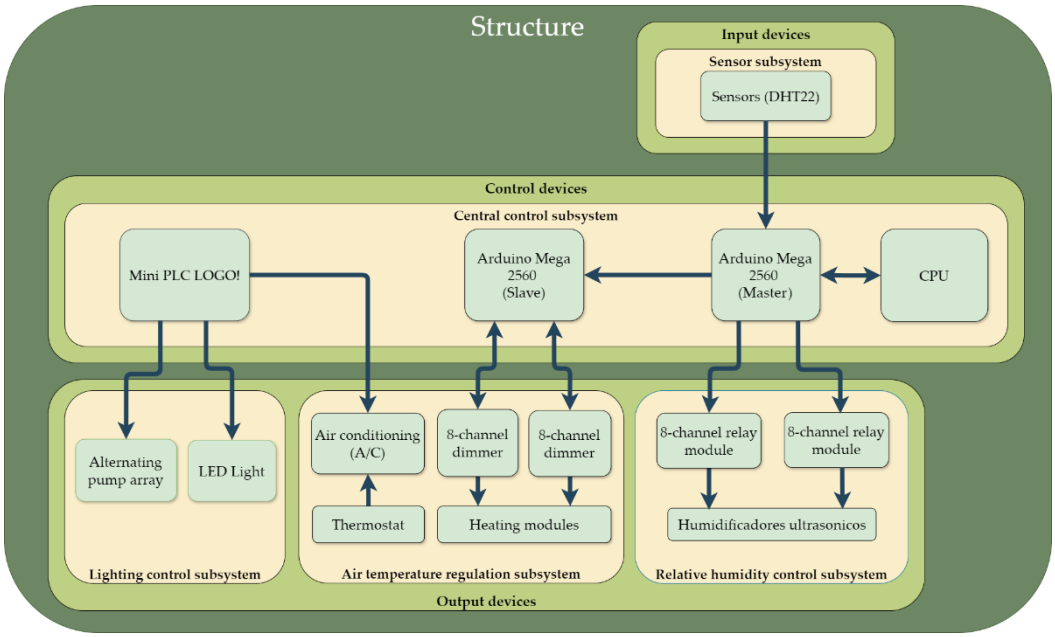

Figure 1. Physical components of the designed multi-chamber environmental control system, including input devices (sensors), output devices (air temperature (*AT*), relative humidity (*RH*), and lighting control subsystems), and central control devices (central control subsystem).

Control algorithms

The system operates through an application developed for the Windows® operating system. In addition, it includes two algorithms programmed in Arduino®, one for each microcontroller (master and slave), and the instructions for the programmable logic controller Mini PLC LOGO! (Siemens; Berlin, Germany) (Figure 2).

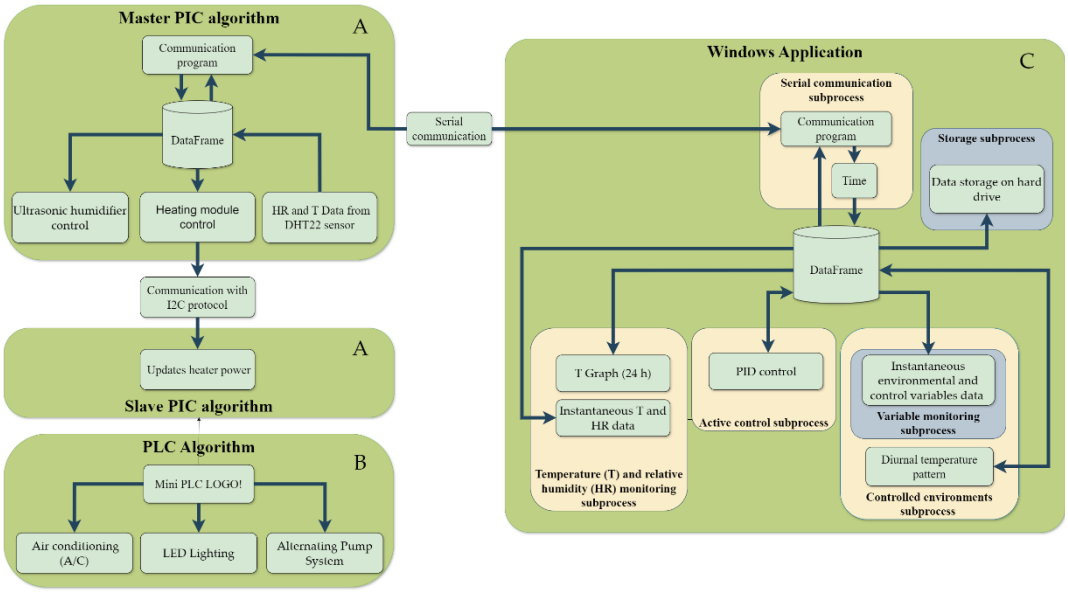

Figure 2. Flow chart of the control algorithms used in the multi-chamber environmental control system. A: Programmable integrated circuits (master and slave); B: programmable logic controller (Mini PLC LOGO!); C: graphical user interface.

Construction of the control system

Structure

The system consists of an angular iron frame with dimensions of 1.22 m long, 2.44 m wide, and 0.75 m high. The structure has 15 compartments or growth chambers organized in a 3 x 5 matrix arrangement. Each growth chamber was delimited with thermal insulation, forming a cube of 0.3 m per side (27 dm^3), excluding the volume of insulation. On the other hand, the lid was designed as a rectangular prism measuring 1.22 m in length, 2.44 m in width and 0.225 m in height. This cover serves several functions: it seals the growth chambers, serves as a base for fixing the lighting system, and acts as the outlet for the air coming from each growth chamber.

Central control subsystem

This subsystem has two microcontrollers: one master and one slave, based on the open-source Arduino® platform. The model used for both microcontrollers was the Mega2560 (Arduino; Ivrea, Italy), built from the ATmega2560 integrated circuit. The master microcontroller is connected to a computer (CPU) via a USB cable. It has 15 digital I/O ports configured as inputs for the DHT22 sensors and 16 digital I/O ports configured as outputs, connected to two mechanical relay modules to manage the switching on and off of the humidifiers. The slave microcontroller is connected to two

8-channel dimmer modules via 16 digital I/O ports configured as outputs. Attenuator modules are used to regulate the intensity of the AC voltage supplying the heating modules (Figure 4). The ignition of both the lighting subsystem and the alternating pumping arrangement for cooling the LEDs was managed by a programmable logic controller (Mini PLC LOGO!).

Sensor subsystem

A DHT22 sensor (Kuongshun Electronic; Shenzhen, China) was placed in each growth chamber to record *AT* and *RH* with an accuracy of ±0.5 °C and ±2 %, respectively. The resulting data were received by the master microcontroller.

Air temperature control subsystem

The *TA* regulating subsystem consists of two components: the cooling module and the heating module. The first consists of an LG® brand A/C unit with a capacity of 3516 kW. In addition, the subsystem has three 0.092 $m^3\ s^{-1}$ extractors (iPower; Beijing, China). A thermostat module with display (Steren; Mexico City, Mexico) was used to control the on/off of the compressor.

The heating module was constructed from a 10 cm ceramic insulating tube (No. 10). A 170 Ω nichrome wire resistor (0.1601 mm) was used to obtain an operation in the module from 0 to 127 V, with a maximum current of 0.74 A. The resistor was wound on a resistor holder constructed from ceramic insulating tube and attached to the inside of the tube by means of two screws with nuts that in turn serve the function of resistor pins. To withstand the high temperatures, the ceramic insulating tube was bonded with thermal silicone to a 25.4 mm coupling and a 25.4 mm hydraulic polyvinyl chloride (PVC) union nut.

The *AT* control process starts when the 16 °C air flow from the A/C coil passes through three lines of hydraulic PVC tubing (10.16 cm) and enters through the base of each chamber to the heating modules, where the air is heated to the target temperature (T_{Obj}). Each of these lines feeds five chambers, and the airflow in each line is regulated with a dimmer-operated exhaust fan RNL06-10Z (Leviton; New York, NY, USA). The hot air then exits through a duct located at the top of each chamber and is collected with 55 mm PVC pipe and released to the outside.

Relative humidity control subsystem

RH control was performed with 16 mm ultrasonic membrane humidifiers inside each growth chamber. This is important because the evaporator of the air conditioning system dehumidifies the air by cooling it (Daou *et al*., 2006).

Lighting control subsystem

A full-spectrum LED light chip for plant cultivation emitting 130 $\mu mol\ s^{-1}\ m^{-2}$ photosynthetic photon flux density at 380 nm (blue light) and 840 nm (red light) was installed in each growth chamber. The LEDs were fixed in copper tubing through

which water was recirculated with two 372.85 W peripheral pumps (Truper; Jilotepec, Mexico) that alternate their operation every 15 min to extract by conduction the heat produced by the LEDs and keep them within the operating temperature range. This cooling method is more efficient compared to the commercial solution of forced convection cooling (using a fan) with an aluminum heatsink attached to the back of the LED, which would increase the *AT* value surrounding the plants. In addition, cold air from the A/C was introduced through 10.16 cm tubing to the inside of the lid where the base of the LEDs is located.

Application for Windows

The application was programmed in Python® and PyQT5® languages. In addition, the simple-pid 1.0.1 library developed by Martin Lundberg, under license from the Massachusetts Institute of Technology (MIT), was used. This library implements a PID control (proportional (Kp), integrative (Ki), and derivative (Kd)) in each chamber in order to regulate the temperature. The Windows® application was installed on a desktop computer (CPU) and has two main functions: to establish bidirectional serial communication with the master microcontroller of the central control subsystem and to control environmental variables such as *AT* and *RH*. For this purpose, two user interfaces were designed: a window to monitor the current status and graphical records of the last 24 h of *RH* and *AT* in each growth chamber, and another interface to program the diurnal and nocturnal pattern of environmental variables. In particular, temperature programming can be performed using two options: maintaining a constant temperature or using an experimental curve, which consists of six set points.

Algorithms in Arduino

The programming of the Arduino® integrated circuits was performed in the Arduino IDE 2.2.1 development environment. The master microcontroller algorithm (Figure 2A) is responsible for establishing bidirectional serial communication with the Windows® application. Through this communication, the microprocessor algorithm receives the pulse width modulation (PWM, 0–255) values and the on/off status (0 or 1) of the humidifiers. It then provides the Windows application with the *AT* and *RH* values measured by the DHT22 sensors in each of the chambers. The master microcontroller also communicates with the slave microcontroller via the I2C (Inter-Integrated Circuit) protocol. Through this communication channel, the PWM values are transmitted to the attenuator modules to regulate the heating level.

PLC Algorithms

The Mini PLC (LOGO!) was programmed using LOGO! Soft Comfort V8.3. The algorithm is responsible for switching the water pumps on and off every 15 min, as well as switching the LEDs on and off.

Evaluation

Experimental conditions

In each growth chamber, a dwarf syngonium plant (*Syngonium podophyllum* Schott), selected because it is an adult plant of small size, was placed. Three constant target temperatures (T_{Obj}) were evaluated: 18, 23, and 40 °C, depending on the operating range of the equipment previously evaluated. The temperature of 23 °C was chosen because of its correspondence with the optimal growth range of dwarf syngnonium, which is between 22 and 25 °C (Salame and Zieslin, 1994; Chao *et al*., 2019). A photoperiod of 12 hours of light and 12 hours of darkness was maintained, with a target relative humidity (RH_{Obj}) of 60 %, which has been used as a standard for growth chamber evaluation (Jamhari *et al*., 2020). *AT* and *RH* data were recorded every 4 min for three days, for each chamber and T_{Obj}.

Evaluation metrics

Three hundred and sixty measurements per day were used to evaluate the precision and accuracy of *AT* and *RH* monitoring. The following statistical metrics were used: absolute error (*AE*) (Equation 1) and relative percent error (*RPE*) (Equation 2) to measure accuracy, and standard deviation (*SD*) (Equation 3) and coefficient of variation (CV, %) (Equation 4) to assess precision (Kokai *et al*., 2021).

$$AE = \sum_{i=1}^{n} |x_i - x_o| \tag{1}$$

where n is the total number of observations, x_i is the observed values, and x_o is the target value.

$$RPE = \sum_{i=1}^{n} \frac{|x_i - x_o|}{x_o} \tag{2}$$

$$SD = \sqrt{\frac{1}{n-1}\sum_{i=1}^{n}(x_i - \bar{x})^2} \tag{3}$$

where $\bar{x}$ is the arithmetic mean of the observed values.

$$CV = \left(\frac{SD}{\bar{x}}\right) \times 100\ \% \tag{4}$$

Similarly, the error (*ERR*) was calculated for the variables *AT* and *RH* (Equation 5). This analysis facilitated the identification of periods with positive or negative errors.

$$ERR_i = x_i - x_o \tag{5}$$

where ERR_i represents the error for the i-th observation.

The confidence interval (CI) for *AT* and *RH* was calculated using the following expression (Equation 6):

$$CI = \left(\bar{x} \mp Z_{\alpha/2}\frac{DS}{\sqrt{n}}\right) \tag{6}$$

where α is the significance level and $Z_{\alpha/2}$ is the critical value of the normal distribution.

RESULTS AND DISCUSSION

During the experimental phase, chambers 1 and 9 presented failures in the heater resistors, while chamber 5 had failures in the temperature sensor on the third day when the target temperature (T_{Obj}) was 40 °C. Because of this, the data corresponding to these chambers were eliminated (Table 1). Average air temperature values were recorded in the 15 chambers for three days, with T_{Obj} of 18, 23, and 40 °C (Table 1). When the target temperature was 18 °C, average maximum (chamber 10, day 1) and

Table 1. Average air temperature (°C) recorded during 24 h and its standard deviation (SD) in growth chambers with plants, evaluated at three target temperatures (n = 360 observations).

CN	18 °C			23 °C			40 °C		
	Day 1	Day 2	Day 3	Day 1	Day 2	Day 3	Day 1	Day 2	Day 3
2	18.47±0.98	18.05±0.28	18.39±0.62	22.97±0.44	22.95±0.42	22.86±0.52	39.83±0.29	39.63±0.61	39.66±0.69
3	18.64±1.22	18.04±0.25	18.54±0.76	23.02±0.32	23.01±0.28	23.00±0.26	40.02±0.38	40.02±0.30	39.97±0.62
4	18.93±1.83	18.02±0.12	18.58±0.84	23.00±0.26	23.02±0.26	23.00±0.20	39.97±0.38	40.00±0.24	39.99±0.47
5†	18.93±1.68	18.06±0.24	18.66±0.99	23.14±0.44	23.30±0.72	23.01±0.31	39.85±0.29	39.64±0.68	NA
6	18.25±0.62	18.01±0.21	18.18±0.34	23.00±0.39	23.00±0.35	23.01±0.30	40.01±0.26	40.01±0.28	39.98±0.59
7	18.29±0.73	18.00±0.15	18.15±0.38	22.99±0.21	23.00±0.20	23.03±0.25	40.01±0.10	40.00±0.11	39.96±0.52
8	18.67±1.16	18.09 ±0.40	18.55 ±0.87	23.04±0.47	23.04±0.53	23.01±0.47	40.04±0.45	40.01±0.36	40.12±0.86
10	19.00±1.70	18.04±0.19	18.63±0.91	23.16±0.46	23.24±0.60	23.00±0.18	39.90±0.34	40.00±0.40	39.98±0.61
11	18.42±0.90	18.02±0.19	18.30±0.53	22.96±0.53	22.92±0.54	22.80±0.65	39.83±0.50	39.91±0.46	39.77±0.79
12	18.68±1.20	18.08±0.27	18.58±0.84	23.00±0.32	23.02±0.39	22.93±0.49	40.00±0.12	39.95±0.19	39.91±0.67
13	18.69±1.26	18.04±0.39	18.55±0.89	23.03±0.56	23.02±0.57	23.00±0.59	40.00±0.27	39.98±0.31	39.93±0.81
14	18.96±1.59	18.09±0.28	18.76±1.05	23.05±0.41	23.09±0.49	23.03±0.42	40.00±0.19	40.00±0.15	39.92±0.67
15	18.46±1.00	18.01±0.19	18.27±0.56	22.98±0.31	23.01±0.30	23.05±0.32	39.69±0.48	39.55±0.69	39.84±0.72

CN: Chamber number; †: NA (value not available).

minimum (chamber 17, day 2) values of 19±1.7 and 18±0.15 °C, respectively, were observed, revealing a consistent deviation towards higher values. In contrast, at 23 and 40 °C, the maximum and minimum averages were 23.24±0.6 (chamber 10, day 2) and 22.8±0.64 °C (chamber 11, day 3), as well as 40.12±0.86 (chamber 8, day 3) and 39.55±0.69 °C (chamber 15, day 2), respectively.

Except when T_{Obj} was 18 °C, the error in *AT* increased during the light period, causing an increase of up to 6.5 °C (Figures 3A, 3B, and 3C). This behavior is attributed to the increase in daytime temperature outside the chambers, which generated an excessive demand on the air conditioning. On the other hand, when the chambers were set at T_{Obj} of 23 and 40 °C, it was found that the thermal disparity was less than 3 °C in some chambers (Figure 3), while in most of them the variations were less than 0.5 °C. Similarly, elevations or reductions of up to 2.5 °C were observed that were not necessarily associated with the light period (Figure 3).

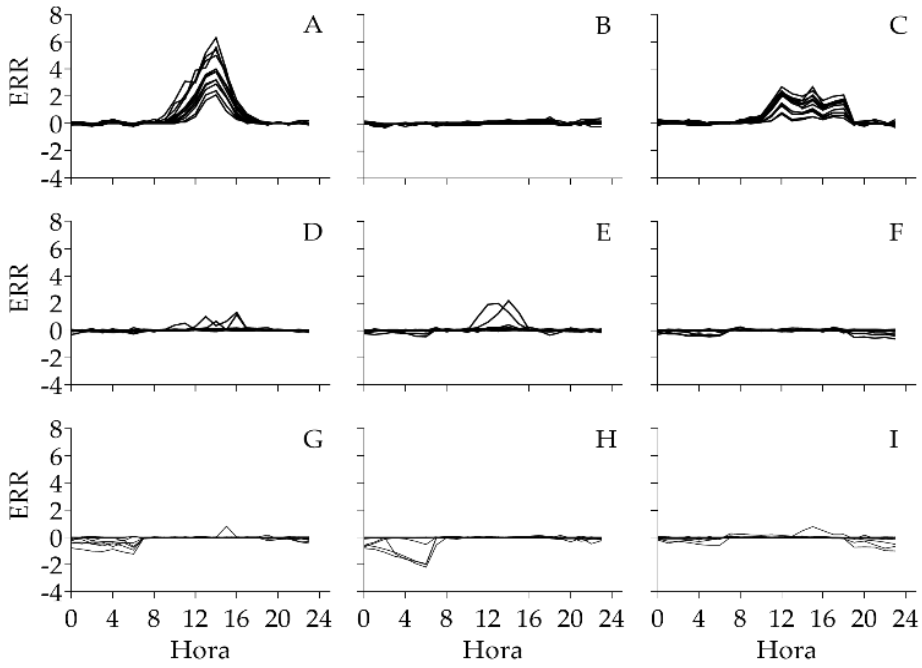

Figure 3. Error (*ERR*) between the target temperature (T_{Obj}) of 18 (A, B, and C), 23 (D, E, and F), and 40 °C (G, H, and I) and the air temperature (*AT*) in the growth chambers with plants, evaluated for three days.

The overall average *AT* plus its *SD* (23.02±0.43 °C) remained in the range of its respective T_{Obj} of 23±0.5 °C (Table 2). An improvement in the precision and accuracy of the system is observed as T_{Obj} increases (Table 2). Furthermore, the 95 % confidence interval (CI) for T_{Obj} confirms this trend, showing narrower intervals and higher precision with increasing T_{Obj}.

Table 2. Descriptive statistics of air temperature (*AT*) (n = 1080) recorded in growth chambers with plants evaluated at three target temperatures (T_{Obj}).

	18 °C	23 °C	40 °C
Mean	18.39	23.02	39.92
Standard deviation	0.93	0.43	0.51
CV (%)	5.05	1.88	1.00
Absolute error	0.59	0.31	0.25
Relative error (%)	3.20	1.36	0.69
CI (95 %)	18.37–18.40	23.01–23.02	39.91–39.93

CV: coefficient of variation; CI: confidence interval.

In relation to daily average relative humidity (*RH*), values greater than 60 % were frequently recorded when T_{Obj} was 18 °C, which contrasted with the results during tests with other T_{Obj}. On the other hand, there was evidence of a decrease in *RH* in the growth chambers as T_{Obj} increased (Table 3).

Table 3. Average relative humidity (*RH*) recorded during 24 h and its standard deviation (*SD*) in growth chambers with plants, evaluated at three target temperatures (n = 360 observations).

CN	18 °C			23 °C			40 °C		
	Day 1	Day 2	Day 3	Day 1	Day 2	Day 3	Day 1	Day 2	Day 3
2	63.03±3.83	59.88±2.61	60.26±2.50	59.80±2.70	59.26±2.54	58.57±2.70	59.87±3.06	59.60±3.47	58.89±2.98
3	60.73±4.03	55.44±4.92	55.96±5.01	53.64±4.03	51.13±4.85	47.82±5.09	46.55±3.94	40.09±80.10	40.73±3.96
4	58.09±6.90	51.59±6.07	52.34±6.70	59.61±2.93	53.33±6.70	44.67±6.87	47.17±8.18	43.43±11.82	31.48±3.79
5†	60.81±6.25	57.20±4.96	57.91±4.40	48.93±8.55	50.24±8.66	50.91±8.93	58.93±2.98	57.35±7.36	NA
6	60.45±3.90	54.74±4.88	56.44±5.75	54.39±4.12	50.88±4.74	47.36±5.02	43.12±3.86	36.51±6.87	35.11±2.93
7	63.01±3.39	59.64±4.13	60.00±3.54	58.70±4.33	59.42±2.33	59.35±2.82	55.09±3.85	48.21±6.06	44.28±4.47
8	62.33±5.16	59.83±4.17	60.01±3.76	57.00±8.15	60.37±3.67	59.83±3.20	56.16±10.91	56.45±8.59	44.34±12.86
10	60.15±4.87	57.84±3.86	57.87±3.82	49.46±7.16	45.19±5.77	48.09±6.28	59.1±2.76	45.34±11.15	32.95±3.36
11	61.75±3.69	59.59±2.89	60.01±2.41	56.22±4.16	56.66±4.13	57.11±3.98	55.92±5.22	49.82±12.34	56.15±5.93
12	63.11±3.12	60.87±2.76	60.91±3.08	60.84±3.20	60.47±3.16	59.69±3.50	60.75±3.32	60.72±3.37	61.04±3.07
13	61.78±3.99	57.24 ±4.02	56.80±4.28	57.12±2.92	56.10±3.28	54.67±4.06	59.01±1.22	57.70±2.20	43.36±6.27
14	61.38±4.18	56.12±4.36	56.22±4.79	56.17±3.36	54.61±3.69	52.51±4.24	57.65±3.44	58.21±3.33	56.73±4.09
15	62.29±3.73	58.75±3.20	59.35±3.04	59.21±3.38	58.70±3.75	57.70±4.08	60.31±40.00	59.68±3.77	59.73±3.61

CN: camera number; †: NA (value not available).

RH does not show a relationship with time of day (Figure 4). However, it is notable that as T_{Obj} increased, a corresponding increase in the magnitude of the error in *RH* was also observed. These errors, for the most part, remained below the RH_{obj} values, reflecting a consistent trend. In addition, a marked dispersion in *RH* values was observed between growth chambers, which was more evident as the T_{Obj} value increased.

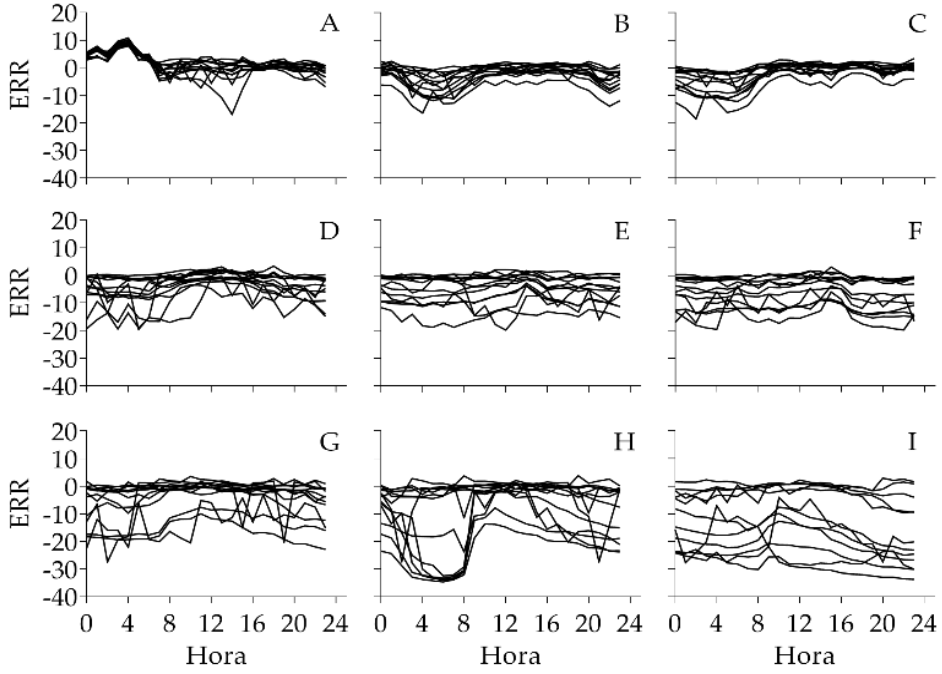

Figure 4. Error (*ERR*) between relative humidity (*RH*) and target relative humidity (RH_{Obj}) (60 %) in the 15 growth chambers with plants evaluated for three days at target temperatures of 18 (A, B, and C), 23 (D, E, and F), and 40 °C (G, H, and I).

The overall average *RH* decreases with increasing T_{Obj} (Table 4). This negative correlation is associated with a decrease in precision (increase in standard deviation (*SD*) and coefficient of variation (CV)) and accuracy (increase in absolute error (*AE*) and relative percent error (*RPE*)). In addition, the confidence interval (CI) increased as a function of T_{Obj}, and the maximum and minimum values in each confidence range moved away from the RH_{Obj} value (60 %). These results suggest the need to increase the

Table 4. Descriptive statistics of relative humidity (RH) (n = 1080) recorded in growth chambers with plants evaluated at three target temperatures.

	18 °C	23 °C	40 °C
Mean	59.02	55.03	51.57
Standard deviation	5.12	6.72	10.77
CV (%)	8.67	12.21	20.89
Absolute error	3.75	5.38	9.23
Relative error (%)	6.36	9.77	17.89
IC (95 %)	58.94–59.10	54.93–55.14	51.39–51.74

CV: coefficient of variation; IC: confidence interval.

humidification capacity of the air inside the growth chambers to maintain humidity as temperature increases.

The results indicate that external environmental conditions influence the ability of the system to regulate *AT* and *RH* in the growth chambers, this effect being more evident at T_{Obj} 18 °C, with greater absolute error during the light period. These results are similar to those of Porter *et al.* (2015), who evaluated multiple environmental variables in eight plant growth chambers (Conviron model BDW40 walk-in) and observed differences between daytime (24.5± 0.98 °C) and T_{Obj} (25 °C) temperatures. In addition, Hagopian *et al.* (2015) report a correlation between internal air temperature in environmental control systems and received solar irradiance. In this research, this could be due to diffuse solar radiation entering through skylights, which contributes to the increase in internal temperature in enclosed spaces. Therefore, it is necessary to improve the thermal insulation of the system.

Although the *AE* of the overall average *RH* at T_{Obj} 23 and 40 °C was considerable, it was observed that some chambers were able to reach the desired humidity level. The increased temperature in the chambers caused the expansion of the air inside, which increased the pressure and accelerated the outward flow of air. This air expansion resulted in a decrease of *RH* in the chamber, requiring the use of humidifiers with a higher water flow rate or a mechanism to regulate the air flow. In addition, this variability could be attributed to possible inconsistencies in the performance of ultrasonic humidifiers.

Another factor that influenced *RH* control was the drying of the air as it passed through the air conditioning (A/C) coil during the initial cooling phase, prior to entering the growth chambers. Katagiri *et al*. (2015) consider that the use of commercial humidifiers does not solve the problem of air dehumidification during the A/C cooling cycle in their environmental control equipment. Therefore, they opted to use an environmental cooling system with an air humidification mechanism to increase the humidity in the controlled atmosphere.

The system studied was stable at the evaluated temperatures of 18.38±0.67, 23.02±0.17, and 39.93±0.16 °C. The operating range exceeds the temperature limit of the "Advanced Plant Habitat" (APH) chamber, proposed by Massa *et al.* (2016), which is limited to temperatures of 18 to 30 °C. However, our system has a narrower thermal range compared to commercial equipment, such as the CARON© brand 7310, 7311, 7312, 7315, and 7317 models, which operate in a range of 15 to 45 °C and consist of a single chamber. A distinctive aspect of our proposal is its capacity to operate 15 cameras simultaneously. This arrangement translates into efficiency when evaluating plant performance in contrasting environments (Edet and Ishii, 2022). It also allows the implementation of diverse experimental designs, which is relevant given that environmental control systems cannot completely eliminate experimental error (Hammer and Hopper, 1997).

Unlike expensive commercial systems such as the Countertop model (Thermo Scientific™), which consists of a single compartment, our proposal offers a more

affordable solution, costing between $1661 and 2767 thousand USD, which represents only one-fifth of the value of commercial equipment. However, our multi-chamber environmental monitoring system has a limitation in the size of each chamber, which is 30 x 30 x 30 cm. This restricts evaluations to objects such as Petri dishes, test tubes, trays with microgreens, seedlings, or small-sized plants in 5 cm-high pots. It is important to note that both the configuration of the programs and the overall structure of the system can be adapted to control larger growth chambers.

CONCLUSIONS

The implementation of open-source technologies allowed the design and construction of a low-cost multi-chamber environmental control system. Despite operating in an unfavorable environmental setting, the system showed precision and accuracy in temperature control, although there were limitations in the regulation of relative humidity.

ACKNOWLEDGMENTS

The main author is grateful for the scholarship of the *Consejo Nacional de Humanidades, Ciencias y Tecnologías* (CONAHCYT) during his PhD, to the staff of the Plant Physiology Laboratory of the *Colegio de Postgraduados* for their invaluable support, and to the Plant Physiology Laboratory of *Universidad Autónoma Chapingo* for their collaboration and access to specialized equipment, which enriched our results.

REFERENCES

Arunachalam A, Andreasson H. 2022. RaspberryPi-Arduino (RPA) powered smart mirrored and reconfigurable IoT facility for plant science research. Internet Technology Letters 5 (1): e272. https://doi.org/10.1002/itl2.272

Bhatta M, Sandro P, Smith MR, Delaney O, Voss-Fels KP, Gutierrez L, Hickey LT. 2021. Need for speed: Manipulating plant growth to accelerate breeding cycles. Current Opinion in Plant Biology 60: 101986. https://doi.org/10.1016/j.pbi.2020.101986

Cazzola F, Bermejo CJ, Guindon MF, Cointry E. 2020. Speed breeding in pea (*Pisum sativum* L.), an efficient and simple system to accelerate breeding programs. Euphytica 216 (11): 178. https://doi.org/10.1007/s10681-020-02715-6

Chao Z, Yin-Hua S, De-Xin D, Guang-Yue L, Yue-Ting C, Nan H, Hui Z, Zhong-Ran D, Feng L, Jing S. 2019. *Aspergillus niger* changes the chemical form of uranium to decrease its biotoxicity, restricts its movement in plant and increase the growth of *Syngonium podophyllum*. Chemosphere 224: 316–323. https://doi.org/10.1016/j.chemosphere.2019.01.098

Daou K, Wang R, Xia Z. 2006. Desiccant cooling air conditioning: A review. Renewable and Sustainable Energy Reviews 10 (2): 55–77. https://doi.org/10.1016/j.rser.2004.09.010

Dasgupta S, Robinson EJZ. 2022. Attributing changes in food insecurity to a changing climate. Scientific Reports 12 (1): 4709. https://doi.org/10.1038/s41598-022-08696-x

Edet OU, Ishii T. 2022. Cowpea speed breeding using regulated growth chamber conditions and seeds of oven-dried immature pods potentially accommodates eight generations per year. Plant Methods 18 (1): 106. https://doi.org/10.1186/s13007-022-00938-3

Fuller S, Greiner B, Moore J, Murray R, van Paassen R, Yorke R. 2021. The python control systems library (python-control). *In* 2021 60th IEEE Conference on Decision and Control (CDC). Institute of Electrical and Electronics Engineers: Austin, TX, USA, pp: 4875–4881. https://doi.org/10.1109/cdc45484.2021.9683368

Grindstaff B, Mabry ME, Blischak PD, Quinn, M, Chris Pires J. 2019. Affordable remote monitoring of plant growth in facilities using Raspberry Pi computers. Applications in Plant Sciences 7 (8): e11280. https://doi.org/10.1002/aps3.11280

Hagopian WM, Schubert BA, Jahren AH. 2015. Large-scale plant growth chamber design for elevated pCO2 and δ13C studies. Rapid Communications in Mass Spectrometry 29 (5): 440–446. https://doi.org/10.1002/rcm.7121

Hammer PA, Hopper DA. 1997. Experimental design. *In* Langhans RW, Tibbitts TW. (eds.), Plant Growth Chamber Handbook. ISU: Ames, IA, USA, pp: 177–187.

He W, Pu M, Li J, Xu ZG, Gan L. 2022. Potato tuber growth and yield under red and blue LEDs in plant factories. Journal of Plant Growth Regulation 41 (1): 40–51. https://doi.org/10.1007/s00344-020-10277-z

Jamhari CA, Wibowo WK, Annisa AR, Roffi TM. 2020. Design and implementation of IoT system for aeroponic chamber temperature monitoring. *In* 2020 Third International Conference on Vocational Education and Electrical Engineering (ICVEE). Institute of Electrical and Electronics Engineers: Surabaya, Indonesia, pp: 1–4 https://doi.org/10.1109/icvee50212.2020.9243213

Jarvis BA, Romsdahl TB, McGinn MG, Nazarenus TJ, Cahoon EB, Chapman KD, Sedbrook JC. 2021. CRISPR/Cas9-Induced *fad2* and *rod1* mutations stacked with *fae1* confer high oleic acid seed oil in pennycress (*Thlaspi arvense* L.). Frontiers in Plant Science 12 (1664–462X): 652–669. https://doi.org/10.3389/fpls.2021.652319

Katagiri F, Canelon-Suarez D, Griffin K, Petersen J, Meyer RK, Siegle M, Mase K. 2015. Design and construction of an inexpensive homemade plant growth chamber. PLoS ONE 10 (5): e0126826. https://doi.org/10.1371/journal.pone.0126826

Kokai O, Kilbreath SL, McLaughlin P, Dylke ES. 2021. The accuracy and precision of interface pressure measuring devices: A systematic review. Phlebology 36 (9): 678–694. https://doi.org/10.1177/02683555211008061

Marchus CRN, Knudson JA, Morrison AE, Strawn IK, Hartman AJ, Shrestha D, Pancheri NM, Glasgow I, Schiele NR. 2022. Low-cost, open-source cell culture chamber for regulating physiologic oxygen levels. HardwareX 11: e00253. https://doi.org/10.1016/j.ohx.2021.e00253

Massa GD, Wheeler RM, Morrow RC, Levine HG. 2016. Growth chambers on the International Space Station for large plants. Acta Horticulturae 1134: 215–222. https://doi.org/10.17660/ActaHortic.2016.1134.29

Mitchell CA. 2022. History of controlled environment horticulture: Indoor farming and its key technologies. HortScience 57 (2): 247–256. https://doi.org/10.21273/hortsci16159-21

Padmanabha M, Streif S. 2019. Design and validation of a low cost programmable controlled environment for study and production of plants, mushroom, and insect larvae. Applied Sciences 9 (23): 5166. https://doi.org/10.3390/app9235166

Porter AS, Evans-Fitz GC, McElwain JC, Yiotis C, Elliott-Kingston C. 2015. How well do you know your growth chambers? Testing for chamber effect using plant traits. Plant Methods 11 (1): 44. https://doi.org/10.1186/s13007-015-0088-0

Reed DW, Vanden Bosch CA. 2023. Engineering perspectives of growing plants in space. Journal of the Indian Institute of Science 103 (3): 797–805. https://doi.org/10.1007/s41745-023-00369-6

Salame N, Zieslin N. 1994. Peroxidase activity in leaves of *Syngonium podophyllum* following transition from *in vitro* to *ex vitro* conditions. Biologia Plantarum 36 (4): 619–622.

Vatistas C, Avgoustaki DD, Bartzanas T. 2022. A systematic literature review on controlled-environment agriculture: How vertical farms and greenhouses can influence the sustainability and footprint of urban microclimate with local food production. Atmosphere 13 (8): 1258. https://doi.org/10.3390/atmos13081258

Agrociencia

STRUCTURAL AND STOCHASTIC BEHAVIOR OF MEXICAN AGRICULTURAL EXPORTS

Miguel Ángel **Martínez-Damián**[1*], Ana Laura **Rivera-Silva**[2], Víctor Ángel **Hernández-Trejo**[3]

[1]Colegio de Postgraduados Campus Montecillo. Carretera México-Texcoco km 36.5, Montecillo, Texcoco, State of Mexico, Mexico. C. P. 56264.
[2]Universidad Anáhuac México Norte. Avenida Universidad Anáhuac 46, Lomas Anáhuac, Naucalpan, State of Mexico, Mexico. C. P. 5278.
[3]Universidad Autónoma de Baja California Sur. Carretera al Sur km 5.5. A. P. 19-B, La Paz, Baja California Sur, Mexico. C. P. 23080.
* Author for correspondence: angel01@colpos.mx

Citation: Martínez-Damián MÁ, Rivera-Silva AL, Hernández-Trejo VÁ. 2024. Structural and stochastic behavior of Mexican agricultural exports. **Agrociencia** 58(7): 896-905. https://doi.org/ 10.47163/agrociencia.v58i7.3210

Editor in Chief:
Dr. Fernando C. Gómez Merino

Received: April 18, 2024.
Approved: September 04, 2024.
Published in Agrociencia: October 09, 2024.

ABSTRACT

Mexican agricultural exports have grown faster than the country's economy, suggesting a foreign exchange inflow and the use of production factors in Mexico. This work examines both the structural behavior of the agricultural exports and its stochastic behavior using data from 1993 to 2023. The structural part is modeled with three explanatory behaviors: first, the influence in exports of the U.S. economy through its Gross Domestic Product (GDP); second, the effect of the Mexican economy through its own GDP; and third, the search for a more profitable price abroad was modeled with the real exchange rate. On the other hand, the stochastic behavior was modeled with lags of the actual exports and other explanatory variables. After adjusting an autoregressive distributed lag model and verifying the existence of a long-term relationship between Mexican agricultural exports, U.S. GDP, Mexican GDP, and the real exchange rate, it was found that the behavior of the export growth is largely explained by the U.S. economy.

Keywords: Autoregressive Distributed Lag, cointegration, bounds test.

INTRODUCTION

Mexican agricultural exports had a value of $442 731 253.9 thousand MXN for 2021, or 0.62 % of the total Gross Domestic Product (GDP) of the country for that year. This contribution in 1994 was 0.028 %, showing their increasing importance to the national economy. Agricultural exports have become increasingly important for the economic activity of the country. The aim of this research is to determine what factors contribute to the increase in Mexican agricultural exports. While the signing of the North American Free Trade Agreement in 1994 was an important factor, this behavior could be due to other reasons such as internal, external, profitability factors, or, of course, a combination of these.

As noted by Macías-Uribe (2019), trade agreements are crucial for increasing exports by removing tariffs and making domestic products more appealing. On the other hand, Lechuga-Montenegro and Vega-Miranda (2018) examine the significance of exchange

and interest rates, both of which are important factors; specifically, the exchange rate may represent not only a better foreign price but also greater purchasing power after payment due to the terms of the exchange rate. Likewise, Galindo and Ríos (2015) highlight the role of both internal and external factors in driving export growth as a growing economy will consider selling abroad, which might influence domestic exports.

Using a dynamic model, we examined the behavior of Mexican agricultural exports in response to the U.S. economy (Y_US), the Mexican economy (Y_MX), and the MXN-USD exchange rate (TCR). Within the same model, the behavior of exports (EXP) is examined in relation to their previous values as well as the lagged values of the three variables mentioned. Initially, the hypothesis to be tested is that these three variables (Y_US, Y_MX, and TCR), their respective lags, and export lags all explain the behavior of Mexican agricultural exports.

MATERIALS AND METHODS

Monthly data on Mexican agricultural exports from the Bank of Mexico website (https://www.banxico.org.mx/SieInternet/) from 1993 to 2023 were used. To standardize the frequency with the other series used, these were converted to a quarterly basis. Exports are reported in United States dollar (USD) and were converted to Mexican peso (MXN) using the exchange rate obtained from the Bank of Mexico website. The data was deflated using the implicit GDP index from the National Institute of Statistics and Geography (INEGI) website (https://www.inegi.org.mx/app/indicadores/). Quarterly Mexican GDP (Y_MX) data from the INEGI portal were also used; the quarterly data for the U.S. GDP (Y_US) were obtained from the Bureau of Economic Analysis website (https://www.bea.gov/). Both GDPs were deflated using the implicit GDP index at 2013 prices obtained from the INEGI and BEA websites, respectively.

Finally, the MXN-USD exchange rate used, originated from the Bank of Mexico website as a variable indicating how profitable placing a domestic product abroad can be. To account for the different inflation rates in each country, the exchange rate was deflated using the implicit GDP price indices, resulting in an indicator of the real exchange rate. These series show fluctuations, hence the use of the Hodrick and Prescott (1997) filter to separate trend and cyclical behavior and estimate the quarterly growth rate in each case using the following growth model (Brambila-Paz, 2011).

$$Y_t = \theta_0 e^{\theta_1 t} + u_t$$

where Y_t is the variable modeled, θ_0 and θ_1 are parameters to be estimated, e is the natural base, t indicates the time in a linear way, and u_t indicates a random term of error. In this model non-linear least squares were used to estimate the growth rate, denoted by parameter θ_1. The quarterly growth rates for agricultural exports, Mexican

GDP, U.S. GDP, and the MXN-USD exchange rate were 1.48, 0.505, 0.528, and 1.089 %, respectively (Figure 1). These rates were converted to annual rates using the formula:

$$\tau_{an} = (1 + \tau_{trim})^4 - 1$$

where τ_{an} and τ_{trim} are the annual and quarterly growth rates. The annual growth rates are 6.072 % for exports, 2.037 % for Mexican GDP, 2.123 % for U.S. GDP, and 4.42 % for the MXN-USD exchange rate.

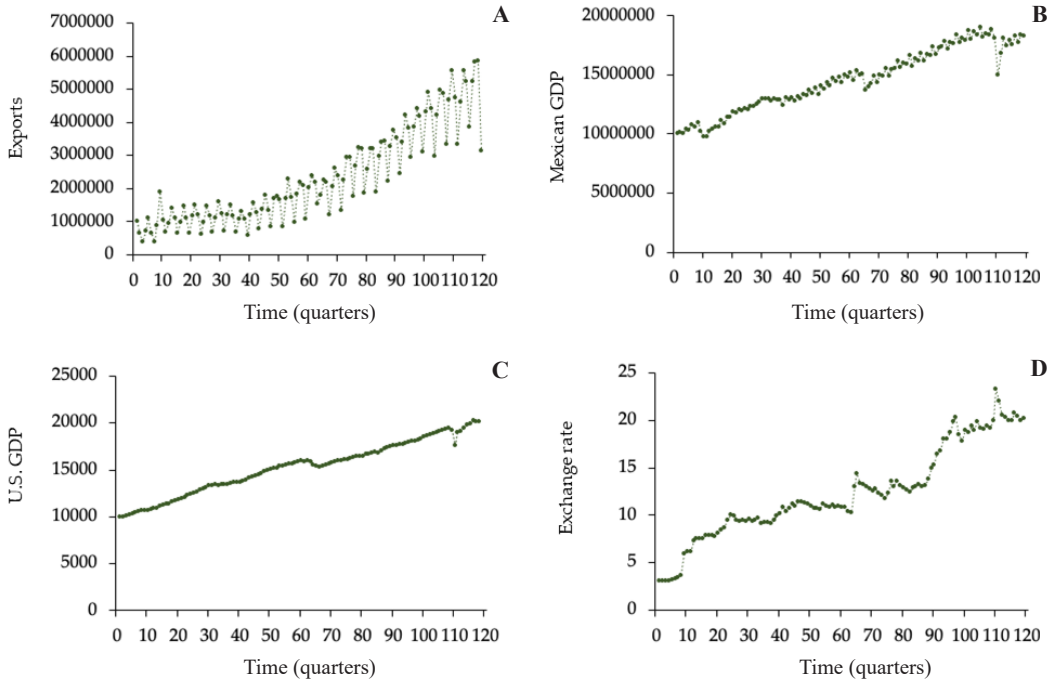

Figure 1. Quarterly growth rates for the economic data used. A: behavior of agricultural exports; B: GDP of Mexico; C: GDP of the U.S.; D: MXN-USD exchange rates.

So, the question is, what can explain export behavior? That is, is the relevant factor domestic economic conditions, or the behavior of the external market, in this case represented by the U.S., Mexico's main export destination, or perhaps the behavior of the exchange rate? The approach is to model Mexican agricultural exports using an autoregressive distributed lag (ARDL). This approach has been used, among others, by Bahmani-Oskooee *et al.* (2016) in the study of Mexico's trade scale with its 13 trade partners; Villarreal-Samaniego (2021), when studying economic growth

and its relationship with stock market capitalization; Valencia-Romero *et al.* (2023), when studying the demand for wheat imports in Mexico; and Gulzar and Li (2018), when examining the leadership between exports and economic growth in China and Pakistan. The ARDL model is formulated as follows:

$$Y_t = \alpha_0 + \sum_{i=1}^{p} \delta_i Y_{t-i} + \sum_{j=1}^{k} \sum_{l=0}^{q_j} \theta_{j,l} X_{j,t-l} + \varepsilon_t \quad (1)$$

where Y_t are agricultural exports in time t, Y_{t-i} are the lagged agricultural exports up to p periods, $X_{j,\,t-l}$ are k explanatory variables (Y_US, Y_MX, and TCR) in period t and its respective lag (q_j), δ_i and $\theta_{j,l}$ are unknown parameters to be estimated, and ε_t is an independent and identically distributed (IID) random error term with expectation $E(\varepsilon_t) = 0$ and $E(\varepsilon_t^2) = \sigma^2$ (zero mean and constant variance). At the time of the analysis, all variables were converted to their natural logarithms, which protects against changes in variance and helps interpret first differences as growth rates.

The model expressed in equation (1) helps explain the behavior of exports (EXP) from their own past as well as other explanatory exogenous variables and their own respective lags. It is worth noting that this is the combination of a structured model and a time series model; the exogenous variables used were the Mexican GDP (Y_MX), the U.S. GDP (Y_US) and the real MXN-USD exchange rate (TCR), as well as their respective lags.

RESULTS AND DISCUSSION

Since the ARDL is a linear regression model and the variables are considered susceptible to contain a unitary root, the problem of a spurious regression may exist. In this regard, Castillo-Ponce and Díaz-Bautista (2002) found an integration order of one for the Mexican GDP, whereas Cushman (2016) found the same for the U.S. GDP. The MXN-USD exchange rate also shows this issue of non-stationarity, according to García *et al.* (2018). Therefore, the data are examined for the presence of a unit root using SAS statistical software. (Table 1).

The set of hypotheses in this test considers that the examined series contains a unit root (non-stationary series). As shown, both the Dickey-Fuller and the Phillips-Perron tests did not reject the presence of a unit root in any of the variables. The null hypothesis is rejected for the version with an intercept for exports (simple mean), with no lags and one lag in the augmented part; if this were the case, an ARDL model is the best approach for extracting long-term behavior because it allows the combination of $I(0)$ and $I(1)$ series.

To recover the coefficients of the model stated in equation (1) and extract a possible long-term component, whether or not the variables that make up the model are

Table 1. Unit root test for: Exports (EXP), Mexico´s GDP (Y_MX), US GDP (Y_US) and MXN-USD Exchange Rate (TCR).

			Dickey-Fuller test		Phillips-Perron test	
EXP	Type	Lags	Tau	Pr < Tau	Tau	Pr < Tau
	Mean zero	0	-1.10	0.246	-1.10	0.246
		1	-0.74	0.393	-0.95	0.304
		2	0.83	0.890	-0.27	0.588
	Simple mean	0	-3.20	0.023	-3.20	0.023
		1	-2.81	0.061	-3.10	0.029
		2	-0.72	0.838	-2.44	0.133
Y_MX	Type	Lags	Tau	Pr < Tau	Tau	Pr < Tau
	Mean zero	0	1.05	0.923	1.05	0.923
		1	1.97	0.988	1.60	0.973
		2	2.00	0.989	1.65	0.976
	Simple mean	0	-1.39	0.585	-1.39	0.585
		1	-1.00	0.750	-1.15	0.693
		2	-1.04	0.738	-1.14	0.697
Y_US	Type	Lags	Tau	Pr < Tau	Tau	Pr < Tau
	Mean zero	0	4.04	1.000	4.04	1.000
		1	4.65	1.000	4.56	1.000
		2	4.43	1.000	4.81	1.000
	Simple mean	0	-0.66	0.853	-0.66	0.853
		1	-0.64	0.857	-0.64	0.857
		2	-0.66	0.852	-0.63	0.859
TCR	Type	Lags	Tau	Pr < Tau	Tau	Pr < Tau
	Mean zero	0	2.70	0.998	2.70	0.998
		1	2.20	0.993	2.54	0.997
		2	2.78	0.999	2.68	0.998
	Simple mean	0	0.06	0.962	0.06	0.962
		1	-0.10	0.946	0.01	0.957
		2	0.16	0.969	0.07	0.962

EXP: exports; Y_MX: Mexican GDP; TCR: MXN-USD exchange rate. Elaborated using SAS statistical software (SAS Institute). Pr refers to probability. Tau means a statistic analogous to a t. Type points to a version of the test without intercept (zero mean) or with intercept (simple mean).

examined, the absence of stationary linear combinations would result in a spurious regression (Granger and Newbold, 1974) in the presence of unit roots. One method for testing multivariate cointegration is suggested by Johansen (1991), known as the trace test or maximum eigenvalue test. However, it requires modeling within an autoregressive vector, which in this case and for the number of variables used (four) requires the estimation of 16 parameters for each possible lag of the vector in question, which implies many degrees of freedom.

Therefore, the procedure suggested by Pesaran and Shin (1995) was followed, which proposes a cointegration test under the structure of an ARDL model, namely, the bounds test. The principle of the test is to compare the statistical significance of the coefficients of the explanatory factors considered at level but lagged for a period within a distributed lag regression of the same variables in first difference. This is accomplished using the F-test principle, though if there are unit roots, the statistic follows a different distribution, the percentiles of which were determined by Pesaran and Shin (1995).

The first step is to determine the best order of representation in equation (1), which is how many lags of the endogenous variable to include, as well as the lags of each independent variable. One way to address this is using the AIC statistic, known as the Akaike information criterion. Under this criterion, the best order in which to represent the lags to be modeled is that which minimizes the AIC statistic. For the data used, the best order of representation for the ARDL model considers six lags of the endogenous variable EXP, five lags for both Y_MX and Y_US, and three lags for the TCR variable, this was estimated using R-Software, (Table 2).

Table 2. Autoregressive distributed lag (ARDL) model estimated for Mexican agricultural exports.

	Estimator	*t* statistic	*p* value
Exp_{t-1}	0.204	2.188	0.031
Exp_{t-2}	-0.009	-0.096	0.924
Exp_{t-3}	0.117	1.889	0.062
Exp_{t-4}	0.733	11.923	0.000
Exp_{t-5}	-0.080	-0.831	0.408
Exp_{t-6}	-0.163	-1.955	0.054
Y_MX_{t}	-0.891	-1.474	0.144
Y_MX_{t-1}	-0.020	-0.027	0.979
Y_MX_{t-2}	2.188	3.209	0.002
Y_MX_{t-3}	-0.741	-1.117	0.267
Y_MX_{t-4}	1.030	1.586	0.116
Y_MX_{t-5}	-1.461	-2.556	0.012
Y_US_{t}	3.198	2.492	0.015
Y_US_{t-1}	0.662	0.397	0.692
Y_US_{t-2}	-4.324	-2.612	0.011
Y_US_{t-3}	0.533	0.321	0.749
Y_US_{t-4}	-1.240	-0.781	0.437
Y_US_{t-5}	2.259	1.777	0.079
TCR_{t}	1.251	7.458	0.000
TCR_{t-1}	-0.999	-4.376	0.000
TCR_{t-2}	0.565	2.327	0.023
TCR_{t-3}	-0.916	-4.798	0.000
Ordinate	-8.152	-2.798	0.006

Source: own elaboration (R and R-Studio).

Agricultural exports displayed a positive contemporary relation with the U.S. GDP (Y_US) and the real exchange rate (TCR), yet a negative—but not significant—contemporary relation with the Mexican GDP (Y_MX). Out of the 24 coefficients estimated, only nine displayed probability values above 10 %, i.e., not significantly different from zero at that level. Coincidentally, this is also true for the first lag of the respective GDPs of Mexico and the U.S., implying that the effect of the lag on these variables takes at least one quarter to impact exports. On the other hand, a definite impact on the real exchange rate is shown.

One potential issue in this regression with variables that do not rule out the presence of a unit root is the presence of a long-term relationship. If there is no such long-term relationship, there is a model that only reflects short-term behavior; in this case, the Pesaran and Shin (1995) bounds test can help identify a long-term relationship. In particular, the bounds test in its F version resulted in a value of 9.329, which exceeds the critical values of the test for probability values below 10 %, which is 3.2 when the series are integrated of order one. In fact, it exceeds the critical value of 4.66 at a significance of 1 % with three degrees of freedom (taken from results obtained using EViews 12). This has an immediate implication; the variables (exports, GDPs, and the real exchange rate) are cointegrated, meaning that they have a long-term relationship. This implies that a representation of the model can be used in terms of an error correction model:

$$\Delta Y_t = \sum_{i=1}^{p-1} \vartheta_i \Delta Y_{t-i} + \sum_{j=1}^{k} \sum_{l=0}^{q_{j-1}} \psi_{j,l} \Delta X_{j,t-l} + \sum_{j=1}^{k} \emptyset_j \Delta X_{j,t} + \varphi EC_{t-1} + \varepsilon_t$$

where $EC_t = Y_t - \sum_{j=1}^{k} \gamma_j X_{j,t} - \gamma_0$ represents the long-term relationship or error correction term; Δ represents the difference operator, and Y_t and $X_{j,\,t-l}$ are as defined in equation (1).

The error correction model estimated with E-Views (Table 3) helps examine short-term relationships. Since the variables used in the model are a transformation into logarithms, this model has an immediate interpretation in terms of growth rates. In this sense, the growth rates of the U.S. GDP (Y_US), Mexican GDP (Y_MX), and real exchange rate (TCR) have a positive contemporary relationship with the growth rate of agricultural exports, whereas their respective lags alternate in signs. Although the long-term relationship shows a contemporary effect on positive levels of both Y_MX and Y_US, despite being negative with the real exchange rate, only the one on Y_US is statistically different from zero.

From both analyses, agricultural exports respond predominantly to the economic activity in the U.S., followed by the economic activity in Mexico. The real exchange rate has expected effects on the short term but little importance in the long term. These results are similar to the findings by Alam and Qazi (2012) for Pakistan, who found

Table 3. Error correction model.

Variable	Coefficient	Estimated error	*t* statistic	*p* value
Δ EXP$_{t-1}$	-0.598	0.084	-7.143	0.000
Δ EXP$_{t-2}$	-0.607	0.086	-7.038	0.000
Δ EXP$_{t-3}$	-0.489	0.088	-5.578	0.000
Δ EXP$_{t-4}$	0.244	0.084	2.910	0.005
Δ EXP$_{t-5}$	0.163	0.080	2.031	0.045
Δ Y_MX$_{t}$	-0.891	0.580	-1.535	0.128
Δ Y_MX$_{t-1}$	-1.016	0.623	-1.629	0.107
Δ Y_MX$_{t-2}$	1.179	0.586	2.000	0.049
Δ Y_MX$_{t-3}$	0.432	0.565	0.765	0.446
Δ Y_MX$_{t-4}$	1.461	0.535	2.733	0.008
Δ Y_US$_{t}$	3.198	1.199	2.665	0.009
Δ Y_US$_{t-1}$	2.772	1.259	2.212	0.029
Δ Y_US$_{t-2}$	-1.553	1.232	-1.260	0.211
Δ Y_US$_{t-3}$	-1.020	1.194	-0.854	0.395
Δ Y_US$_{t-4}$	-2.259	1.174	-1.924	0.058
Δ TCR_$_{t}$	1.251	0.138	9.051	0.000
TCR_$_{t-1}$	0.351	0.182	1.925	0.057
TCR_$_{t-2}$	0.916	0.181	5.037	0.000
CointEq(-1)*	-0.198	0.028	-6.981	0.000

Note: CointEq is the Cointegrating equation:

Variable	Coefficient	Estimated error	*t* statistic	*p* value
Y_MX	0.529	1.845	0.287	0.775
Y_US	5.487	2.561	2.143	0.035
TCR	-0.497	0.312	-1.593	0.115
Intercept	-41.094	15.843	-2.593	0.011

Source: own elaboration (EViews 12).

a predominant explanation of exports in the income of trade partners. However, this contradicts Bahmani-Oskooee *et al*. (2016), who discovered that currency depreciation benefits exports. In turn, Gulzar and Li (2018) and Sanjuán-López and Dawson (2010) found a leading relationship where exports drive economic growth. The immediate implication for decision-makers in the scope of agricultural exports in Mexico is to focus their attention on the behavior of the economy of its main trade partner, considering the signal from the domestic economy and, to a lesser extent, the real exchange rate.

CONCLUSIONS

Agricultural exports in Mexico have grown since 1994 at a rate that surpasses the growth rate of the economy and of its main trade partner. An examination of the

hypothesis that internal and external factors, as well as the exchange rate, explain this growth in equal parts leads to the rejection of this hypothesis in favor of the fact that this behavior in the long term is predominantly explained by the tendency of the U.S. economy. As a result, it is worth recommending agricultural exporters closely monitor the behavior of the U.S. economy, particularly on the long-term, followed, to a lesser extent, by the behavior of the Mexican economy and the real exchange rate.

REFERENCES

Alam S, Qazi M. 2012. Exchange rate volatility and aggregate exports demand through ARDL framework: An experience from Pakistan economy. Review of Applied Economics 8 (1): 79–94. https://doi.org/10.22004/ag.econ.143465

Bahmani-Oskooee M, Halicioglu F, Hegerty SW. 2016. Mexican bilateral trade and the J-curve: An application of the nonlinear ARDL model. Economic Analysis and Policy 50: 23–40. https://doi.org/10.1016/j.eap.2016.02.003

Brambila-Paz JJ. 2011. Bioeconomía: instrumentos para su análisis económico. Secretaría de Agricultura y Desarrollo Rural: Ciudad de México, México. 312 p.

Castillo-Ponce RA, Díaz-Bautista A. 2009. Testing for unit roots: México´s GDP. Revista Momento Económico 124: 2–10.

Cushman DO. 2016. A unit root in postwar U.S. real GDP still cannot be rejected, and yes, it matters. Econ Journal Watch 13 (1): 5–45.

Galindo M, Ríos V. 2015. Exportaciones. Serie de Estudios Económicos. Ciudad de México, México. 8 p.

García S, Saucedo E, Velasco A. 2018. The effects of oil prices on the spot exchange rate (MXN/USD) a var analysis for Mexico from 1991 to 2017. Análisis Económico 34 (84): 33–56.

Granger CWJ, Newbold P. 1974. Spurious regressions in econometrics. Journal of Econometrics 2 (2): 111–120. https://doi.org/10.1016/0304-4076(74)90034-7

Gulzar A, Li Z. 2018. Exports-led growth or growth-led exports in the case of China and Pakistan: An empirical investigation from the ARDL and Granger causality approach. The International Trade Journal 32 (3): 293–314. https://doi.org/10.1080/08853908.2017.1379449

Hodrick RJ, Prescott EC. 1997. Postwar U.S. business cycles an empirical investigation. Journal of Money, Credit and Banking 29 (1): 1–16. https://doi.org/10.2307/2953682

Lechuga-Montenegro J, Vega-Miranda F. 2018. El impacto de la tasa de interés y del tipo de cambio en las exportaciones agrícolas en México: un estudio para el periodo 1993-2017. Revista Textual 72: 125–150. https://doi.org/10.5154/r.textual.2017.72.008

Johansen S. 1991. Estimation and hypothesis testing of cointegration vectors in Gaussian vector autoregressive models. Econometrica 59 (6): 1551–1580. https://doi.org/10.2307/2938278

Macías-Uribe C. 2019. Reforma del comercio agrícola mundial: Inserción del sector agrícola de México bajo el TLCAN y el acuerdo sobre agricultura de la OMC, de 1994 a 2012. Revista Textual 74: 13–49. https://doi.org/10.5154/r.textual.2018.74.01

Pesaran H, Shin Y. 1995. An autoregressive distributed lag modeling approach to co-integration analysis. *In* Steinar S. (ed.), Econometrics and Economic Theory in the 20st Century. Cambridge University Press: Cambridge, UK, pp: 371–413. https://doi.org/10.1017/ccol521633230.011

Sanjuán-López AI, Dawson PJ. 2010. Agricultural exports and economic growth in developing countries: a panel cointegration approach. Journal of Agricultural Economics 61 (3): 565–583. https://doi.org/10.1111/j.1477-9552.2010.00257.x

Valencia-Romero R, Trejo-García JC, Ríos-Bolívar H. 2023. Wheat import demand in Mexico: Evidence of quantile cointegration. Agriculture 13 (5): 980. https://doi.org/10.3390/agriculture13050980

Villarreal-Samaniego JD. 2021. Desarrollo del mercado accionario y crecimiento económico en México: un examen mediante los enfoques ARDL y no causalidad. Contaduría y Administración 66 (3): 1–23. https://doi.org/10.22201/fca.24488410e.2021.2259

Agrociencia

WATER RESOURCE BALANCE AND PROPOSED MEASURES FOR SUSTAINABLE MANAGEMENT IN THE FOUR SECTIONS OF CHAPULTEPEC FOREST

Héctor Alonso **Ballinas-González**[1], Rodrigo **Roblero-Hidalgo**[1*], José Avidán **Bravo-Jácome**[1], Beatriz **García-Vázquez**[2], María Teresa **Cruz-Cruz**[2], Margarita Elizabeth **Preciado-Jiménez**[1], Citlalli **Astudillo-Enríquez**[1], Julio César **Soriano-Monzalvo**[1]

[1]Instituto Mexicano de Tecnología del Agua. Coordinación de Sistemas Hídricos. Paseo Cuauhnáhuac 8532, Colonia Progreso, Jiutepec, Morelos, Mexico. C. P. 62550.
[2]Universidad Autónoma de Chapingo. Departamento de Irrigación. Carretera México-Texcoco km 38.5, Chapingo, Texcoco, State of Mexico, Mexico. C. P. 56227.
* Author for correspondence: rodrigo_roblero@tlaloc.imta.mx

Citation: Ballinas-González HA, Roblero-Hidalgo R, Bravo-Jácome JA, García-Vázquez B, Cruz-Cruz MT, Preciado-Jiménez ME, Astudillo-Enríquez C, Soriano-Monzalvo JC. 2024. Water resource balance and proposed measures for sustainable management in the four sections of Chapultepec forest. **Agrociencia** 58(7): 906-921. https://doi.org/ 10.47163/agrociencia.v58i7.3136

Editor in Chief:
Dr. Fernando C. Gómez Merino

Received: December 18, 2023.
Approved: September 01, 2024.
Published in Agrociencia: November 06, 2024.

ABSTRACT

This study examined the water resources in four sections of Chapultepec Forest (CF) to assess their current state and propose strategies for proper management. The forest is significant for Mexico City due to its historical and cultural value, ecological relevance, and contribution to the quality of life of its residents. For diagnosis, a water balance was carried out under current conditions, and water supply and demand were projected to the year 2050. The results show that there is currently a water deficit in sections 1, 2, and 3, mainly due to the demand for irrigation water. Towards 2050, and considering the trend of climatological variables, an increase in the deficit is expected for the entire CF due to increased evaporation and water demand in its various uses.

Key words: supply, demand, water use, deficit, consumption, rainwater harvesting.

INTRODUCTION

Since pre-colonial times, Chapultepec was regarded as a sacred garden, as well as a place of leisure and recreation for its rulers. After 1930, with the expansion of the population, the surrounding areas of the forest began to be settled in a disorderly fashion. Today, the forest continues to serve as a recreational space; however, with the increase in visitors and the reduction in water availability, water resources are beginning to be compromised.

The administration of the Federal Government and Mexico City carried out the Chapultepec Forest (CF) Cultural Complex Project with the purpose of increasing the services that the forest offers from a cultural, environmental, and social perspective. However, several problems affect water resources, starting with the lack of knowledge of water supply and demand for planning under current and future conditions to

manage its balanced use. Therefore, it is important to carry out a diagnosis of the site in order to implement actions and achieve sustainable management of the water resources.

The CF is located in the Miguel Hidalgo mayoralty of Mexico City (Figure 1). It has an area of 686.01 ha, divided into three sections: the First Section, with 274.08 ha; the Second Section, with 168.03 ha; and the Third Section, with 243.90 ha (Gobierno del Distrito Federal, 2003). In addition, there is a proposal for its expansion, including a fourth section.

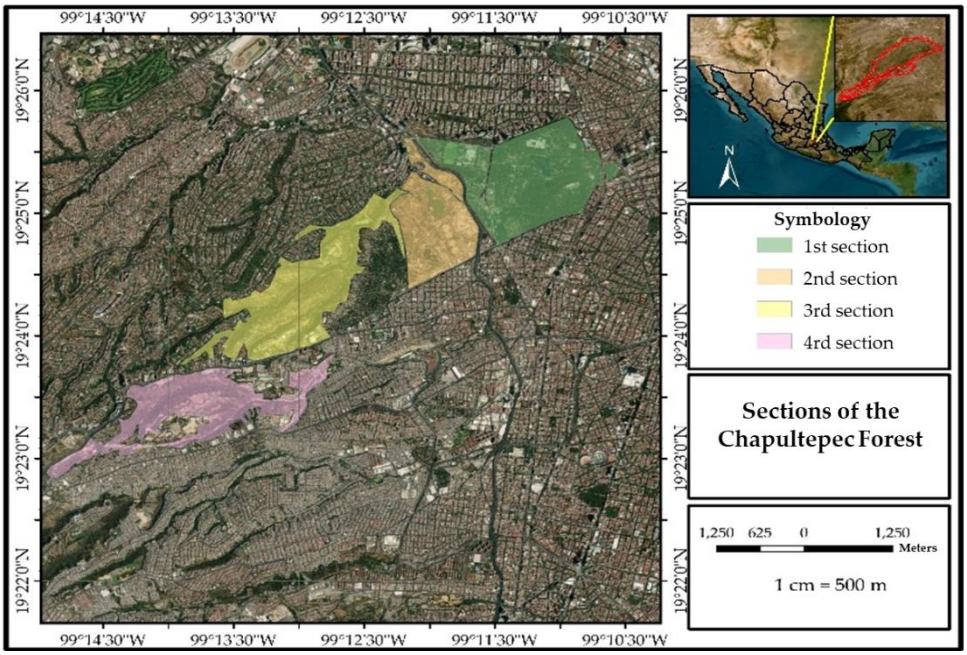

Figure 1. Sections of Chapultepec Forest in Mexico City, Mexico.

The First Section, under the custody of the National Institute of Anthropology and History (INAH), belongs to the historic sector of the park, with 182 ha of green areas. It has two lakes and five museums, including the Chapultepec Castle. There are approximately 55 thousand trees, among which the cedar (*Cupressus lusitanica* Mill.), the thunder tree (*Ligustrum lucidum* W.T. Aiton), and the ahuehuete (*Taxodium mucronatum* Ten.) predominate (SEDEMA, 2011). The Second Section was inaugurated in 1964 for recreational purposes. It is an open space with two lakes, four museums, and approximately 17 500 trees. The Presidential House of Los Pinos and the Papalote Children's Museum are located in this area (SEDEMA, 2011).

The Third Section, inaugurated in 1974 with an environmental vocation, was decreed a Natural Protected Area in 1992. It has extensive green areas and 137.71 ha corresponding to ravines, making it the least known area of the forest. It has an

estimated 85 550 trees (SEDEMA, 2011). The project of the Fourth Section of the CF takes place in what used to be the former Army Weapons Factory, an area that will become an artistic and cultural space, with almost 100 ha destined to the care and conservation of the environment.

In order to understand the current and future state of CF's water resources, a water balance of the area was carried out, for which available information was collected to characterize the region and quantify the current water supply and demand. Subsequently, the predicted water volume for the year 2050 was estimated. The supply is the sum of the annual water volume provided by the various supply sources, whether surface or groundwater, and the demand is the ideal (annual) water consumption resulting from the occupation by visitors and the various services provided.

The CF is located within basin 2670 Mexico City (SINA, 2020a) and aquifer 901 Mexico City Metropolitan Zone (SINA, 2020b). The basin has an available volume of surface water of 1.26 Mm^3 (DOF, 2020a), while the aquifer is unavailable, with a deficit of 507.23 Mm^3 (DOF, 2020b). Although the basin has surface water availability, Breña-Puyol and Breña-Naranjo (2017) showed that in the Hydrological Administrative Region XIII, where CF is located, the degree of water availability is of extreme scarcity. In both cases, the estimation of these volumes is based on NOM-011-CONAGUA-2015 (DOF, 2015), which establishes the specifications and method for determining the average annual availability of national waters in Mexico. Silva-Hidalgo *et al.* (2013) state that there are several manuals for determining the availability of water in a basin, but they refer to the natural availability of the resource or the natural runoff generated in it, which is different from the legal-administrative or regulatory context contained in the standard.

Many works directed towards the calculation of natural availability can be found in scientific publications. For example, López-García *et al.* (2017), in their work, show a water balance to obtain the natural availability under climate change scenarios of the aquifer in the Galeana Valley in the State of Nuevo León, Mexico. Other studies, such as the one conducted by Ordóñez-Gálvez (2011), show a methodology for estimating the natural surface water balance in Peru.

Very similar methodologies were applied by Gómez-Reyes (2013) and UNESCO (2006) to obtain the surface water balance of the Valley of Mexico basin. These works include the incorporation of the variable of uses of consumption (Uc) and the calculation of the variability and uncertainty of the components of the water balance. On the other hand, according to Silva-Hidalgo *et al.* (2013), scientific publications on the subject of water availability in legal-administrative or regulatory terms are scarce. However, countries such as Chile, Spain, Mexico, and the United States have regulatory documents for water resource management, with some variations, but all focused on the regulatory framework.

In general, the methodologies for obtaining the natural water balance or for regulatory purposes are very similar in their formulation, i.e., they are all based on the basic equation $dV/dt = E-S$, which expresses that the variation in volume (V) is equal to the

inputs (E) minus the outputs (S) of water for a specific time interval (t) (UNESCO, 2006). The only thing that changes in each methodology are the methods for processing the data that feed the water balance equation.

With the implementation of NOM-011-CONAGUA-2015, it is possible to know the availability of water resources in the four sections of CF for its current state and for the year 2050. It is taken into account that, in the variable of consumptive use from urban public use, an increase in the number of inhabitants of the CF is not expected, except in the Fourth Section, where there is a residential land use that is fully occupied. However, the main increase in water use in the four sections will be due to the increase in visitors to the CF. In addition, due to the increase in temperature, an increase in evapotranspiration is expected, causing a water deficit in the projected period.

The objective of this work is to conduct a water balance to determine the current status of the resource as well as its status in 2050, in order to determine its availability and, if necessary, propose a specific action to help minimize any potential water deficits.

MATERIALS AND METHODS

The balance for each of the CF sections was performed by applying the general storage change equation:

$$\frac{\partial V}{\partial t} = E - S$$

where $\partial v / \partial t$ is the change in storage over time, E are the inputs, and S are the outputs. From the equation, the general elements for the water balance are broken down:

$$\Delta V = (Vp + Ear + Im + Re + B + Vm) - (Ev + ET + Eaa + Ex + Uc + f + In + Int)$$

where ΔV is the change in storage, Vp the precipitated volume, Ear the upstream runoff, Im the imports from external basins, Re the returns, B the pumped withdrawals within the polygon, Vm the volume contributed by springs, EV the evaporation from water bodies, ET the evapotranspiration, Eaa the downstream runoff, Ex the exports, Uc the consumptive uses, f the leaks in the drinking water distribution network, In the infiltration, and Int the interception.

However, if we express the volume of runoff per proper basin (Cp), the equation is expressed as:

$$Cp = Vp - ET - In - Int$$

which is reduced to:

$$\Delta V = (Cp + Ear + Im + Re + B + Vm) - (Ev + Eaa + Ex + Uc + f)$$

The origin of the information for the variables considered in the latter equation is explained below.

Runoff per own basin (*Cp*)

The drainage polygons to the four sections of the CF were estimated and subdivided into micro-watersheds. Rainfall-runoff modeling was performed for the whole set with the SWMM application (James *et al*., 2010).

Land use was classified as residential, built urban, and streets, among others, to delimit the impervious and permeable zones within each micro-watershed. In addition, it was combined with the soil type from the soil cartography of the National Institute of Statistics and Geography (INEGI) Series I of 2005 and Series II of 2013 for the calculation of infiltration losses (variable *In*). Edaphology and land use were also used to calculate infiltration losses in the microbasins using the Soil Conservation Service method, Curve Number (CN) (NRCS, 1986; SCS, 1991). Likewise, Manning's n coefficient was defined for conduits, impermeable surfaces, permeable surfaces, depression storage height above the impermeable area, and depression storage height above the permeable area.

An analysis of stations of the National Meteorological Service (SMN) with daily precipitation record (variable *Vp*) was performed, where the area of influence of the stations was verified from the Thiessen polygons. A greater influence of the Colonia America station (code 9010) was identified, with information from 1980 to 2017. During this time period, the years with the highest and lowest annual precipitation were obtained, and it was determined that the year 2017 represents an average year of precipitation, on which hydrological modeling was performed. Since the linear correlation is greater than or equal to 0.8, the missing precipitation and evaporation data were supplemented with data from the Tacubaya station (code 9048). Evaporation was included because it is a necessary component for the SWMM model to calculate the variable *Int*. The *ET* variable is estimated by the *Uc* component.

The model calibration considered the operation of the intake works at Dolores Dam. Because there is no information on dam levels or hydrometric stations recording runoff at any site in CF and its contributing watersheds, the outflow of 6.9 $m^3 s^{-1}$ was matched to the simulation using 2017 precipitation. Furthermore, the purpose of this dam is to regulate floods during storms, not to store water. The reference expenditure was taken from Trujillo (2016).

Upstream runoff (*Ear*)

To estimate upstream runoff, it was necessary to identify the streams that interconnect the microbasins. This value was obtained using the SWMM hydrologic model.

Imports from external basins (Im_e)

For the First Section, the only import considered is the discharge from the Chapultepec treatment plant (PTAR), which is sent to the minor lake and then to the major lake with a flow rate of 60 L s^{-1}. Then, 40 L s^{-1} are sent to the Acequia canal, where a portion is divided to the pumping sump for the irrigation network of the First Section, and the 15 L s^{-1} surplus is sent to the Reforma Avenue collector.

In the second section, the outflow from the PTAR is considered, with an outflow of 60 L s^{-1} to the minor lake, and then 55 L s^{-1} are sent to the major lake. A portion of this discharge is sent to the pumping sump for the irrigation network, and 20 L s^{-1} are sent to the Avenida Reforma collector.

In the Third Section, the discharges coming from an industrial use register were quantified, which is reported in supply sources as discharges. For the Fourth Section, the discharges presented in the Public Registry of Water Rights (REPDA), corresponding to domestic and service use, are considered.

Imports by potable water network (Im_p)

Information was compiled from plans of the drinking water network for the CF area from the Mexico City Water System (SACMEX). The water volume in each section was estimated based on the pipe diameters, using the Bresse equation (Bresse, 1860), which starts from a very elementary and conservative criterion by using a constant velocity of 0.57 m s^{-1}, which turns out to be a velocity widely surpassed nowadays. This equation is expressed as:

$$D = 1.2\sqrt{Q}$$

Clearing the expense, it remains:

$$\left(\frac{D}{1.2}\right)^2 = Q$$

where Q is the flow rate (m^3 s^{-1}), and D is the diameter (in meters).

For water distribution, it was assumed that the supply is made every day of the week in a range of 2 h per day, and that the overall efficiency in the water network in the four sections is 100 %.

Returns (Re)

A percentage was considered for each use (DOF, 2015): 75 % for urban public, 55 % for industrial, and 20 % for irrigation, based on the estimated volume of the drinking water network by SACMEX, pumping reported by REPDA (CONAGUA, 2020), and volume going to the pumping sump intended for irrigation, respectively.

Extractions by pumping within the polygon (*B*)

From the extractions reported by REPDA, only the total volume destined for industrial use was considered, since pumping wells were identified within the CF polygons. This volume of water is included in the initial analysis, but because the flow distribution within the CF is unknown due to a lack of micro-metering and because it is not an industrial zone, it is excluded from the final balance.

Volume supplied by springs (*Vm*)

Based on field surveys, a spring was discovered in the Tacubaya River ravine, just a few meters upstream from the Fourth Section. This spring is pumped by SACMEX and distributed to the drinking water network, but the flow to the CF is unknown. As a result, the drinking water network considers it a component of the variable (*Im*) because the estimated flow includes extractions from supply sources.

Evaporation of water bodies (*Ev*)

Evaporation was taken from climatological station 9048 (Tacubaya), located 1.18 km from the First Section of the CF. This station was considered because it has the longest record. The average monthly evaporation (in millimeters) was applied to the surface of the water bodies as a function of height to obtain the average evaporated water volume per month. In the First Section, the maximum evaporation surface of Chapultepec Lake was considered, which was 68 036.23 m^2. The Second Section has a maximum evaporation surface of 92 656.56 m^2. The Dolores Dam is located in the Third Section, but it does not store water, so it was not included in the analysis. The Tacubaya Dam is located in the Fourth Section and has a maximum evaporation surface of 20 278.64 m^2. In all scenarios, May has the highest evaporation, with 182 mm.

Downstream runoff (*Eaa*)

Downstream runoff was obtained using the SWMM hydrologic model to obtain the runoff described in basin proper (Cp).

Exports (*Ex*)

As stated in the demand of water bodies, of the 60 L s^{-1} that arrive from the PTAR, 15 L s^{-1} leave the basin as part of what was considered in the First Section. The discharge that is sent to the Reforma Avenue collector, with a flow rate of 20 L s^{-1}, was considered for the Second Section as part of the flow that exits the polygon. There were no sub-basin exports considered in the third and fourth sections.

Uses of consumption (*Uc*)

This index represents the total estimated consumption by type of water use for each section. To determine the type of water use based on land use and vegetation, a land use map was created using a vector map of blocks (INEGI, 2020c) and satellite imagery. The Cropwat application was used to estimate irrigation water use for different soils

(Swennenhuis, 2009), and it calculates the annual lamina required for irrigation. The First and Second Sections are irrigated primarily through a water network fed by pumping sumps, with a flow rate of 35 L s^{-1} applied via sprinkler irrigation at a 70 % efficiency.

The irrigation requirement data was generated using 10-year irrigation schedules, and the irrigation requirement method was based on crop evapotranspiration estimation. The consumption volume for the water bodies was calculated using the volume assigned to each, with flows from the PTAR. The volume of water for urban public use was estimated using records of visitors and employees from the First, Second, and Third Sections, as provided by CF authorities. The demographic data for the fourth section came from the population and housing census (INEGI 2020a).

Leaks in the potable water distribution network by SACMEX (*f*)

The system is considered to be 70 % efficient. This value is similar to the data provided by Bourguett-Ortiz and Ochoa-Alejo (1996), which found that in various cities across the country, leaks in intakes account for 24.5 % of losses on average.

Projection to 2050

The CF polygons are areas where no urban sprawl or land use change is expected, as they are protected areas by INAH, the Secretariat of the Interior and Ministry of National Defense (SEDENA) in the First, Second, and Fourth Sections, respectively, with the Third Section being a natural protected area. The water balance to 2050 was projected using climate change models and linear trends in climate variables such as temperature, precipitation, and evaporation. Similarly, visitor projections were made for the four sections using the population growth model. The Fourth Section projected only the population of the currently urbanized area. Based on the findings, each parameter in the forward water balance equation was calculated.

RESULTS AND DISCUSSION

The CF and its hydrographic system are located in the Lake Texcoco and Zumpango sub-basin of the Moctezuma River basin, which is one of three basins that comprise Hydrological Region No. 26 of the Pánuco River. Within the CF area, a series of ravines can be identified where rivers run off in a flowing manner during the rainy season. According to the Watershed Water Flow Simulator (SIATL) (INEGI, 2020b), these rivers are classified as intermittent streams because they do not present runoff during the dry season. The Third Section of the CF is formed by the Dolores River; the First and Second Sections do not have watercourses due to their flat topography, and the Fourth Section is crossed by the Tacubaya River, with runoff from wastewater discharges to the dam of the same name.

The study area belongs to the Anahuac Lakes and Volcanoes physiographic subprovince, which is part of the Neovolcanic Axis. The highest point in the basin has an altitude of 2850 m, while the lowest part of the basin reaches approximately

2200 m (INEGI, 2010). The maximum daily rainfall found is between 25 and 95 mm. In this study, 2017 was used as a reference because it was an average year with 943.1 mm of precipitation. The data for evaporation in the microbasins showed an average maximum rate of 6.4 mm d^{-1} and an average minimum rate of 3.8 mm d^{-1}.

The dominant soil in the CF area and catchment basin is Feozem, which has a medium texture. Their impervious areas of each micro-watershed range from 1.39 to 100 %. The curve numbers obtained range from 76 to 91. This is because each micro-watershed has a weighted value (based on different land uses). The calibration of the simulated model with the average rainfall represented by the 2017 precipitation revealed that by matching the outflow through the intake work of 6.9 $m^3 s^{-1}$, a flow of 0.37 m within the dam was generated.

Current water balance in the CF sections

The water balance was performed using the general equation of storage change, which included input variables (supply) such as runoff from the hydrological model, imports, and the drinking water network, as well as outputs such as evaporation, leaks, transfers, and consumptive uses in the area (demand). As a result, the First, Second, and Fourth Sections experience an annual water surplus. The Third Section has a deficit of almost 400 thousand m3 per year (Table 1).

Table 1. Current potential water balance of the Chapultepec Forest sections in Mexico City, Mexico.

	Variable	First Section (m^3 $year^{-1}$)	Second Section (m^3 $year^{-1}$)	Third Section (m^3 $year^{-1}$)	Fourth Section (m^3 $year^{-1}$)
(+)E	*Cp*	1 258 456	1 075 281	2 625 404	5 357 618
	Ear	125 129	2 427 445	0	2 518 747
	Im	2 539 614	2 199 589	66 200	1 136 982
	Re	752 406	451 669	46 045	570 250
	B	200 000	0	0	0
	Vm	0	0	0	0
(-)S	*Ev*	111 115	151 324	0	33 119
	Eaa	1 548 275	87 223	2 359 257	675 165
	Ex	474 336	632 448	0	0
	Uc	1 847 416	389 975	759 886	473 003
	f	252 681	90 673	18 418	228 100
(+)E	Total	4 875 605	6 153 984	2 737 649	9 583 597
(-)S	Total	4 233 823	1 351 643	3 137 561	1 409 387
ΔV	Total (m^3)	641 782	4 802 341	-399 912	8 174 210

(+)E: inflow volume; (-)S: outflow volume; ΔV: change in storage volume; *Cp*: volume of runoff by own basin; *Ear*: volume of runoff from upstream; *Im*: import volume; *Re*: return volume; *B*: volume of extraction by pumping; *Vm*: volume contributed by springs; *EV*: volume loss due to evaporation from water bodies; *Eaa*: downstream runoff volume; *Ex*: export volume; *Uc*: volume of consumption use; *f*: losses due to leaks in the distribution network.

However, it is important to consider that pumping (*B*) represents the volume supplied by REPDA supply sources, the amount of water and proportion that it contributes to each section being unknown, as they also supply other neighboring areas outside the CF polygons. Therefore, only the volume estimated using the pipe diameters of the potable water network, which supplies the four sections in total, is considered. Water from runoff and returns was also eliminated due to poor quality (IMTA, 2022), resulting in a water balance of -146, 935, -712, and 402 thousand m^3 in the First, Second, Third, and Fourth Sections, respectively.

With this consideration, the First Section also suffers from water deficit. However, if the balance is separated by use, that is, what comes from the PTAR that is used for irrigation and water bodies, and what comes from the potable water network for urban public use minus what is lost in leaks, the available water for irrigation in the First, Second, and Fourth Sections is obtained. Nonetheless, for urban public use, there is a deficit in the First, Second, and Third Sections (Table 2).

Table 2. Current effective water balance of the Chapultepec Forest sections in Mexico City, Mexico.

Variable	First Section (m^3 $year^{-1}$)	Second Section (m^3 $year^{-1}$)	Third Section (m^3 $year^{-1}$)	Fourth Section (m^3 $year^{-1}$)
+ PTAR supply	1 897 344	1 897 344	4 807	376 648
+ Drinking water supply network	642 270	302 245	61 393	760 334
- Irrigation demand	1 223 984	92 794	668 207	268 210
- Lake demand	632 448	632 448	0	0
- Urban public demand	623 432	297 181	91 679	204 793
- Leaks	252 681	90 673	18 418	228 100
Irrigation availability	40 912	1 172 102	-663 400	108 438
Urban public availability	-233 843	-85 609	-48 704	327 441

PTAR: Chapultepec wastewater treatment plant.

Projections to 2050

By 2050, the average temperature will oscillate between 12 and 14 °C. For precipitation, based on a linear trend, rainfall of up to 300 mm is expected in August, while climate change projections show a reduction to around 200 mm.

In 2019, there were approximately 19 million visitors per year in the first three sections of the CP, with a projected 28.7 million in 2050. The Fourth Section is expected to receive 3.2 million visitors, as its doors have been opened as a tourist destination until 2022. Finally, by 2050, the four sections are expected to receive 31.9 million visitors per year. In terms of population, no significant growth is expected by 2050, with a projected increase from 3879 (2020) to 5333 people, with the Fourth Section accounting for 80 % of the total.

Water supply to 2050

For the four sections, the WWTP and supply network are expected to remain constant, while surface water runoff volume per basin will decrease due to increased evaporation, resulting in a reduction in total supply volume. Given that it is not feasible to use surface water, including returns, due to the difficulties associated with treating wastewater in the area (IMTA, 2022), it is assumed that the supply in 2050 will remain constant as in the current situation.

Water demand to 2050

Irrigation for pasture and eucalyptus was calculated using climate variables projected to 2050, while land use areas remained unchanged. Finally, for the human consumption demand variable, the projected numbers of visitors and residents in each section were used. The demand or consumption use (*Uc*) increased from 1.8 to 3.2 million m^3 in the first section, 0.4 to 0.6 million m^3 in the second section, 0.76 to 2 million m^3 in the third section, and 0.47 to 1 million m^3 in the fourth section.

Water balance to 2050

Considering the constant supply, the increase in demand due to population, visitors, and irrigation volume, the separation by balance by use, the volume coming from the PTAR for irrigation and water bodies, and the volume of the potable water network for urban public use deducting what is lost in leaks, we have that the Second Section maintains a volume of water available for irrigation but not for urban public use. The Fourth Section would not be able to meet its irrigation needs, but would maintain a slight volume available for human consumption (Table 3). The First and Third Sections will be in deficit of water for irrigation, lakes, and urban public.

Table 3. Projected effective water balance for the year 2050 in the Chapultepec Forest sections of Mexico City, Mexico.

Variable	First Section (m^3 $year^{-1}$)	Second Section (m^3 $year^{-1}$)	Third Section (m^3 $year^{-1}$)	Fourth Section (m^3 $year^{-1}$)
+ PTAR supply	1 897 344	1 897 344	4807	376 648
+ Drinking water network supply	642 270	302 245	61 393	760 334
- Irrigation demand	2 265 917	171 385	1 901 854	500 449
- Lake demand	474 336	632 448	0	0
- Urban public demand	951 533	442 426	117 624	513 327
- Leaks	252 681	90 673	18 418	228 100
Irrigation and lake availability	-842 909	1 093 511	-1 897 047	-123 801
Urban public availability	-561 944	-230 854	-74 649	18 907

PTAR: Chapultepec wastewater treatment plant.

Sustainable management measures within the CF

The measures analyzed to reduce the existing water gap and to 2050 addressed four issues (available water, flood reduction, groundwater recharge, and water quality improvement). In principle, the limited treatment that wastewater can receive (IMTA, 2022) influenced the selection of these measures, as the rugged topography prevents the use of natural wastewater treatment systems, which require significant surface area extensions. It is possible to treat wastewater in a specific way in each discharge using mechanical means; however, this requires significant economic investment (IMTA, 2022).

With the proposed aquifer recharge and flood reduction measures, it is not possible to include the contribution to the volume of water consumed. As a result, rainwater harvesting was chosen to take advantage of the existing and planned building extensions. Rainwater harvesting systems (SCALL) are made up of five basic components: the catchment area, pipelines for conveying water, treatments, storage tank size, and complements. The volume of rainwater harvested in the current and projected 2050 scenarios is roughly 65 thousand m^3 per year (Table 4).

When these volumes are compared to the current and 2050 urban public use demand, it is clear that it is not possible to meet the water needs, but it is possible to significantly reduce the volume of water in the rainy months for specific uses such as sanitary use (Figure 2).

Table 4. Volume of water captured (m^3 $year^{-1}$) in the sections of the Chapultepec Forest in Mexico City, Mexico.

Scenario	First Section	Second Section	Third Section	Fourth Section	Total
Current	28 594	10 014	0	26 858	65 466
2050	23 291	10 751	8105	21 387	63 534

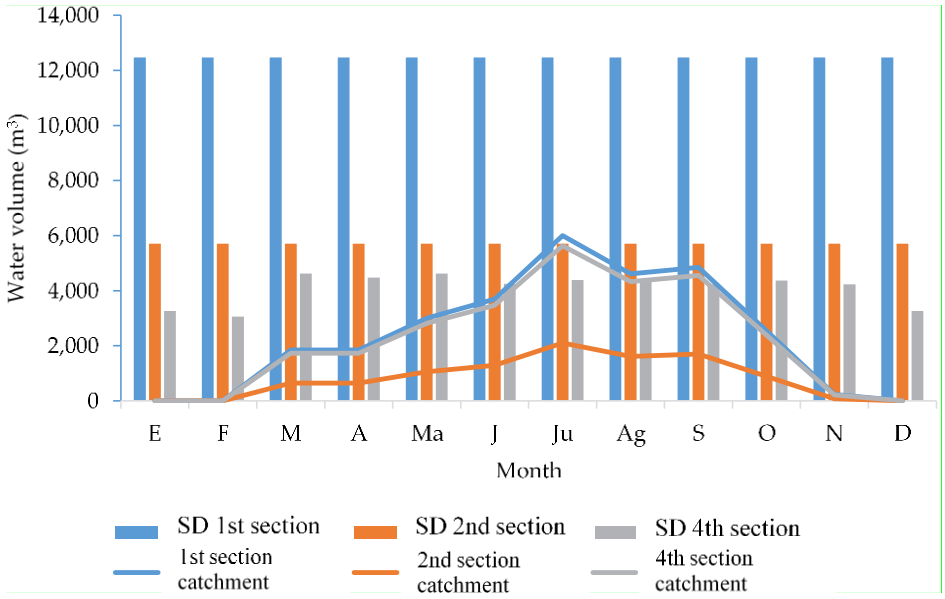

Figure 2. Water catchment volume versus demand volume for monthly sanitary use in the current scenario in three sections of Chapultepec Forest. SD: sanitary demand.

CONCLUSIONS

Currently, the four sections of Chapultepec Forest are in water balance, tending to deficit during dry seasons. However, if the Cultural Complex Project is implemented in the future, it will not be possible to supply water resources to visitors due to the deficit of the aquifer. Towards 2050, an increase in precipitation is observed, but also in temperatures, which leads to an increase in evaporation and a greater demand for consumption. With an increase in the visiting population, a greater demand for urban public use is expected, so the water balance is expected to be negative in the future.

Rainwater harvesting is a major contributor to water supply, which could partially pay, in the months of March to October, a percentage of the water demanded for sanitary use of the buildings. More rainwater could be captured; however, there is a restriction due to the division of the administrative management of Chapultepec Forest, resulting in inadequate and suboptimal water management, which is only possible in the Third Section but requires a large investment in infrastructure. To deal with the low availability of water, volumetric meters must be installed to count consumption and detect leaks or losses, so that they can be repaired and drinking water is not wasted.

ACKNOWLEDGMENTS

To the *Fondo Institucional para el Desarrollo Científico, Tecnológico y de Innovación* FORDECYT-PRONACES (Institutional Fund for Scientific, Technological and Innovation Development) of the Consejo Nacional de Humanidades, Ciencias y Tecnologías (CONAHCYT) (National Council of Humanities, Sciences and Technologies).

REFERENCES

Breña-Puyol AF, Breña-Naranjo JA. 2017. Disponibilidad de agua en el futuro de México. Ciencia 1 (3): 64–71.

Bresse JAC. 1860. Cours de mécanique appliquée. Kessinger Publishing: Paris, France. 504 p.

CONAGUA (Comisión Nacional del Agua). 2020. Base de datos del Registro Público de Derechos de Agua (REPDA). Gobierno de México, Comisión Nacional del Agua. Ciudad de México, México. https://app.conagua.gob.mx/consultarepda.aspx (Retrieved: May 2020).

DOF (Diario Oficial de la Federación). 2015. NORMA Oficial Mexicana NOM-011-CONAGUA-2015, conservación del recurso agua, que establece las especificaciones y el método para determinar la disponibilidad media anual de las aguas nacionales. Gobierno de México. Secretaría de Medio Ambiente y Recursos Naturales. Comisión Nacional del Agua. Ciudad de México, México. https://www.dof.gob.mx/nota_detalle.php?codigo=5387027&fecha=27/03/2015#gsc.tab=0 (Retrieved: May 2020).

DOF (Diario Oficial de la Federación). 2020a. ACUERDO por el que se actualiza la disponibilidad media anual de las aguas nacionales superficiales de las 757 cuencas hidrológicas que comprenden las 37 Regiones Hidrológicas en que se encuentra dividido los Estados Unidos Mexicanos. Gobierno de México. Secretaría de Medio Ambiente y Recursos Naturales. Comisión Nacional del Agua. Ciudad de México, México. https://dof.gob.mx/nota_detalle.php?codigo=5712948&fecha=28/12/2023#gsc.tab=0 (Retrieved: May 2020).

DOF (Diario Oficial de la Federación). 2020b. ACUERDO por el que se actualiza la disponibilidad media anual de agua subterránea de los 653 acuíferos de los Estados Unidos Mexicanos, mismos que forman parte de las regiones hidrológico-administrativas que se indican. Gobierno de México. Secretaría de Medio Ambiente y Recursos Naturales. Comisión Nacional del Agua. Ciudad de México, México. https://dof.gob.mx/nota_detalle.php?codigo=5708074&fecha=09/11/2023#gsc.tab=0 (Retrieved: May 2020).

Gobierno del Distrito Federal. 2003. Gaceta oficial del Distrito Federal del 2 de diciembre de 2003. Ciudad de México, México. 92 p.

Gómez-Reyes E. 2013. Valoración de las componentes del balance hídrico usando información estadística y geográfica: la cuenca del Valle de México. Realidad, datos y espacio. Revista Internacional de Estadística y Geografía 4 (3).

Bourguett-Ortiz V, Ochoa-Alejo L. 1996. Recuperación integral de pérdidas de agua potable. Diagnóstico, eliminación y control de pérdidas en sistemas de agua potable. Instituto Mexicano de Tecnología del Agua. Facultad de Ingenieros Topógrafos e Hidráulicos. Comisión Municipal de Agua Potable y Alcantarillado de Reynosa, Tamaulipas. Jiutepec, México. 449 p.

IMTA (Instituto Mexicano de Tecnología del Agua). 2022. Diagnóstico y propuestas para la gestión de los recursos hídricos en las cuatro secciones del bosque de Chapultepec. Instituto Mexicano de Tecnología del Agua. Consejo Nacional de Humanidades, Ciencias

y Tecnologías. Ciudad de México, México. http://chapultepec.centrogeo.org.mx/cms/multimedia/ChapultepecGeo/menuSect-6-132 (Retrieved: August 2020).

INEGI (Instituto Nacional de Estadística y Geografía). 2010. Modelos digitales de elevación de alta resolución LiDAR, con resolución de 5 m. Ciudad de México, México. https://www.inegi.org.mx/app/mapas/?tg=1015 (Retrieved: August 2020).

INEGI (Instituto Nacional de Estadística y Geografía). 2020a. Censo de población y vivienda 2020. Ciudad de México, México. https://www.inegi.org.mx/programas/ccpv/2020/#:~:text=El%20Censo%20de%20Poblaci%C3%B3n%20y,viviendas%20para%20obtener%20informaci%C3%B3n%20sobre (Retrieved: August 2020).

INEGI (Instituto Nacional de Estadística y Geografía). 2020c. Marco geoestadístico, diciembre 2021. Ciudad de México, México. https://www.inegi.org.mx/app/biblioteca/ficha.html?upc=889463849568 (Retrieved: August 2020).

INEGI (Instituto Nacional de Estadística y Geografía). 2020b. SIATL. Simulador de flujos de agua de cuencas hidrográficas. Ciudad de México, México. http://antares.inegi.org.mx/analisis/red_hidro/siatl/?s=geo&c=1693&e=04 (Retrieved: August 2020).

James W, Rossman LE, James WRC. 2010. User's guide to SWMM5 (13th edition). CHI Press: Guelph, Canada. 905 p.

López-García TG, Manzano MG, Ramírez AI. 2017. Disponibilidad hídrica bajo escenarios de cambio climático en el Valle de Galeana, Nuevo León, México. Tecnología y Ciencias del Agua 8 (1).

NRCS (Natural Resource Conservation Service). 1986. Urban hydrology for small watersheds, technical release 55 (Second edition). U.S. Department of Agriculture: Washington, DC, USA. 164 p.

Ordóñez-Gálvez JJ. 2011. Cartilla técnica: balance hídrico superficial. Contribuyendo al desarrollo de una cultura del agua y la gestión integral de recurso hídrico. Sociedad Geográfica de Lima. Foro Peruano para el Agua. Lima, Perú. 41 p.

SCS (Soil Conservation Service). 1991. Soil-plant-water relationships. National engineering handbook. Section 15, irrigation, chapter 1. U.S. Department of Agriculture: Washington, DC, USA. 56 p.

SEDEMA (Secretaría del Medio Ambiente). 2011. Bosque de Chapultepec. Gobierno de la Ciudad de México. Ciudad de México, México. http://data.sedema.cdmx.gob.mx/bosquedechapultepec/index.php?option=com_content&view=article&id=45&Itemid=28 (Retrieved: June 2020).

Silva-Hidalgo H, Aldama ÁA, Martín-Domínguez IR, Alarcón-Herrera MT. 2013. Metodología para la determinación de disponibilidad y déficit de agua superficial en cuencas hidrológicas: aplicación al caso de la normativa mexicana. Tecnología y Ciencias del Agua 4 (1): 27–50.

SINA (Sistema de Información Nacional del Agua). 2020a. Mapa vectorial de cuencas 2020. Gobierno de México. Comisión Nacional del Agua. Ciudad de México, México. https://sinav30.conagua.gob.mx:8080/SINA/?opcion=cuencas (Retrieved: June 2020).

SINA (Sistema de información Nacional del Agua). 2020b. Mapa vectorial de acuíferos 2020. Gobierno de México. Comisión Nacional del Agua. Ciudad de México, México. https://sinav30.conagua.gob.mx:8080/SINA/?opcion=acuiferos (Retrieved: June 2020).

Swennenhuis J. 2009. CropWat 8.0. FAO water development and management unit. Rome, Italy. https://www.fao.org/land-water/databases-and-software/cropwat/en/ (Retrieved: June 2020).

Trujillo J. 2016. Desarrollo de estudio hidrológico y proyecto conceptual hidráulico de la Tercera Sección del Bosque de Chapultepec. Taller de Ingeniería y Diseño S. A. de C. V. Consejo Nacional de Humanidades, Ciencias y Tecnologías. Ciudad de México, México. 49 p.

UNESCO (Organización de las Naciones Unidas para la Educación, la Ciencia y la Cultura). 2006. Evaluación de los recursos hídricos: elaboración del balance hídrico integral por cuencas hidrográficas. Documento técnico del PHI-LAC 4. Montevideo, Uruguay. 95 p.

Agrociencia

INSECTICIDE SUSCEPTIBILITY IN TWO POPULATIONS OF *Aedes aegypti* L. (Diptera: Culicidae) FROM GUERRERO, MEXICO, AND RECOMMENDATIONS FOR THEIR MANAGEMENT

Nelson Erik **López-Zerón**[1], J. Concepción **Rodríguez-Maciel**[2*], Claudia Yanet **Wilson-García**[3], Ángel **Lagunes-Tejeda**[1], Gonzalo **Silva-Aguayo**[4]

[1]Centro de Bachillerato Tecnológico Agropecuario No. 178. Carretera San Luis Horcasitas km 0.5, San Luis Acatlán, Guerrero, Mexico. C. P. 41600.
[2]Colegio de Postgraduados Campus Montecillo. Posgrado en Fitosanidad-Entomología y Acarología. Carretera México-Texcoco km 36.5, Montecillo, Texcoco, State of Mexico, Mexico. C. P. 56264.
[3]Universidad Autónoma Chapingo. Sede San Luis Acatlán. Carretera San Luis Acatlán-Tlapa de Comonfort km 5, San Luis Acatlán, Guerrero, Mexico. C. P. 41600.
[4]Universidad de Concepción. Facultad de Agronomía, Departamento de Producción Vegetal. Casilla 537, Chillán, Ñuble, Chile.
* Author for correspondence: concho@colpos.mx

Citation: López-Zerón NE, Rodríguez-Maciel JC, Wilson-García CY, Lagunes-Tejeda Á, Silva-Aguayo G. 2024. Insecticide susceptibility in two populations of *Aedes aegypti* L. (Diptera: Culicidae) from Guerrero, Mexico, and recommendations for their management. **Agrociencia** 58(7): 922-933. https://doi.org/ 10.47163/agrociencia.v58i7.3041

Editor in Chief:
Dr. Fernando C. Gómez Merino

Received: July 03, 2023.
Approved: August 29, 2024.
Published in Agrociencia: October 03, 2024.

ABSTRACT

The *Aedes aegypti* L. mosquito is a vector of diseases such as classic and hemorrhagic dengue (DENV), chikungunya (CHIKV), Zika (ZIKV), yellow fever (YFV), and Mayaro (MAYV). In 2019 alone, in Latin America, there were 2.7 million cases and 1206 deaths. In Mexico, government programs for managing this pest include the elimination of larval habitats and chemical control of larvae and adults. The objective of this study was to evaluate the response of two larvae and adult populations of *A. aegypti* from the state of Guerrero, Mexico, under laboratory conditions, to insecticides with different modes of action and to make considerations for their management. In the bioassays, larvae showed susceptibility to permethrin, malathion, deltamethrin, and *Bacillus thuringiensis* var. *israelensis;* low resistance to Temephos and propoxur; as well as moderate resistance to Spinosad. Both adult populations showed resistance to permethrin and susceptibility to deltamethrin, while the Acapulco population showed resistance to alpha-cypermethrin. For larvae, Spinosad is suggested to be used in times of high incidence of dengue. During drought, it is advisable to include rotations of *B. thuringiensis* var. *israelensis* with organophosphates. For adults, the use of imidacloprid in combination with botanical insecticides is considered a rational alternative to rotations with organophosphates and pyrethroids.

Keywords: vector control, yellow fever mosquito, dengue mosquito, plague, resistance management.

INTRODUCTION

The yellow fever mosquito, *Aedes aegypti* L. (Diptera: Culicidae), is one of the most important insect species in public health, as it is a vector of viral diseases such as classical and hemorrhagic dengue (DENV), chikungunya (CHIKV), Zika (ZIKV), Mayaro fever (MAYV), and yellow fever (YFV) (WHO, 2019). In Mexico, during the 33rd epidemiological week of 2022, 3134 cases of dengue were confirmed. The highest number of cases coincides with the rainy season (CENAPRECE, 2022). Regarding confirmed cases of Zika, a total of 12 996 have been documented between 2015 and 2022. In February 2017, the first case of microcephaly due to Zika virus infection was also detected (CENAPRECE, 2022).

The species *A. aegypti* was considered to colonize only regions with an elevation below 1700 m; however, at the end of the last decade, its presence was documented in Mexico City at 2200 m (Kuri-Morales *et al*., 2017). Currently, management strategies for this species are based on awareness campaigns to promote the elimination of breeding sites and the use of insecticides against larvae and adults (WHO, 2019). In Mexico, for more than 30 years, Temephos (organophosphate) insecticides have been applied uninterruptedly against larvae, and for the last 10 years, permethrin (pyrethroid) has been used against adults (Flores *et al*., 2013). Consequently, in both biological states, numerous cases of resistance have been documented in the states of Veracruz (Flores *et al*., 2013), Coahuila (Flores *et al*., 2009), Quintana Roo (Flores *et al*., 2006), Guerrero (Chino-Cantor *et al*., 2014), and Baja California (Flores *et al*., 2005).

The use of Spinosad, *Bacillus thuringiensis* var. *israelensis*, and Temephos to control *A. aegypti* larvae is authorized in Mexico, but Temephos is the most widely used larvicide. The active ingredients permethrin, deltamethrin, chlorpyrifos, malathion, and propoxur are authorized against adults of this vector (CENAPRECE, 2017). Currently, the number of insecticides used to reduce the density of the dengue mosquito has diversified, so it is expected that the resistance levels that were present when chemical control was based on a few options have decreased. Therefore, the present study aimed to evaluate the response to insecticides in two populations of *A. aegypti* from the state of Guerrero, Mexico, and to make recommendations for their management.

MATERIALS AND METHODS

Populations

During April and May 2017, 148 ovitraps for *A. aegypti* mosquitoes were placed in Acapulco, Guerrero, Mexico (16° 51′ 46′′ N, 99° 53′ 13′′ W), and 165 in San Luis Acatlán (16° 48′ 23″ N, 98° 43′ 58″ W). The ovitraps were kept at the peridomestic sites and checked weekly. Subsequently, they were sent to the Toxicology Laboratory of the Colegio de Postgraduados Montecillo Campus to obtain enough F_1 individuals for the bioassays. The New Orleans race of *A. aegypti* was used as the susceptible reference population. Field and reference populations were bred using the method proposed by the World Health Organization (WHO, 2005).

Insecticides used

For the larvae bioassays, the commercial formulations used were Spinosad (NATULAR EC CLARKE®, 20.6 %, emulsifiable concentrate, 230 g active ingredient (a. i.) L^{-1}; Public Health Supply and Equipment de México S. A. de C. V., Mexico); *Bacillus thuringiensis* var. *israelensis* (VECTOBAC WDG®, 34.7 % water-soluble granules; Bayer de México S. A. de C. V., Mexico); Temephos (TEMEPHOS 500 CE, 500 g a.i. L^{-1}, emulsifiable concentrate; Química Lucava S.A. de C.V., Mexico); chlorpyrifos ethyl (CLORPIRIFÓS, 122.8 g a. i. L^{-1}, liquid in mineral oil; Public Health Supply and Equipment de México S. A. de C. V., Mexico); permethrin (AQUA RESLIN SUPER®, 108.7 g a. i. L^{-1}, aqueous solution; Bayer de México S. A. de C. V., Mexico); deltamethrin (AQUA K-OTHRINE®, aqueous emulsion 20 g a.i. L^{-1}; Bayer de México S. A. de C. V., Mexico); deltamethrin (AQUA K-OTHRINE®, aqueous emulsion 20 g a. i. L^{-1}; Bayer de México S. A. de C. V., Mexico); malathion (VERTHION®, 410 g i. a. L^{-1} concentrated solution; Agricultura Nacional S.A. de C.V., Mexico), and technical grade propoxur (99.5 % purity; Chem service, West Chester, PA, USA).

For the adult bioassays, permethrin (technical grade, mixture of isomers, 99.4 % purity; Chem service, West Chester, PA, USA), deltamethrin (technical grade, 99.1 % purity; Chem service, West Chester, PA, USA), and alpha-cypermethrin (technical grade, 99.5 % purity; Chem service, West Chester, PA, USA) were used. For the formulated insecticides, distilled water was used to prepare the required concentrations, and for the active ingredients, analytical-grade acetone (Meyer®; Tláhuac, Mexico City, Mexico) was used.

Bioassays with larvae

Bioassays with larvae were performed according to the standardized procedure of the World Health Organization (WHO, 2012). In 120 mL polystyrene containers, 100 mL of distilled water and 20 early fourth instar larvae were placed. Subsequently, 1 mL of the required concentration of the insecticide treatment to be evaluated was added.

Initially, the biological response window was determined with the range of concentrations that caused between 0 and 100 % mortality. Subsequently, for each insecticide, nine intermediate concentrations were evaluated to cover this range. After 24 h of exposure to the toxicant, larvae that were not able to perform vertical movements or that did not show the characteristic diving reaction when the water was disturbed were considered dead (Flores, 2014).

Five replicates of each insecticide concentration were made, and each replicate included an untreated control. The maximum natural mortality accepted for the control was 10 %, and this was adjusted with the formula by Abbott (1925). Resistance ratio values at the level of the lethal concentrations LC_{50} (RR_{50}) and LC_{95} (RR_{95}) were obtained by dividing $LC_{50(95)}$ of the field population by $LC_{50(95)}$ of the susceptible population. The Mazzarri and Georghiou (1995) criterion was considered to define the resistance level. It was established that a resistance factor < 5 indicates a low resistance level, between 5 and 10 it is considered moderate resistance, and > 10 is high resistance.

Bioassays with adults

For bioassays with *A. aegypti* adults, the recommended diagnostic doses of alpha-cypermethrin, deltamethrin (10 µg per bottle), and permethrin (15 µg per bottle) were evaluated (CDC, 2010). The required concentrations were prepared using a micropipette (Thermo Fisher Scientific, Waltham, MA, USA) of 1 mL capacity in amber glass bottles, and analytical grade acetone was used as diluent (Meyer®, Mexico City, Mexico). Individually, 1 mL of the insecticide concentration was added to the 250 mL Wheaton glass bottles, while 1 mL of acetone was applied to the control. To form a uniform layer of the insecticide inside the bottles, these were capped and placed in an inverted position for 30 s. Subsequently, they were laid horizontally. The lid was removed and placed on a rotating roller machine (Star MFG International Inc., Maplewood, MO, USA) until the acetone evaporated, which occurred in approximately 10 min.

With a manual aspirator, 20 females (1–2 days old) previously in blood quarantine were introduced and provided with 10 % sugar water *at libitum*. The treated insects were checked every 5 min for half an hour, and this period was considered the diagnostic time. The exposure time was approximately 30 min. Adult mosquitoes that could not remain in normal position or fly in a coordinated manner were categorized as knocked down (Flores, 2014). The maximum number of downed mosquitoes accepted in the control was 10 %. Five replicates of each insecticide were conducted on different days, and a control was included in each replicate. Mortality was adjusted using the Abbott (1925) formula.

The World Health Organization (WHO, 2016) criteria were used to categorize resistance as follows: with 98–100 % knockdown, the population was considered susceptible; with 90–97 %, it was considered as possible resistance, in which case the bioassay was repeated to confirm; and with a knockdown value of less than 90 %, the population was considered resistant to the insecticide evaluated (WHO, 2016).

Data analysis

Data from the larval bioassays were analyzed using the PROC PROBIT SAS procedure ver. 9.4 (SAS Institute, 2016). The slope values and their standard error, the mean, 95 % lethal concentrations (LC_{50} and LC_{95}), and their respective confidence intervals (95 %) were estimated. The significant difference in response between the two populations at the LC_{50} or LC_{95} level was determined by the absence of overlap between their confidence intervals (Mazzarri and Georghiou, 1995). The mortality result with the adult diagnostic dose was plotted with the Excel 2013 software package (Microsoft Corporation, USA).

RESULTS AND DISCUSSION

The two mosquito larvae populations showed susceptibility to *Bacillus thuringiensis* var. *israelensis*, as their resistance factor (RR_{50}) was 1.14 × (Acapulco) and 0.95 × (San

Luis Acatlán), and there was overlap of their confidence intervals (LC_{50} and LC_{95}) with the susceptible New Orleans control population (Table 1). These results agree with reports of *A. aegypti* from the field that have shown susceptibility to *B. thuringiensis* var. *israelensis* (Araújo *et al*., 2013; IRAC, 2017). For more than 10 years, populations under selection pressure have been studied under laboratory conditions and showed no changes in susceptibility to this insecticide. This can be attributed to the composition of the commercial product containing a mixture of four proteins from this bacterium (Cry4Aa, Cry4Ba, Cry11Aa, and Cyt1Aa), each with different receptors or active sites, with activity in the midgut of mosquito larvae (Tetreau *et al*., 2013).

Table 1. Toxicity of microbial insecticides on the larval population of *Aedes aegypti* L. from the state of Guerrero, Mexico.

Insecticide	Population	†n	¶b ± EE	§LC_{50} (LC 95 %)	ᵖPr> χ^2	¤RR_{50}	LC_{95} (LC 95 %)	RR_{95}
Spinosad	New Orleans	500	3.78 ± 0.36	0.11 (0.10–0.12)	0.23		0.31 (0.25–0.41)	
	San Luis Acatlán	500	3.13 ± 0.23	0.18 (0.16–0.20)	0.63	1.63	0.62 (0.51–0.79)	2.00
	Acapulco	600	3.37 ± 0.29	0.15 (0.13–0.17)	0.75	1.36	0.47 (0.38–0.62)	1.51
Bacillus thuringiensis var. *israelensis*	New Orleans	500	2.11 ± 0.16	0.021 (0.018–0.025)	0.40		0.12 (0.099–0.180)	
	San Luis Acatlán	500	2.67 ± 0.27	0.02 (0.017–0.023)	0.20	0.95	0.083 (0.062–0.120)	0.69
	Acapulco	500	3.26 ± 0.31	0.024 (0.021–0.028)	0.30	1.14	0.079 (0.062–0.110)	0.65

†*n*: total number of treated insects; ¶b ± EE: slope and standard error; §LC: lethal concentration (mg L^{-1}); ᵖPr > χ^2: Chi-square probability of fit to a straight line; ¤RR: resistance factor.

In the case of Spinosad, the San Luis Acatlán population showed low levels of resistance (RR < 5 ×), both at the LC_{50} and LC_{95} levels, while the Acapulco population was only at the LC_{50} level. Therefore, it is necessary to implement rational management of this insecticide to avoid higher levels of resistance, as well as to monitor the biological effectiveness in the field that contributes to making the right decisions, as suggested by Marina *et al*. (2012).

Both larvae populations showed susceptibility to deltamethrin (Table 2). This insecticide is a type II pyrethroid, with a metabolic mechanism of resistance based on the action of Multiple Function Oxidases (MFO), unlike type I pyrethroids such as permethrin, which produce MFO and are also metabolized by esterases. (Atencia *et al*., 2016). Both larval populations reported low LC_{50} levels to malathion (FR < 5 ×). Chino-Cantor *et al*. (2014) found similar results when evaluating three field populations with this insecticide and determined resistance levels < 5 ×.

Table 2. Toxicity of synthetic insecticides on the population of *Aedes aegypti* L. larvae from the state of Guerrero, Mexico.

Insecticide	Population	†*n*	¶b ± EE	§LC_{50} (LC_{95} %)	ᵖPr > χ^2	¤RR_{50}	LC_{95} (LC_{95} %)	RR_{95}
Permethrin	New Orleans	800	1.65 ± 0.19	0.0098 (0.0069–0.0130)	0.052		0.096 (0.054–0.250)	
	San Luis Acatlán	500	2.24 ± 0.19	0.045 (0.040–0.052)	0.67	4.50	0.24 (0.18–0.37)	2.50
	Acapulco	600	2.19 ± 0.25	0.014 (0.011–0.017)	0.52	1.42	0.08 (0.055–0.140)	0.83
Deltamethrin	New Orleans	900	1.97 ± 0.13	0.0083 (0.0070–0.0097)	0.98		0.056 (0.042–0.079)	
	San Luis Acatlán	600	2.07 ± 0.25	0.01 (0.008–0.012)	0.63	1.20	0.062 (0.043–0.110)	1.10
	Acapulco	600	2.53 ± 0.22	0.0028 (0.0024–0.0032)	0.69	0.33	0.012 (0.0098–0.0170)	0.21
Temephos	New Orleans	600	2.48 ± 0.22	0.017 (0.014–0.019)	0.73		0.077 (0.058–0.110)	
	San Luis Acatlán	500	2.31 ± 0.20	0.076 (0.067–0.087)	0.34	4.47	0.39 (0.29–0.58)	5.06
	Acapulco	600	3.10 ± 0.25	0.032 (0.028–0.036)	0.88	1.88	0.10 (0.08–0.18)	1.29
Propoxur	New Orleans	500	3.67 ± 0.37	0.014 (0.012–0.016)	0.73		0.039 (0.031–0.054)	
	San Luis Acatlán	600	2.36 ± 0.21	0.024 (0.021–0.028)	0.10	1.71	0.12 (0.09–0.18)	3.07
	Acapulco	700	2.39 ± 0.30	0.028 (0.021–0.040)	0.039	2.00	0.13 (0.082–0.360)	3.33
Malathion	New Orleans	600	1.56 ± 0.18	0.017 (0.014–0.022)	0.22		0.19 (0.11–0.45)	
	San Luis Acatlán	600	2.31 ± 0.21	0.031 (0.026–0.036)	0.74	1.82	0.16 (0.11–0.24)	0.84
	Acapulco	600	1.88 ± 0.18	0.03 (0.025–0.037)	0.87	1.76	0.22 (0.15–0.4)	1.15
Chlorpyrifos	New Orleans	900	1.48 ± 0.15	0.096 (0.07–0.13)	0.074		1.23 (0.68–3.00)	
	San Luis Acatlán	800	1.65 ± 0.14	0.29 (0.24–0.36)	0.18	3.02	2.92 (1.90–5.26)	2.37
	Acapulco	800	1.12 ± 0.19	0.33 (0.19–0.77)	0.0083	3.43	9.50 (2.61–212.10)	7.72

†*n*: total number of treated insects; ¶b ± EE: slope and standard error; §LC: lethal concentration (mg L^{-1}); ᵖPr > χ^2: Chi-square probability; ¤RR: resistance factor.

In the case of Temephos, at the LC_{50} level, the Acapulco and San Luis Acatlán populations showed low resistance, whereas the latter showed moderate resistance at the LC_{95} level. Both populations also had low resistance to propoxur at the LC_{50}

level. These results agree with Chino-Cantor *et al*. (2014), who documented moderate resistance to Temephos in larvae populations of this species from Guerrero. According to Marina *et al*. (2011), this can be attributed to the fact that Temephos has been used for more than 35 years to combat *A. aegypti* larvae in that place; in addition, this insecticide and other organophosphates are also used in agriculture and may come into contact with breeding sites located in bodies of water, contributing to resistance development. This could be the case of chlorpyrifos, which registered a RR_{95} of 7.72 × in the Acapulco population, indicating moderate resistance.

Adults of both populations showed susceptibility to deltamethrin (Figure 1). At the diagnostic dose evaluated (10 µg per bottle) and 30 min of exposure, a value > 98 % mortality was recorded. Because this insecticide was used extensively and intensively in the past (Flores *et al*., 2013), this population is likely to contain resistance alleles not detectable by the methodology used, as suggested by Atencia *et al*. (2016).

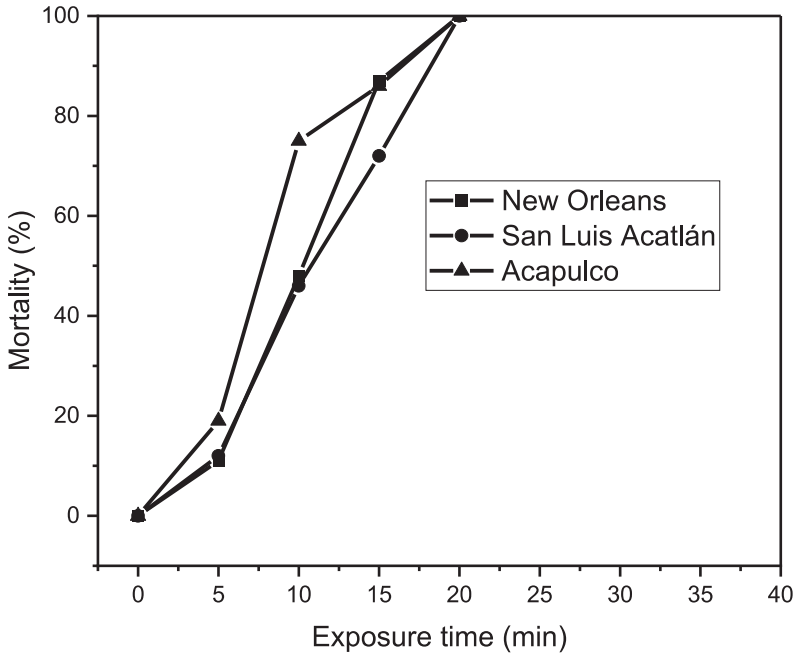

Figure 1. Toxicity of deltamethrin on *Aedes aegypti* L. populations from the state of Guerrero, Mexico, at a dose of 10 µg per bottle.

The San Luis Acatlán population was susceptible to alpha-cypermethrin since 100 % mortality was reached before the diagnostic time; however, the Acapulco population showed possible resistance to this insecticide since only 97 % mortality was reached at the diagnostic time and dose (30 min) (Figure 2).

The Acapulco population showed resistance to permethrin (Figure 3), which could be due to the use of this insecticide in Mexico for more than a decade (Flores *et al*., 2014).

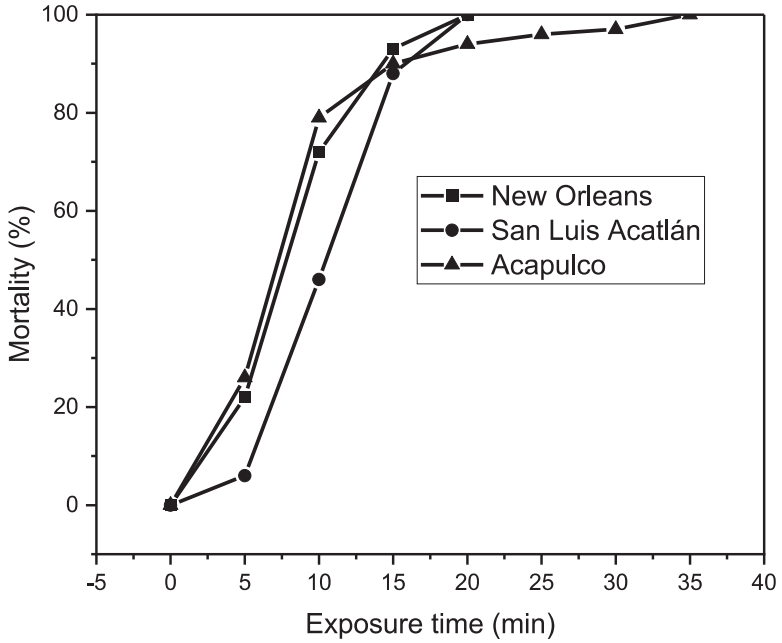

Figure 2. Toxicity of alpha-cypermethrin on *Aedes aegypti* L. populations from the state of Guerrero, Mexico, at a dose of 10 µg per bottle.

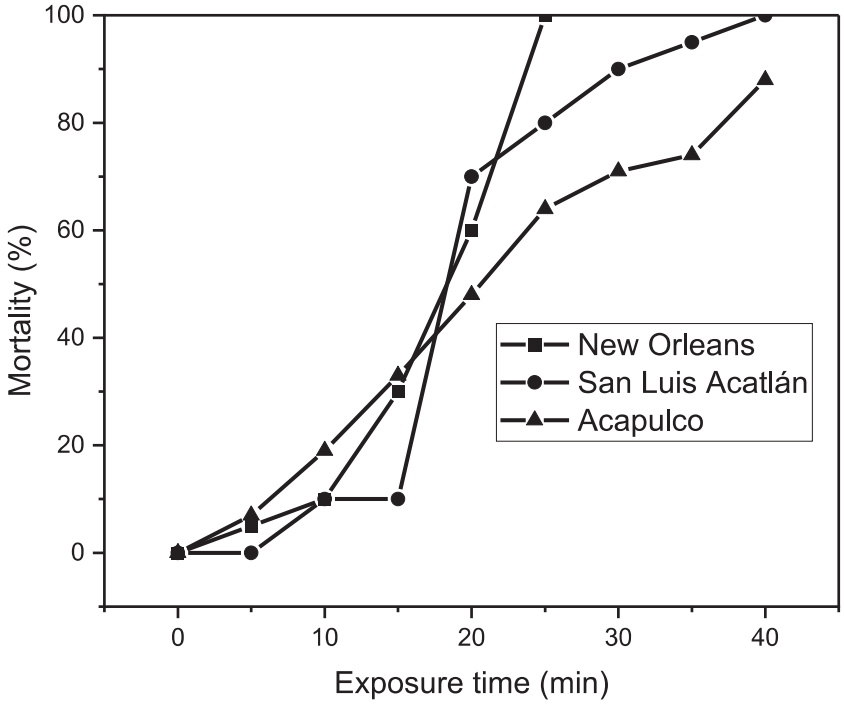

Figure 3. Toxicity of permethrin in *Aedes aegypti* L. populations from the state of Guerrero, Mexico, at a dose of 10 µg per bottle.

The results above agree with Deming *et al*. (2016), who evaluated field populations from municipalities near Mérida, Yucatán, and found that the Mérida population of adults presented higher resistance levels than nearby municipalities. This was because the frequency of application is higher in larger cities than in small towns. However, although the adults of the Acapulco population showed resistance to permethrin, the larvae were susceptible to this insecticide. Similarly, Chaverra-Rodríguez *et al*. (2012) detected a population of *A. aegypti* adults with field resistance to this insecticide and susceptibility in larval stages.

The use of Spinosad and *B. thuringiensis* var. *israelensis* as mosquito larvicides started in Mexico in 2012 (Marina *et al*., 2012). Their use is not yet widespread since, in most cases, Temephos is used, which could explain the low resistance values in the populations evaluated.

In the case of larvae, it is advisable to use microbial insecticides such as Spinosad; however, it has a high cost, so it is recommended to apply in rainy seasons. However, *B. thuringiensis* var. *israelensis* can be used at any time of the year in rotation with organophosphates since they have a low propensity to resistance (Tetreau *et al*., 2013). In the case of adults, although resistance occurs locally, it is suggested to restrict the use of pyrethroid insecticides because they are highly prone to resistance. Where pyrethroids are used, rotation with other groups, such as organophosphates, neonicotinoids, carbamates, or botanicals, is recommended (Rodríguez *et al*., 2014). For adults, the use of permethrin in public health programs should be avoided until resistance levels to this adulticide decrease and it can be used in rotation with other insecticides.

In Mexico, the highest incidence of dengue cases and mosquito density coincides with the rainy season, that is, from July to September (CENAPRECE, 2022). On the other hand, in the first months of the year (January to June), cases decrease, so it is suggested to apply pyrethroids in rotation with organophosphates, mainly chlorpyrifos, at the beginning of the year in the dry months (Marina *et al*., 2012). At the start of the rainy season, it is suggested to apply mixtures of imidacloprid with botanicals since adult density increases, and these products maintain their biological efficacy (Ahmed and Matsumura, 2012). However, they are highly prone to resistance and are also more expensive than carbamates and pyrethroids.

In Mexico, mixtures of botanical insecticides such as neem (*Azadirachta indica* A. Juss) and cinnamon (*Cinnamomum zeylanicum* Blume) are used to combat adult populations of *A. aegypti*, in addition to including them in mixtures with imidacloprid and pyrethrins. This option is considered adequate to diversify the tools to combat this vector, in addition to the use of biopesticides with less adverse effects on the environment and human health (CENAPRECE, 2017).

CONCLUSIONS

A. aegypti larvae showed susceptibility to permethrin, malathion, deltamethrin, and *Bacillus thuringiensis* var. *israelensis*, low resistance to Temephos and propoxur,

and moderate resistance to Spinosad. Adults of the San Luis Acatlán population were susceptible to alpha-cypermethrin; however, the Acapulco population was resistant. Adults from Acapulco were resistant to permethrin, but their larvae showed susceptibility to this insecticide. Adults are resistant to permethrin because it has been used to control this insect for over 30 years.

Studies revealed that Spinosad can be helpful in times of high incidence of dengue; likewise, in times of drought, it is advisable to include rotations with *Bacillus thuringiensis* var. *israelensis* and organophosphates. For adults, using imidacloprid in mixture with botanical insecticides is considered an alternative to carrying out rotations with organophosphates and pyrethroids.

ACKNOWLEDGEMENTS

Our thanks to the Consejo Nacional de Humanidades, Ciencias y Tecnologías (CONAHCYT) and Colegio de Postgraduados for funding and supporting the project.

REFERENCES

Abbott WS. 1925. A method of computing the effectiveness of an insecticide. Journal of Economic Entomology 18: 265–267. https://doi.org/10.1093/jee/18.2.265a

Ahmed MAI, Matsumura F. 2012. Synergistic actions of formamidine insecticides on the activity of pyrethroids and neonicotinoids against *Aedes aegypti* (Diptera: Culicidae). Journal of Medical Entomology 49 (6): 1405–1410. https://doi.org/10.1603/me12030

Araújo AP, Araujo-Diniz DF, Helvecio E, de Barros RA, de Oliveira CMF, Ayres CFJ, de Melo-Santos MAV, Regis LN, Silva-Filha MHNL. 2013. The susceptibility of *Aedes aegypti* populations displaying Temephos resistance to *Bacillus thuringiensis israelensis*: a basis for management. Parasites and Vectors 6 (1): 297. https://doi.org/10.1186/1756-3305-6-297

Atencia MC, Pérez M de J, Jaramillo MC, Caldera SM, Cochero S, Bejarano EE. 2016. Primer reporte de la mutación F1534C asociada con resistencia cruzada a DDT y piretroides en *Aedes aegypti* en Colombia. Biomédica 36: 432–437. https://doi.org/10.7705/biomedica.v36i3.2834

CDC (Centers for Disease Control and Prevention). 2010. Guideline for evaluating insecticide resistance in arthropod vectors using the CDC bottle bioassay. Center for Global Health (U.S.). Division of Parasitic Diseases and Malaria. Atlanta, GA, USA. 28 p.

CENAPRECE (Centro Nacional de Programas Preventivos y Control de Enfermedades). 2017. Productos recomendados por el CENAPRECE para el combate de insectos vectores de enfermedades. Gobierno de México. Secretaría de Salud. Ciudad de México, México. https://www.gob.mx/salud/documentos/productos-recomendados-por-el-cenaprece-para-el-combate-de-insectos-vectores-de-enfermedades-2017?tab= (Retrieved: March 2020).

CENAPRECE (Centro Nacional de Programas Preventivos y Control de Enfermedades). 2022. Panorama epidemiológico del dengue 2022. Gobierno de México. Secretaría de Salud. Ciudad de México, México. https://www.gob.mx/salud/documentos/panorama-epidemiologico-de-dengue-2022 (Retrieved: August 2022).

Chaverra-Rodríguez D, Jaramillo-Ocampo N, Fonseca-González I. 2012. Selección artificial de resistencia a lambda-cialotrina en *Aedes aegypti* y resistencia cruzada a otros insecticidas. Revista Colombiana de Entomología 38 (1): 100–107.

Chino-Cantor AH, Sánchez-Arroyo H, Ortega-Arenas LD, Castro-Hernández E. 2014. Insecticide susceptibility of *Aedes aegypti* L. (Diptera: Culicidae) in Guerrero, México. Southwest. Southwestern Entomologist 39 (3): 601–612. https://doi.org/10.3958/059.039.0319

Deming R, Manrique-Saide P, Barreiro PM, Cardeña EUK, Che-Mendoza A, Jones B, Liebman K, Vizcaino L, Vázquez-Prokopec G, Lenhart A. 2016. Spatial variation of insecticide resistance in the dengue vector *Aedes aegypti* presents unique vector control challenges. Parasites and Vectors 9 (1): 67. https://doi.org/10.1186/s13071-016-1346-3

Flores AE, Albeldaño-Vázquez W, Salas IF, Badii MH, Becerra HL, Garcia GP, Fuentes SL, Brogdon WG, Black IV WC, Beaty B. 2005. Elevated α-esterase levels associated with permethrin tolerance in *Aedes aegypti* (L.) from Baja California, Mexico. Pesticide Biochemistry and Physiology 82 (1): 66–78. https://doi.org/10.1016/j.pestbp.2004.12.007

Flores AE, Grajales JS, Salas IF, García GP, Becerra MHL, Lozano S, Brogdon WG, Black WC, Beaty B. 2006. Mechanisms of insecticide resistance in field populations of *Aedes aegypti* (L.) from Quintana Roo, Southern Mexico. Journal of the American Mosquito Control Association 22 (4): 672–677. https://doi.org/10.2987/8756-971x(2006)22[672:moirif]2.0.co;2

Flores AE, Reyes-Solís G, Fernández-Salas I, Sánchez-Ramos FJ, Ponce-García G. 2009. Resistance to Permethrin in *Aedes aegypti* (L.) in Northern Mexico. Southwestern Entomologist 34 (2): 167–177. https://doi.org/10.3958/059.034.0207

Flores AE, Ponce G, Silva BG, Gutiérrez SM, Bobadilla C, López B, Mercado R, Black WC. 2013. Wide spread cross resistance to pyrethroids in *Aedes aegypti* (Diptera: Culicidae) from Veracruz State Mexico. Journal of Economic Entomology 106 (2): 959–969. https://doi.org/10.1603/ec12284

Flores AE. 2014. Detección de resistencia a insecticidas en mosquitos con énfasis en *Aedes aegypti*. Artrópodos y Salud 1 (2): 21–36.

IRAC (Insecticide Resistance Action Committee). 2017. Arthropod pesticide resistance database. Michigan State University. East Lansing, MI, USA. https://www.pesticideresistance.org/ (Retrieved: March 2017).

Kuri-Morales P, Correa-Morales F, González-Acosta C, Sánchez-Tejeda G, Dávalos-Becerril E, Fernanda Juárez-Franco M, Díaz-Quiñonez A, Huerta-Jiménez H, Mejía-Guevara MD, Moreno-García M, González-Roldán JF. 2017. First report of *Stegomyia aegypti* (= *Aedes aegypti*) in Mexico City, Mexico: *Stegomyia aegypti* in Mexico City. Medical and Veterinary Entomology 31 (2): 240–242. https://doi.org/10.1111/mve.12225

Marina CF, Bond JG, Casas M, Muñoz J, Orozco A, Valle J, Williams T. 2011. Spinosad as an effective larvicide for control of *Aedes albopictus* and *Aedes aegypti*, vectors of dengue in southern Mexico. Pest Management Science 67 (1): 114–121. https://doi.org/10.1002/ps.2043

Marina CF, Bond CJ, Muñoz J, Valle J, Chirino N, Williams T. 2012. Spinosad: A biorational mosquito larvicide for use in car tires in southern Mexico. Parasites and Vectors 5 (1): 95. https://doi.org/10.1186/1756-3305-5-95

Mazzarri MB, Georghiou GP. 1995. Characterization of resistance to organophosphate, carbamate, and pyrethroid insecticides in field populations of *Aedes aegypti* from Venezuela. Journal of the American Mosquito Control Association 11 (3): 315–322.

Rodríguez MM, Hurtado D, Severson DW, Bisset JA. 2014. Inheritance of resistance to deltamethrin in *Aedes aegypti* (Diptera: Culicidae) from Cuba. Journal of Medical Entomology 51 (6): 1213–1219. https://doi.org/10.1603/me13237

SAS Institute. 2016. SAS/Stat® 9.1 User's Guide. SAS Institute, Inc., Cary, NC, USA.

Tetreau G, Stalinski R, David JP, Després L. 2013. Monitoring resistance to *Bacillus thuringiensis* subsp. *israelensis* in the field by performing bioassays with each Cry toxin separately. Memórias do Instituto Oswaldo Cruz 108 (7): 894–900. https://doi.org/10.1590/0074-0276130155

WHO (World Health Organization). 2005. Guidelines for laboratory and field testing of mosquito larvicides. Geneva, Switzerland. 41 p.

WHO (World Health Organization). 2019. Global strategy for dengue prevention and control, 2012-2020. Geneva, Switzerland. 43 p.

WHO (World Health Organization). 2016. Test procedures for insecticide resistance monitoring in malaria vector mosquitoes (Second edition). Geneva, Switzerland. 54 p.

VOLUME 58, NUMBER 7 | OCTOBER 01 - NOVEMBER 15, 2024 | MEXICO